

Enzymes for Industrial Acrylation:

Redesign of *Candida antarctica* Lipase B and Characterization
of a New Cutinase from *Alternaria brassicicola*

Von der Fakultät Energie-, Verfahrens- und Biotechnik der Universität
Stuttgart zur Erlangung der Würde eines
Doktors der Naturwissenschaften (Dr. rer. nat.) genehmigte Abhandlung

Vorgelegt von

Danni Liu

aus Xi'an (V. R. China)

Hauptberichter: Prof. Dr. Rolf D. Schmid

Mitberichter: Prof. Dr. Georg Sprenger

Tag der mündlichen Prüfung: 29. Juli 2009

Institut für Technische Biochemie der Universität Stuttgart

2009

Eidesstattliche Erklärung

Hiermit versichere ich, dass ich die vorliegende Arbeit selbstständig und nur unter Angabe der angegebenen Hilfsmittel und Literatur angefertigt habe.

Stuttgart, den

Acknowledgements

This thesis could not be finished without the help and support of many people who are gratefully acknowledged here.

Foremost, I wish to express my deepest gratitude to Prof. Dr. Rolf D. Schmid for the opportunity to perform my PhD-project in his research group. I particularly appreciate his teaching on the way of life as well as many aspects of scientific research. Without the encouragement and continual support from Prof. Dr. Rolf D. Schmid in my time of difficulties, this work would have been not possible.

I wish to extend my thanks to the chemical company BASF for the financial support. Special thanks go to Prof. Dr. Bernhard Hauer for his fruitful discussion about the Project.

I would also like to express my gratitude to Prof. Dr. Georg Sprenger for his willingness to act as my “Mitberichter” (co-examiner) for my examination.

I thank Dr. Steffen C. Maurer, Dr. Monika Müller and Dr. Sabine Eiben for being my supervisor and for their help in the lab work. Special thanks go to the head of biocatalysis, PD Dr. Vlada Urlacher, for her good suggestions for scientific presentation. I would also like to thank the members of my reading committee, Prof. Dr. Robin Ghosh, Dr. Josef Altenbuchner and Dr. Katja Koschorreck, for their critical review of my thesis and fruitful discussions about my dissertation study.

Also, thanks to my friendly colleagues in the Institute of Technical Biochemistry for creating such a nice work atmosphere. Special thanks go to my friends Dr. Xin Xiong and Dipl. Biol. Tianqi Sun for improving the English version of my thesis and giving further additional critique and enriching remarks. I thank Dipl. Chem. Holger Beuttler

for refining the german summary. I acknowledge Dr. Peter Trodler for the bioinformatic support. I thank also Dipl. Biol. Evelyne Weber for her help in the Analysis of GC-MS.

Finally, I would like to thank those closest to me, my family. My gratitude goes to my parents for their support. Most of all, I thank you, Yijian Wu, for your endurance, unconditional love and support.

Index

Index	I
Abbreviations	VI
Zusammenfassung	VIII
Abstract	XIV
1 Introduction	1
1.1 Enzymes for industrial biocatalysis	1
1.1.1 Biocatalysis	1
1.1.2 <i>Candida antarctica</i> lipase B.....	1
1.1.2.1 Brief introduction of hydrolase and lipase	1
1.1.2.2 Structure of lipases	2
1.1.2.3 Catalytic reactions and mechanisms of lipases.....	5
1.1.2.4 Chirality and Enantioselectivity	7
1.1.2.4.1 Chirality.....	7
1.1.2.4.2 Enantioselectivity of CALB	8
1.1.2.4.3 Determination of enantiomeric rate <i>E</i>	9
1.1.2.5 Immobilization of lipases	11
1.1.2.6 Application of lipases in biotechnology	12
1.1.3 Cutinase	13
1.1.3.1 Structure of cutinase.....	14
1.1.3.2 Immobilization of cutinase.....	15
1.1.3.3 Biotechnological application of cutinase.....	15
1.2 Heterologous expression system for recombinant protein	16
1.2.1 Heterologous gene expression.....	16
1.2.2 <i>E. coli</i> expression system	17
1.2.3 <i>P. pastoris</i> expression system	17
1.2.3.1 Advantages of <i>P. pastoris</i> versus <i>E. coli</i> expression system.....	17
1.2.3.2 Expression of recombinant genes in <i>P. pastoris</i>	18
1.3 Modification of the enzyme properties	20
1.3.1 Directed evolution	22
1.3.2 Rational protein design.....	22
1.3.3 Combination of directed evolution and rational protein design.....	23
1.4 Acrylation	25
1.4.1 Acrylation of hydroxypropylcarbamate	25

1.4.2 Acrylation of 6-mercaptohexanol.....	26
1.5 Goals of this work.....	27
2 Materials and Methods.....	29
2.1 Materials	29
2.1.1 Instruments	29
2.1.2 Consumables	31
2.1.3 Databases and programs.....	31
2.1.4 Chemicals	33
2.1.5 Enzymes	34
2.1.6 Oligonucleotides and plasmids.....	35
2.1.7 Strains.....	36
2.1.8 Commercial Kits	37
2.1.9 Commonly used buffer and media	37
2.1.10 Stock solutions	40
2.2 Methods.....	40
2.2.1 Molecular biological methods.....	40
2.2.1.1 Purification of total RNA from filamentous fungi	40
2.2.1.2 Isolation of plasmid DNA from <i>E. coli</i> and DNA sequencing.....	41
2.2.1.3 Quantification of RNA or DNA	41
2.2.1.4 Polymerase chain reaction.....	42
2.2.1.5 cDNA synthesis.....	43
2.2.1.6 Mutagenesis by PCR	44
2.2.1.6.1 Error-prone PCR	44
2.2.1.6.2 Single site-directed mutagenesis (QuikChange [®]).....	45
2.2.1.6.3 Sequential introduction of mutations.....	47
2.2.1.6.4 Multi site-directed mutagenesis (QuikChange [®]).....	48
2.2.1.7 Colony PCR	49
2.2.1.7.1 Bacterial Colony PCR	49
2.2.1.7.2 Yeast Colony PCR	50
2.2.1.8 DNA digestion with restriction endonucleases	51
2.2.1.9 Dephosphorylation of DNA	52
2.2.1.10 Ligation of DNA with T4 DNA ligase.....	52
2.2.1.11 Agarose gel electrophoresis of DNA.....	53
2.2.1.12 Isolation of DNA from agarose gel	54
2.2.2 Microbiological Methods	54
2.2.2.1 Methods for <i>E. coli</i>	54
2.2.2.1.1 Storage and cultivation of <i>E. coli</i> strains.....	54

2.2.2.1.2	Transformation of <i>E. coli</i> by heat shock (Mandel and Higa 1970)	55
2.2.2.1.3	Transformation of <i>E. coli</i> by electroporation (Neumann et al. 1982)	56
2.2.2.1.4	Expression of recombinant lipase in <i>E. coli</i>	57
2.2.2.1.5	Disruption of <i>E. coli</i> cells	58
2.2.2.2	Methods for <i>P. pastoris</i>	59
2.2.2.2.1	Storage and cultivation of <i>P. pastoris</i> strains	59
2.2.2.2.2	Transformation of <i>P. pastoris</i>	59
2.2.2.2.3	Expression of recombinant lipase in <i>P. pastoris</i>	60
2.2.2.3	Methods for <i>A. brassicicola</i>	60
2.2.2.3.1	Cultivation of <i>A. brassicicola</i>	60
2.2.2.3.2	Expression of a cutinase from <i>A. brassicicola</i>	61
2.2.3	Biochemical methods	61
2.2.3.1	Concentration of protein	61
2.2.3.2	Determination of protein concentration	61
2.2.3.3	Sodium dodecyl sulphate - polyacrylamide gel electrophoresis	62
2.2.3.4	Densitometric analysis	64
2.2.3.5	Purification of recombinant pCUTAB1	64
2.2.3.6	Biochemical characterization	65
2.2.3.6.1	pH-stat assay	65
2.2.3.6.2	Spectrophotometric assay	65
2.2.3.6.3	Substrate specificity of pCUTAB1	67
2.2.3.6.4	Temperature and pH optima of pCUTAB1	67
2.2.3.6.5	Temperature and pH stability of pCUTAB1	67
2.2.3.6.6	Kinetic measurements	67
2.2.4	Immobilization of enzyme	68
2.2.5	Assay systems	68
2.2.5.1	Screening of lipase activity with tributyrin agar plate assay	68
2.2.5.2	Hydrolysis assay for hzca	69
2.2.5.3	Analysis of the enantioselectivity of lipases by gas chromatography	69
2.2.5.4	Analysis of activity of lipase and cutinase by GC/MS	70
3	Results	72
3.1	Improved acylation of hydroxypropylcarbamate by rational protein design of <i>C. antarctica</i> lipase B	72
3.1.1	Rational protein design by molecular modeling	73
3.1.2	Expression of <i>CALB</i> in the <i>E. coli</i> for library screening	76
3.1.2.1	Summary of functional expression of <i>CALB</i> in the <i>E. coli</i> cytoplasm	76
3.1.2.2	Optimization of transformation efficiency for library creation	76
3.1.2.3	Increasing mutagenesis efficiency of library	77
3.1.2.4	Development and validation of a high-throughput assay for the created library	79

3.1.3	Modification of enzyme properties	80
3.1.3.1	Directed evolution using epPCR	80
3.1.3.2	Site-directed mutagenesis.....	80
3.1.3.3	Saturation mutagenesis at positions L277, L278 and A281	82
3.1.3.4	Two-site saturation mutagenesis library (L278X/W104X).....	83
3.1.4	Expression of <i>CALB</i> variants in <i>P. pastoris</i> and characterization.....	85
3.1.4.1	Subcloning of <i>CALB</i> variants into <i>P. pastoris</i>	85
3.1.4.2	Expression of <i>CALB</i> variants in <i>P. pastoris</i>	88
3.1.4.3	Characterization of <i>CALB</i> variants.....	89
3.1.5	Immobilization of <i>CALB</i> variants.....	92
3.1.6	Acrylation of hpc catalyzed by <i>CALB</i> variants	94
3.2	Cloning, expression and characterization of a cutinase from <i>A. brassicicola</i> for acrylation of 6-mercaptohexanol	95
3.2.1	Cloning of a cutinase from <i>A. brassicicola</i> in <i>P. pastoris</i>	95
3.2.1.1	Homology alignment and 3D structure of a cutinase from <i>A. brassicicola</i>	95
3.2.1.2	Cloning of <i>CUTAB1</i> in pPICZαA	100
3.2.2	Expression of <i>CUTAB1</i> in <i>P. pastoris</i>	103
3.2.2.1	Selection of highest expression strains for expression in small batch experimental shake flask	104
3.2.2.2	Expression of <i>CUTAB1</i>	105
3.2.2.3	Purification of recombinant pCUTAB1	106
3.2.2.4	Glycosylation of recombinant pCUTAB1.....	107
3.2.2.5	Putative signal peptide of pCUTAB1.....	109
3.2.3	Biochemical characterization of pCUTAB1	110
3.2.3.1	Kinetic constants of pCUTAB1	110
3.2.3.2	Substrate specificity of pCUTAB1.....	111
3.2.3.3	Temperature optimum of pCUTAB1	113
3.2.3.4	pH optimum of pCUTAB1.....	113
3.2.3.5	Temperature and pH stability of pCUTAB1	114
3.2.4	Immobilization of pCUTAB1 on MP1000.....	116
3.2.5	Acrylation of 6-mercaptohexanol catalyzed by lipase and cutinase	117
4	Discussion.....	119
4.1	Improved acrylation of hydroxypropylcarbamate by rational protein design of <i>C. antarctica</i> lipase B.....	119
4.1.1	Library creation for <i>CALB</i> using the <i>E. coli</i> expression system	119
4.1.2	Modification of enzyme properties	120
4.1.3	Expression of <i>CALB</i> variants in <i>P. pastoris</i> and characterization.....	123
4.1.4	Acrylation of hpc with methyl acrylate by <i>CALB</i> variants	124

4.2 Cloning, expression and characterization of a cutinase from <i>A. brassicicola</i> for acrylation of 6-mercaptohexanol	125
4.2.1 Homology alignment and cloning of <i>CUTAB1</i> in <i>P. pastoris</i>	125
4.2.2 Expression of <i>CUTAB1</i> in <i>P. pastoris</i>	127
4.2.3 Biochemical characterization of pCUTAB1	129
4.2.4 Acrylation of 6-mercaptohexanol.....	130
References	132
Appendix	147
Curriculum vitae	148
Publications.....	149

Abbreviations

A	Absorbance
ab.	Abbreviation
APS	Ammonium persulfate
bp	Base pair(s)
BSA	Bovine serum albumin
CALA	<i>Candida antarctica</i> lipase A
CALB	<i>Candida antarctica</i> lipase B
CIAP	Calf intestinal alkaline phosphatase
Da	Dalton
DMSO	Dimethyl sulfoxide
DNA	Deoxyribonucleic acid
dNTP	Dexynucleoside-5'-triphosphate
DTT	Dithiothreitol
EDTA	Ethylendiaminetetraacetic acid
<i>ee</i>	Enantiomeric excess
GC	Gas chromatography
GC-MS	Gas chromatography-mss spectroscopy
hpc	Hydroxypropylcarbamate
hpca	Hydroxypropylcarbamate acrylate
IPTG	Isopropyl- β -D-thiogalactoside
kb	Kilobases
kDa	Kilo Dalton
LB	Luria-Bertani
OD	Optical dencity
PAGE	Polyacrylamide gel electrophoresis
pCUTAB1	Cutinase von <i>Alternaria brassicicola</i>
PCR	Polymerase chain reaction
PDB	Protein Data Bank
<i>p</i> NPB	<i>p</i> -nitrophenyl butyrate
<i>p</i> NPP	<i>p</i> -nitrophenyl palmitate

Abbreviations

rpm	Revolutions per minute
SDS	Sodium dodecyl sulfate
TAE	Tris/acetate/EDTA buffer
TE	Tris/EDTA buffer
TEMED	N,N,N',N'-tetramethyl-ethylendiamine
Tris	Tris-(hydroxymethyl)-aminomethane
U	Unit(s) of protein activity
UV	Ultraviolet
WT/wt	Wild-type
w/v	weight/volume
v/v	volume/volume

Zusammenfassung

Die Acylierung ist eine Methode zur Einführung von polymerisierbaren Gruppen in Zielverbindungen. In den letzten beiden Jahrzehnten wurde die Verwendung von Lipasen zur Acylierung von einigen Arbeitsgruppen berichtet. In ersten Berichten wurde die *Candida antarctica* (*C. antarctica*) Lipase B (CALB) (EC 3.1.1.3) (Novozym 435) für die Umesterung von Methylacrylat oder für die direkte Veresterung von Acrylsäure verwendet. Wir berichten hier über die Verbesserung der Acylierung von Hydroxypropylcarbamate (Hpc) durch rationales Design von CALB und die Klonierung, Expression und Charakterisierung einer neuen Cutinase aus *Alternaria brassicicola* (*A. brassicicola*) für die Acylierung von 6-Mercaptohexanol.

CALB ist eine Serin-Hydrolase mit einer α/β -Hydrolasefaltung (α/β hydrolase fold). Ihre hohe Stereoselektivität, Aktivität und Stabilität in organischen Lösungsmitteln, auch bei erhöhter Temperatur, machen CALB zu einem idealen Katalysator für chemische Umsetzungen im industriellen Maßstab. Beim von der BASF durchgeführten Screening von bekannten Enzymen für die Umesterung von Methylacrylat mit Hydroxypropylcarbamaten (Hpc), einer Mischung aus *R*- und *S*-Enantiomeren von primären und sekundären Alkoholen, zeigte CALB die höchste Aktivität der getesteten α/β -Hydrolasen. Jedoch kann der CALB Wildtyp (WT) einen vollständigen Umsatz in annehmbarer Zeit nicht erreichen. Industrielle Ansprüche erforderten es, die Gesamtaktivität des WT-Enzyms zu erhöhen und auch gleichzeitig die Enantioselektivität zu erniedrigen, um einen vollständigen Umsatz zu erreichen. Es wurde gerichtete Evolution und rationales Proteindesign durchgeführt, um eine Mutante von CALB zu erhalten, die sowohl eine hohe Aktivität gegen die Edukte (Hpc) also auch eine geringere Enantioselektivität zeigt.

In der durch Error-Prone PCR erstellten Bibliothek war die Mutageneserate zu hoch und damit die Anzahl der Kolonien mit aktiver Lipase zu niedrig. Deshalb war es nicht möglich eine geeignete Mutante zu finden. Rationales Design von Enzymen kann die Möglichkeit für das Screening einer großen Zahl von Biokatalysatoren eröffnen. Es erlaubt die Anpassung des Enzyms für eine Zielreaktion und die Einführung von neuen oder verbesserten enzymatischen Aktivitäten. Für das rationale Proteindesign wurden Molekulardynamik-Simulationen (MD-Simulationen) (Trodlér 2008) und das Docking von Substraten zur Analyse der Wechselwirkung zwischen Substraten und Aminosäuren rund um das aktive Zentrum der Lipase durchgeführt (Trodlér 2008). Das *S*-Enantiomer des sekundären Alkohols (2Hpc)

wurde als Hindernis für das Erreichen des vollständigen Umsatzes identifiziert. Für das rationale Proteindesign wurden Positionen für Mutationen in der Verbindungstasche identifiziert, um die stereospezifische Tasche zu vergrößern und damit die Bindungsfähigkeit des *S*-Enantiomers des sekundären Alkohols für den vollständigen Umsatz zu erhöhen.

Die mit Hilfe der MD-Simulationen identifizierte Mutante L278A zeigte eine höhere Aktivität als der WT in der Hydrolyse von Tributyrin und H_pca. Daher wurde die ortsgerichtete Mutagenese an der Position 278 durchgeführt, um die Bindungstasche für das *S*-Enantiomer des sekundären Alkohols zu vergrößern und die Aktivität zu erhöhen. Außerdem wurde an den Positionen 277, 278 und 281 eine Sättigungsmutagenese durchgeführt und die Bibliothek gescreent. Die genannten Positionen liegen in einer langen α -Helix, die den Eingang in das aktive Zentrum von CALB formt. Obwohl die Anzahl (~ 400) der gescreente Kolonien nicht groß war, zeigte eine Substitution von L278 mit Alanin aus der Bibliothek den höchsten Einfluss auf die Aktivität gegen Tributyrin und die Hydrolyse im H_pca-Assay. Allerdings war in einer präparativen Hydrolyse die Reaktionsrate von L278A leicht im Laufe der Zeit zurückgegangen. Die Enzymaktivität war durch Wiederverwendung der Lipase stabil. Der im Laufe der Reaktion leichte Rückgang der Aktivität könnte eine Folge des Verbrauchs des als Substrat günstigeren *R*-Enantiomers und der generell niedrigeren Aktivität gegen das *S*-Enantiomer des sekundären Alkohols sein. Um die Aktivität gegen das *S*-Enantiomer zu erhöhen, d.h. die Enantioselektivität zu erniedrigen, wurden die Positionen T42, S47 und W104, die einen hohen Einfluss auf die Stereoselektivität von CALB zeigen, zur Mutation ausgewählt. Zur Senkung der Stereoselektivität von CALB wurden Substitutionen von T42 und S47 mit kleineren Aminosäuren (z. B. Alanin) und W104 mit Phenylalanin vorgenommen. Diese Mutanten bieten mehr Platz in der Stereoselektivitätstasche, die von den Resten T42, S47 und W104 gebildet wird. Zur Erweiterung der Stereoselektivitätstasche für das *S*-Enantiomer des sekundären Alkohols und gleichzeitigen Erhöhung der Aktivität von CALB wurde zusätzlich eine Zweifachsättigungsmutagenese-Bibliothek (L278X/W104X) erstellt. Diese wurde erfolgreich mit einem Plattenassay mit Tributyrin als Substrat und dem H_pca-Assay gescreent. Die Mutante L278A/W104F aus dem Screening der Bibliothek (~ 4000 Kolonien) zeigte eine höhere Aktivität als der WT und gleichzeitig eine verringerte Stereoselektivität, die durch Bestimmung der Enantioselektivität nachgewiesen wurde (Tabelle 1). Diese Befunde stimmen mit den Ergebnissen der Molekularen Modellierung überein und korrelieren mit den Vorhersagen, dass Position L278 für die Aktivität und W104 für die Stereoselektivität zuständig ist. Darüber hinaus ist S47 in CALB in der so genannten Stereoselektivitätstasche hinter dem aromatischen Ring von W104 positioniert. Die Effekte

aus einer Kombination der Mutante S47A mit den beiden besten Mutanten, L278A und L278A/W104F wurden gegen Hpca nach Expression in *Pichia pastoris* (*P. pastoris*) weiter untersucht.

Tabelle 1: Charakterisierung von CALB Varianten.

CALB Variante	Aktivität gegen Tributyrin [U/mg] ^a	Aktivität gegen Hpca [$\Delta A_{581} \text{ min}^{-1} \text{ mg}^{-1}$] ^b	<i>E</i> ^c
WT	740 ± 30	89 ± 3	> 300
T42A	494 ± 14	n.d. ^d	205
S47A	850 ± 29	64 ± 3	> 300
T42A/S47A	536 ± 16	n.d. ^d	216
W104F	500 ± 18	26 ± 1	30
L278V	3573 ± 171	n.d. ^d	n.d. ^d
L278A	4390 ± 204	195 ± 8	95
L278A/W104F	1770 ± 29	130 ± 3	4
L278A/S47A	1800 ± 55	207 ± 9	80
L278A/W104F/S47A	1618 ± 67	223 ± 11	5

^a Als Aktivität in der Hydrolyse von Tributyrin wurde 1 U als Umsatz von 1 $\mu\text{mol/min}$ definiert.

^b Als Aktivität in der Hpca-Hydrolyse wurde die ΔA_{581} als die Absorptionsverringerng bei 581 nm definiert.

^c Enantioselektivität (*E*) in der Hydrolyse von Phenylethylpropionat.

^d n.d.: Die Aktivität und die Enantioselektivität wurden nicht bestimmt.

Für das oben genannte Screening der Bibliothek wurden die CALB-Varianten in *Escherichia coli* (*E. coli*) exprimiert (Liu et al. 2006). *E. coli* als Expressionssystem ist besser für das Hochdurchsatzscreening im Hinblick auf die Expressionszeit und die Anzahl der Kolonien geeignet. Aufgrund des sehr niedrigen Expressionsniveaus der aktiven CALB-Varianten in *E. coli*, wurde *P. pastoris* als deutlich besserer Expressionswirt zur Charakterisierung ausgewählter CALB-Varianten verwendet. Eine hohe Ausbeute der Lipasen mit einer hohen Reinheit wurde in diesem Expressionssystem durch die Sekretion der Lipasen in das Medium ermöglicht. Die Transformanten wurden im Hinblick auf die Aktivität bei der Hydrolyse von Tributyrin sowie Hpca und der Stereoselektivität in der Hydrolyse von Phenylethylpropionat charakterisiert.

Beim Vergleich der CALB-Varianten (Tabelle 1) zeigte L278A die höchste spezifische Aktivität (4390 U/mg) gegen Tributyrin und eine sechsfach höhere spezifische Aktivität als

der Wildtyp. Außerdem waren die spezifischen Aktivitäten der Mutanten L278V, L278A/S47A, L278A/W104F, L278A/W104F/S47A und S47A ebenfalls höher als die des Wildtyps. Allerdings zeigten T42A/S47A, T42A und W104F, im Gegensatz zum WT, etwas niedrigere Aktivitäten gegen Tributyrin. Darüber hinaus zeigten die CALB-Varianten L278A, L278A/S47A, L278A/W104F, L278A/W104F/S47A höhere Aktivitäten gegen die Hydrolyse von Hpca als der WT. Weiterhin wurde die Enantioselektivität der CALB-Varianten mit 1-Phenylethylpropionat als Edukt gemessen. Dabei zeigte sich, dass die Auswirkungen der Mutation an Position 47 stark abhängig von den Aminosäuren an den Positionen 104 und 278 waren. Auf der einen Seite zeigte die Einzel-Mutante S47A eine geringere Aktivität als der WT in der Hpca-Hydrolyse und eine vergleichbare Enantioselektivität ($E > 300$). Auf der anderen Seite führte die Kombination von S47A mit L278A beziehungsweise mit L278A/W104F zu einem starken Anstieg der Hydrolysegeschwindigkeit beider Substrate und zu einer verringerten Enantioselektivität ($E = 80$ bzw. $E = 5$).

Mit der Mutante W104F wurde eine geringere Enantioselektivität ($E = 30$, WT $E > 300$) erreicht, die allerdings mit einem Aktivitätsverlust bei der Hydrolyse von Tributyrin und Hpca einherging. In Kombination mit der Mutation L278A zeigte sich eine 1,5-fach höhere Aktivität bei der Hydrolyse von Hpca als beim WT. Gleichzeitig wurde die Enantioselektivität von 30 auf 4 weiter reduziert.

Die lyophilisierte CALB zeigte keine Aktivität in der Acylierung von Hpc in organischen Lösungsmitteln. Daher wurden der WT und die Mutanten L278A, L278A/W104F und L278A/W104F/S47A, welche alle eine höhere Aktivität als der WT gegen Hpca aufwiesen, auf zwei hydrophoben Trägern (MP1000, HP20L) erfolgreich immobilisiert. Mit den immobilisierten Lipasen wurde die Aktivität bei der Umesterung von Methylacrylat und Hpc verglichen. Gleiche Mengen an immobilisiertem CALB-WT und immobilisierten CALB-Mutanten (L278A, L278A/W104F und L278A/W104F/S47A) wurden für die Messung der Aktivität in der Acylierungsreaktion von Hpc benutzt. Der zeitliche Verlauf der Umsetzung zum Produkt (Hpca) wurde mittels GC/MS-Messungen analysiert. Es lässt sich feststellen, dass alle auf MP1000 immobilisierte Mutanten nach drei Stunden Reaktion eine ungefähr 10-20% höhere Aktivität als der WT und die auf HP20L immobilisierten Mutanten nach einer Stunde eine 7-9% höhere Aktivität als der WT zeigten. Ferner war die Tatsache interessant, dass unter Verwendung von L278A, L278A/W104F und L278A/W104F/S47A nach 24 (MP1000) und 29 Stunden (HP20L) Hpc zu 90% umgesetzt werden konnte, während dies beim WT erst nach 48 Stunden unabhängig vom verwendeten Trägermaterial gelang. Obwohl die auf MP1000 immobilisierte CALB-Mutante L278A am schnellsten Hpc zu 90% umsetzte,

war die Reaktionszeit von L278A/W104F und L278A/W104F/S47A wegen der erniedrigten Enantioselektivität ebenfalls stark reduziert. Die Stereoselektivitätstasche der Doppel- und Dreifach-Mutanten war stark vergrößert, deshalb konnten alle Hpc-Enantiomere in die Taschen gelangen. Dadurch wurde die Enantioselektivität gesenkt. Dies stimmte gut mit den Vorhersagen der molekularen Modellierung überein und sprach für die Zuverlässigkeit der Bibliothek der Zweifachsättigungsmutagenese.

Um ein Enzym zu finden, das die Umesterung von Polyacrylat und Amino- oder Mercapto-Alkohol katalysieren kann, wurde ein Screening einer Enzybibliothek von der BASF durchgeführt. Eine Cutinase von *Humicola insolens* (*H. insolens*), welche die höchste Aktivität für diese Reaktion zeigte, wurde gefunden. Allerdings ist diese Cutinase bereits patentiert und daher nicht ohne Weiteres für industrielle Anwendungen verwendbar. Deshalb war das Ziel dieser Arbeit, ein Enzym zu finden, das neben der Homologie zur Cutinase aus *H. insolens* (Hi_Cutinase) auch die Umesterung von Polymer (Polyacrylat) oder Monomer (Methylacrylat) mit Amino- oder Mercapto-Alkoholen katalysiert.

Bei der Analyse der Sequenz verschiedener Cutinasen und der abgeleiteten 3D-Modelle zeigte die Cutinase pCUTAB1 aus *A. brassicicola* eine Sequenzidentität von 61% zur Hi_cutinase. Sie war somit der ideale Kandidat für eine tiefere Untersuchung. Nach der erfolgreichen Klonierung des Gens *CUTAB1* in pPICZ α A und der Überprüfung der entsprechenden Transformante mit Hilfe der Kolonie-PCR, wurde *CUTAB1* in *P. pastoris* funktionell exprimiert. Die Ausbeute betrug 224 mg/l. Nach der Expression der *CUTAB1* und Aufkonzentrierung des Kulturmediums wurde das rekombinante pCUTAB1 in einem Schritt unter nativen Bedingungen mit einer HIC-Säule (HiTrap™ Phenyl FF (low sub)) aufgereinigt. Die Ausbeute betrug 70%, der Aufreinigungsfaktor 1,6. Die kinetischen Konstanten K_m (0,55 mM) und V_{max} (31 U/mg) des aufgereinigten pCUTAB1 wurden mit pNPP als Substrat bestimmt. Das rekombinante pCUTAB1 wurde nach der Expression in *P. pastoris* in einer glykosylierten und in einer unglykosylierten Form gefunden. Außerdem wurde gefunden, dass neben den vier konservierten Cysteinen ein zusätzliches Cystein im N-terminalen Segment von pCUTAB1 vorkommt, welches sich in der Signalsequenz befindet und nach der Expression abgespalten wurde. Das Vorkommen der Signalsequenz wurde mit Hilfe des Programms SignalP 3.0-Server vorhergesagt. Daher enthielt das exprimierte Protein nur 195 Aminosäuren. Die molekulare Masse wurde mit dem Programm Vector NTI Advance 10.3 (Invitrogen™ Corporation) mit 20,1 kDa vorhergesagt.

Die spezifische Aktivität des aufgereinigten pCUTAB1 wurden mit *p*NPB, *p*NPP, Buttersäure- und Caprylsäureethylester, Olivenöl, verschiedenen Glycerinestern und Methylestern von Fettsäuren mit geradzahligem Kohlenstoffanzahl von C₂ (Essigsäure) bis C₁₄ (Myristinsäure) gemessen. Die höchste spezifische Aktivität wurde gegen Tributyrin (3302 U/mg) beobachtet. Gegen *p*NPB und *p*NPP betrug die spezifische Aktivität von pCUTAB1 2868 U/mg beziehungsweise 17 U/mg. Mit steigender Kettenlänge des Acylrestes nahm die Aktivität der pCUTAB1 ab. Obwohl die Cutinase pCUTAB1 eine hydrolytische Aktivität gegen eine große Zahl von Estern, die von löslichen synthetischen Estern (z. B. *p*NP-Ester) bis hin zu unlöslichen Glycerinestern mit langen Ketten reichen, zeigte, war der Glycerinester Tributyrin das äußerst bevorzugte Substrat für die Cutinase pCUTAB1. Dieses Ergebnis entspricht dem Ergebnis, das für die Hi_Cutinase erhalten wurde. Das pH-Optimum von pCUTAB1 lag bei etwa 7-10 und das Temperaturoptimum bei etwa 40°C. In den Untersuchungen zur Stabilität von pCUTAB1 wurde mehr als 80% Aktivität nach einer vierundzwanzigstündigen Inkubation bei 40°C und pH 8 in einem Triton X-100 enthaltenden Reaktionspuffer erhalten. Der gleiche Effekt wurde bei pH 8 sowie bei Raumtemperatur in dem Reaktionspuffer beobachtet.

Die Cutinase pCUTAB1 wurde erfolgreich auf MP1000 immobilisiert. Bei einem Umsatz von 6-Mercaptohexanol mit Methylacrylat mit der Lipase CALB und der Cutinase pCUTAB1 unter Verwendung vergleichbarer Enzymmengen, zeigte die Cutinase pCUTAB1 die höchste Aktivität. Unter Verwendung der Cutinase pCUTAB1 wurde ein Umsatz von 90% nach 3 Stunden erzielt, während dies bei der Lipase CALB erst nach 7 Stunden gelang.

Abstract

Acrylation is a means to introduce polymerizable groups into target compounds. A few groups reported the use of lipases for acrylation during the last two decades. First reports employed *Candida antarctica* (*C. antarctica*) lipase B (CALB) (Novozym 435) for transesterification of methyl acrylate or for direct esterification of acrylic acid. We reported here the improved acrylation of hydroxypropylcarbamate (hpc) by rational design of CALB, and the cloning, the expression as well as the characterization of a new cutinase from *Alternaria brassicicola* (*A. brassicicola*) for the acrylation of 6-mercaptohexanol.

CALB shows activity in the transesterification of hydroxypropylcarbamates containing a mixture of enantiomers of primary and secondary alcohols with methyl acrylate. However, for industrial purposes it was necessary to increase the activity of the wild-type enzyme. By molecular modeling the *S*-enantiomer of the secondary alcohol was identified as the bottleneck for reaching full conversion. In order to improve the acrylation, the stereospecificity pocket was redesigned using predictions from molecular modeling. Amino acid positions 42, 47, 104 and 278 were targeted and a library for two-site saturation mutagenesis at positions 104 and 278 was constructed. For library screening a new assay for the hydrolysis of acrylated hydroxypropylcarbamates was developed. The best mutants L278A, L278A/W10F and L278A/W104F/S47A showed an increased activity in hydrolysis and transesterification of more than 10-20% within 3 hours. We could reach 90% conversion after one day catalyzed by these mutants, while the wild-type reached this level of conversion only after two days regardless of the used carrier material.

From analysis of the alignment of cutinases and the deduced 3D conformational models, a cutinase (pCUTAB1) from *A. brassicicola* showed homology to the proprietary cutinase from *Humicola insolens* (Hi_cutinase) with a sequence identity of 61%. As far as we know, this is the first time that the cutinase pCUTAB1 was cloned into the pPICZaA and integrated into the genome of the methylotrophic yeast *Pichia pastoris* X-33. The cutinase was expressed and secreted using α -factor signal peptide from *Saccharomyces cerevisiae* under control of the methanol inducible promoter of the alcohol oxidase 1 gene (AOX1). After expression at flask level, the supernatant was concentrated by ultrafiltration with a 10 kDa cut off membrane and purified to apparent homogeneity with hydrophobic interaction chromatography in a single step under native conditions using HiTrap™ Phenyl FF. The purified pCUTAB1 showed both the glycosylated and the unglycosylated forms, with distinct molecular weights of 24 kDa and

20 kDa respectively. The cutinase prefers relatively bulky glycerol esters to single chain aliphatic esters, and showed the highest activity towards tributyrin. The optimum temperature and pH of the recombinant pCUTAB1 was 40°C, and pH 7-10 respectively. For acrylation of 6-mercaptohexanol, the cutinase immobilized on MP1000 showed higher activity than the immobilized CALB. 90% conversion after 3 h was reached using the cutinase pCUTAB1, while the lipase CALB reached this level of conversion only after 7 h.

1 Introduction

1.1 Enzymes for industrial biocatalysis

1.1.1 Biocatalysis

Biocatalysts are involved in the usage of enzymes to catalyze chemical conversions and play an important role in modern biocatalytic processes for their high selectivity and high activity in mild reaction conditions (pH, temperature and solvent), which are crucial when the process contains sensitive substrates or products and are beneficial for the environment.

More than one hundred years ago, it was shown that enzymes could be used in organic solvents (Hill 1898; Kastle and Loevenhart 1900). The high selectivity and activity of enzymes in organic solvents make them ideal catalysts for chemical conversions. Moreover, the interest for biocatalysis boosted from the 1980's with the general acceptance that enzymes can catalyze unnatural reactions efficiently in organic solvents (Klibanov 1986). The development of recombinant protein technology has dramatically decreased the production costs of enzymes. The utility of molecular biological methods has also increased the possibility to improve enzyme properties. With the increasing demand of enantiopure compounds for the pharmaceutical industry, biocatalytic processes have been developed. Nowadays, enzyme catalysis is considered as an important tool for industrial synthesis (Koeller and Wong 2001; Schoemaker et al. 2003).

Given the large expansion in the area of biocatalysis, there are still a vast number of catalytic processes that lack a suitable enzyme. The discovery of new enzymes and the improvement of current enzymes for the process requirements are much in demand.

1.1.2 *Candida antarctica* lipase B

1.1.2.1 Brief introduction of hydrolase and lipase

Hydrolases is a large family of enzymes in biocatalysis. They can break down amide and ester type bonds of many kinds of substrate molecules and catalyze a wide variety of natural and unnatural substrates in organic solvents. These characters make them to be suitable stereoselective catalysts in the synthesis of optically pure molecules which are major products in the pharmaceutical and agrochemical industries.

Lipases (triacylglycerol ester hydrolases, EC 3.1.1.3) forming an important part of hydrolases are ubiquitous enzymes that catalyze the hydrolysis of fats and oils (Schmid and Verger 1998; Jaeger et al. 1999; Villeneuve et al. 2000; Klibanov 2001; Koeller and Wong 2001; Schmid et al. 2001). In addition, lipases act on the hydrolysis of a broad range of natural and unnatural esters, and possess high chemo-, regio- and/or stereoselectivity. Besides high selectivity and broad substrate spectrum, lipases also catalyze hydrolysis of water-insoluble substrates. One lipase from *Thermomyces lanuginose* (*T. lanuginose*) (formerly *Humicola lanuginosa*) produced by Novozymes is added into a large number of the detergents sold all over the world. This lipase has an optimal activity at pH 10.5-11 and 40°C, and is stable under the harsh laundry conditions. It has broad substrate specificity, and can degrade various fat stains found on fabrics. Moreover, lipases are also widely used in the food industry for processing fats and oils (Sharma et al. 2001).

Candida antarctica (*C. antarctica*) lipase A and B (CALA and CALB) (Kirk and Christensen 2002) were produced by the yeast *C. antarctica* which was originally isolated from Antarctica. Until now, CALA has been found to be probably the most thermostable one in all known lipolytic enzymes. Using a method of differential scanning calorimetry (DSC), the thermal denaturation temperature (T_d) values were determined up to 96°C, 95°C and 93°C at the pH values 4.5, 5 and 7, respectively.

CALB belongs to the enzyme class of hydrolases (E.C.3) and acts on ester bonds (E.C.3.1) of carboxylic esters (E.C.3.1.1). It is a triacylglycerol lipase (E.C.3.1.1.3) which can hydrolyze triacylglycerols to fatty acids, diacylglycerol, monoacylglycerol and glycerol. Moreover, it has been used in organic, regioselective and enantioselective synthesis. Therefore, CALB is usually mentioned among the most used lipases and reviewed for its applications (Anderson et al. 1998). This lipase is a rather unique protein with a high stability. Although the optimal pH for catalysis is 7, it is stable in aqueous media within the pH range of 3.5-9.5. It has been reported that immobilized CALB showed high thermostability (Arroyo and Sinisterra 1994). CALB showed high stability and activity in polar organic solvents. Whereas, most enzymes are only stable and active in non-polar organic solvents (Reslow et al. 1987).

1.1.2.2 Structure of lipases

In past decade, numerous crystal structures of lipases were dissolved (Grochulski et al. 1994; Noble et al. 1994; Uppenberg et al. 1994). Lipases have a common fold, the α/β -hydrolase fold (Ollis et al. 1992; Schrag and Cygler 1997), which is composed of a central β sheet

consisting of up to eight different β strands (β_1 - β_8) which are connected by up to six α helices (Figure 1.1). These elements occur in the same order in all lipase amino acid sequences and are oriented in the same three-dimensional direction in all structures.

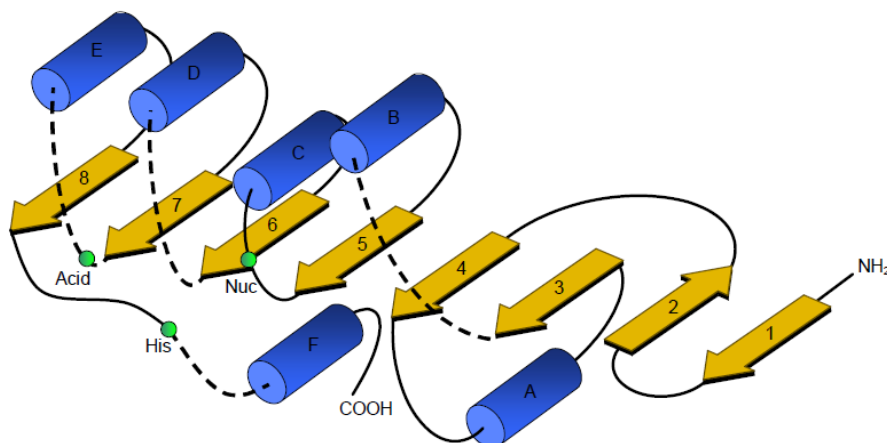


Figure 1.1: The α/β -hydrolase fold of serine hydrolases (Trodler 2008). α -helices are marked with blue cylinders (A-F), β sheets with yellow arrows (1-8). The dashed lines indicate variable fields. The nucleophilic elbow is indicated between β -sheet 5 and α -helix C. The positions of the amino acids of the catalytic triad are marked with green dots.

The protein structural features underlying these observations have been unraveled with the determination of open and closed structures of *Rhizomucor miehei* (*R. miehei*) lipase in 1990 (Brzozowski et al. 1991). The X-ray structures of these lipases indicated the presence of a helical amphiphilic unit (lid or flap) covering the active site of the enzyme in solution. It was shown that a lipid-induced change in the lid orientation causes interfacial activation. Lipases possess poor activity towards soluble substrates in aqueous solutions because the lid is closed. During binding to a hydrophobic interface (e.g. a lipid droplet), the lid opens resulting in increase of catalytic activity. Additionally, the opening of the lid introduces one of the oxyanion-stabilising residues into catalytic orientation.

However, the presence of a lid-like structure is not essentially correlated with interfacial activation (Verger 1997). Most lipases including CALA show interfacial activation, while CALB does not show such behavior and is therefore not considered to be a true lipase (Martinelle et al. 1995). This lid structure which covers the active site of true lipases is absent or very small in CALB. The three-dimensional (3D) structure of CALB has been determined by X-ray crystallography (Protein Data Base (Berman et al. 2002) entries: 1LBS, 1LBT, 1TCA, 1TCB and 1TCC) (Uppenberg 1994; Uppenberg 1995) and is shown in Figure 1.2.

CALB belongs to the α/β -hydrolase-fold superfamily (Ollis 1992). It is built up of 317 amino acids and has a molecular weight of 33 kDa. The active site of CALB is characterized by the triad composed of Ser (S105), His (H224) and Asp (D187) (**Figure 1.2**). Such active sites are conserved in all Ser hydrolases and acyl-enzyme complexes being the crucial intermediates in all lipase-catalyzed reactions (Schmid and Verger 1998; Jaeger 1999; Villeneuve 2000). The Ser residue usually appears in the conserved pentapeptide G-X-S-X-G. However, the highly conserved motif around the Ser of the active site was found to be T-W-S-Q-G in CALB. The active site of CALB possesses an oxyanion hole that stabilizes the transition state and the oxyanion in the reaction intermediate by three hydrogen bonds: one with Q106 and two with T40 (**Figure 1.2** and **Figure 1.3**). Furthermore, the active site also contains a small cavity called the stereospecificity pocket including T42, S47 and W104 (**Figure 1.3**) (Uppenberg 1995), in which secondary alcohols have to orient one substituent during catalysis (Orrenius et al. 1998; Rotticci et al. 1998). This gives CALB a high enantioselectivity towards chiral secondary alcohols (Rotticci 2000).

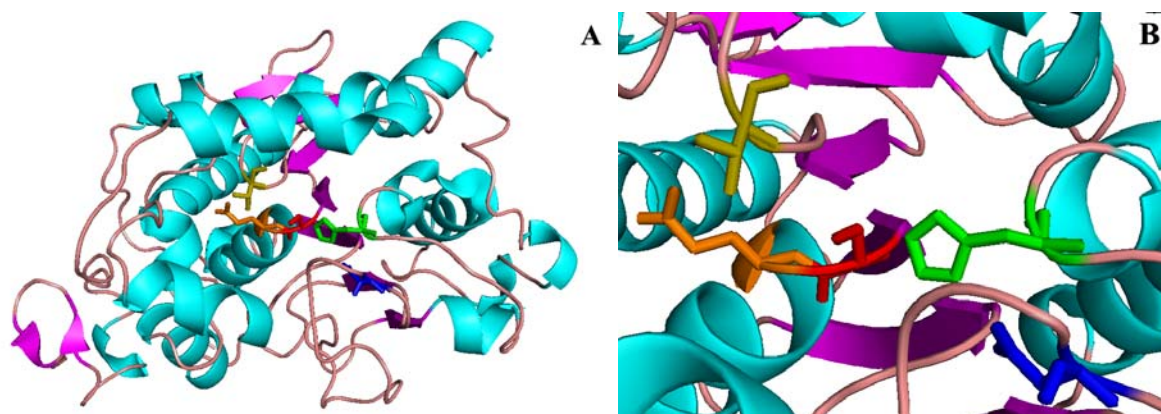


Figure 1.2: (A) Structure of *C. antarctica* lipase B that belongs to the α/β -hydrolase-fold superfamily. The α -helices are shown in cyan and the β -sheets in magenta. The amino acids of the catalytic triad are colored in red for Ala, green for His and blue for Asp. The residues T40 and Q106 in oxyanion hole are presented in olive and orange sticks respectively. (B) A close-up of the active site.

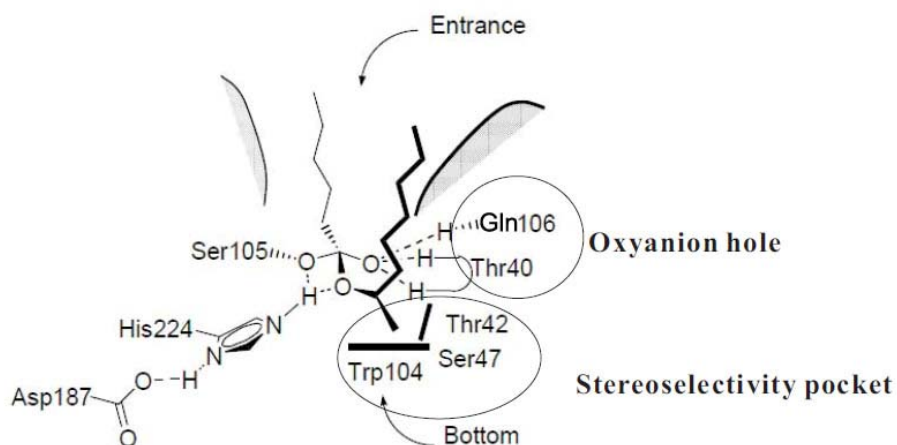


Figure 1.3: Schematic illustration of the catalytic triad (S105, H224 and D187), oxyanion hole and stereoselectivity pocket of CALB in the transition state with 2-octyl hexanoate (the charges are omitted). Modified from (Rotticci 2000).

1.1.2.3 Catalytic reactions and mechanisms of lipases

Lipases are used not only in the hydrolysis of ester bonds, but also in the esterification, the reverse reaction of hydrolysis (**Figure 1.4**). In the transesterification, the alcohol group of the first ester is exchanged by another alcohol to produce a new ester. The exchange depends on both the concentrations of substrates and the substrate specificity of lipase (Soares et al. 2003). In a system with low water content, lipase can catalyze the ester linkages from free carboxylic acids and alcohols. The esterification is easier to control than the hydrolysis, since full conversion can be achieved by steady removal of the final product.

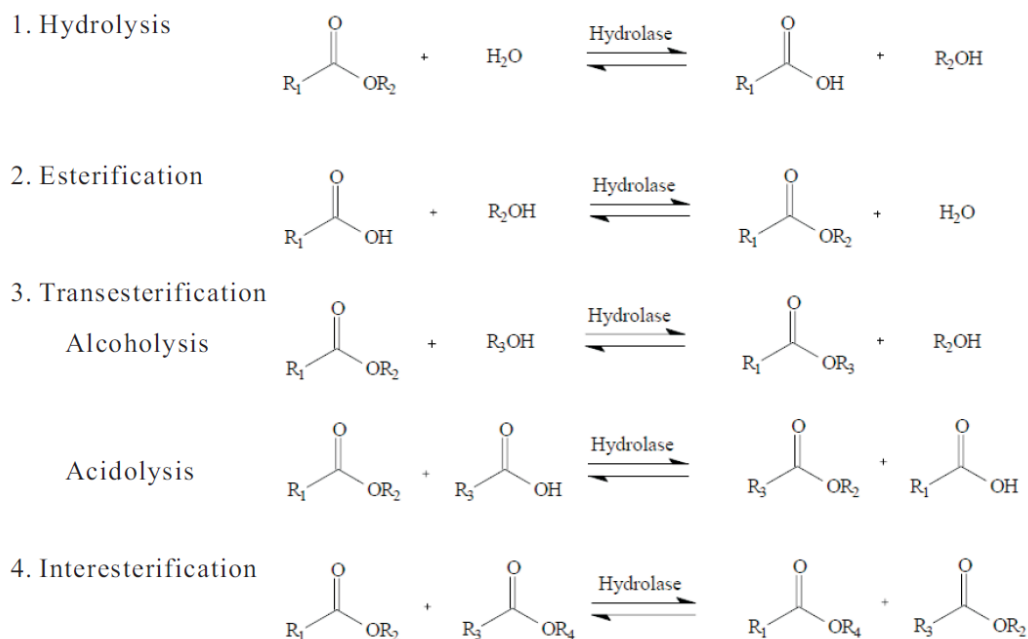


Figure 1.4: Reactions catalyzed by lipases and carboxylesterases.

The mechanism of esterification catalyzed by lipases is comparable with the serine proteases (Carter and Wells 1988). The assumed catalytic mechanism of transesterification for CALB (**Figure 1.5**) is centered on the active site Ser. Firstly, the ester binds to the enzyme and the catalytic Ser attacks the carbonyl forming the first tetrahedral intermediate (**Figure 1.5**). Collapse of this tetrahedral intermediate liberates the alcohol and provides an acyl enzyme intermediate. In a hydrolytic reaction, water attacks this acyl enzyme to form a second tetrahedral intermediate. While in a transesterification, an alcohol or an acid attacks this acyl enzyme to form the second tetrahedral intermediate. Dissociation of this intermediate releases a new alcohol or a new acid and a new ester. In most cases, it appears that the formation of the acyl enzyme is fast and the deacylation is the rate-determining step. CALB can catalyze acyl-transfer reactions between varied compounds. Depending on the R-groups (shown in **Figure 1.5**), the reaction can be an ester hydrolysis, an esterification or a transesterification. The second substrate can also be an amine, which would result in an aminolysis. CALB can accept several types of acyl-donors, e.g. esters, acids, thioesters, carbonates and carbamates.

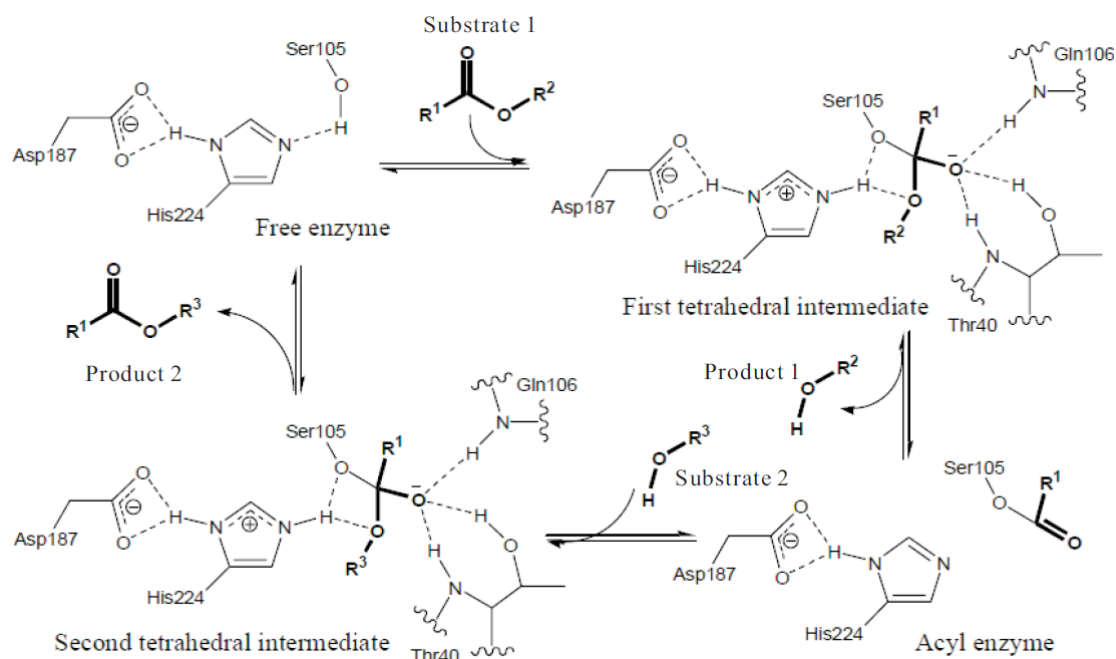


Figure 1.5: Reaction mechanism of CALB which is modified from the literature (Magnusson 2005; Magnusson et al. 2005b). The first substrate enters the active site and forms the first tetrahedral intermediate. The first product leaves the active site, and then the acyl-enzyme is formed. The second substrate enters the active site and forms the second tetrahedral intermediate. The second product leaves the active site and enzyme becomes free and is ready for another catalytic cycle.

1.1.2.4 Chirality and Enantioselectivity

1.1.2.4.1 Chirality

"I call any geometrical figure, or group of points, chiral, and say it has chirality, if its image in a plane mirror, ideally realized, cannot be brought to coincide with itself."

This is the celebrated definition stated by Lord Kelvin in 1904 and universally accepted as the definition of chirality. In nature, many molecules are chiral. A chiral object is defined as being nonsuperimposable on its mirror image. Two objects being mirror images of each other are *enantiomers*. **Figure 1.6** is an example of chiral molecules. The (*R*)-3-methylheptane and the reflection (and rotated reflection) (*S*)-3-methylheptane are mirror images and non-superimposable. Thus, they are enantiomers and chiral.

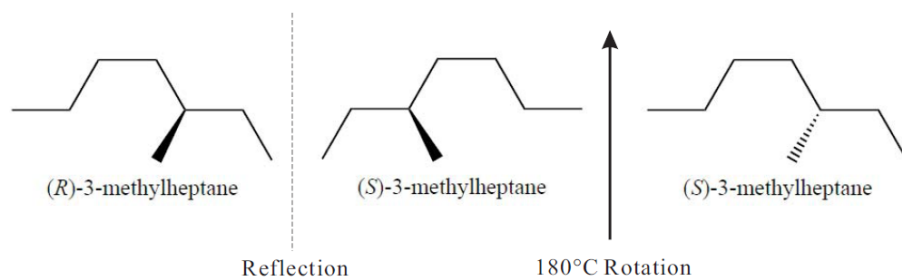


Figure 1.6: Example of chiral molecules. Starting with the (*R*)-3-methylheptane, reflection in the plane generates a new structure (reflection) (*S*)-3-methylheptane. A 180° rotation at a vertical axis generates the rotated reflection. Although the heptane chain of the (*R*)-3-methylheptane and the rotated reflection (*S*)-3-methylheptane can be perfectly overlaid, the 3-CH₃ group of the (*R*)-3-methylheptane points toward the viewer whereas the 3-CH₃ group of the rotated reflection (*S*)-3-methylheptane points away from the viewer. The third carbon is a stereocenter.

1.1.2.4.2 Enantioselectivity of CALB

As early as 1848, Pasteur discovered the optical isomerism of tartaric acid crystals and explained the phenomenon of chirality (Pasteur 1906). Since then, the knowledge and interest in chiral molecules increased continuously. The synthesis of pure enantiomer products is often difficult by chemical separation of racemic mixtures, whereas enzymes offer one of the best routes to enantiomerically pure building blocks for the synthesis of bioactive compounds such as pharmaceuticals, pheromones, fragrances and fine chemicals (Faber 2000). Hydrolases including lipases, esterases, and proteases are catalysts commonly used for the production of optically active carboxylic acids, alcohols, amino acids and amines (Bornscheuer and Kazlauskas 2006).

Lipases showed enantioselective toward alcohols and amines. Kazlauskas et al. reported proposed rules about the enantioselectivity of lipases (Kazlauskas et al. 1991). The rules can be used to simply and accurately predict which enantiomer reacts faster (**Figure 1.7**). This rule predicts in general the *R*-enantiomer as the fast reacting enantiomer. This empirical rule has later been rationalized for CALB at a molecular level (Haeffner et al. 1998). The steric requirements of the stereospecificity pocket determine the enantioselectivity of CALB towards secondary alcohols. The large substituent of the fast-reacting enantiomer of the secondary alcohols situates in the active-site entrance and its medium-sized substituent in the stereospecificity pocket. In order to perform reaction, the slow-reacting enantiomer has to have the opposite orientation for its substituents compared to the fast-reacting enantiomer.

The large substituent which is not easily accommodated in the stereospecificity pocket results in the low reaction rate of this enantiomer (Rotticci 1998).

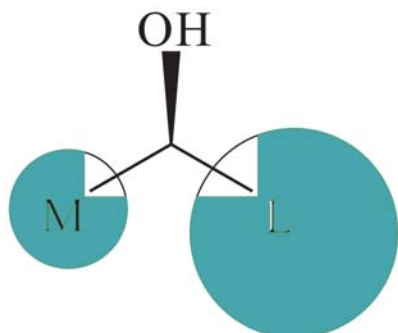


Figure 1.7: The conformations of the medium (M) and large (L) substituent and the hydroxyl group of the fast reacting enantiomer of secondary alcohols as predicted by Kazlauskas rule (Kazlauskas 1991).

1.1.2.4.3 Determination of enantiomeric rate E

To measure the enantiomeric purity of the products produced by enzyme, the enantiomeric excess (ee) indicating the enantiomeric purity is calculated according the following Equation 1.

$$ee_p = \frac{[P1] - [P2]}{[P1] + [P2]} \quad \text{Equation 1}$$

In Equation 1, the concentration of the product 1 ($P1$) is higher than that of the product 2 ($P2$). For accurate evaluation of the stereo preference of an enzyme in the conversion of a given substrate, this value is not suitable, since ee is highly dependent on the substrate concentration. In the course of the reaction, the concentration of the preferred substrate-enantiomer decreases faster than that of the less suitable substrate-enantiomer. Thus, the relative turnover of the less suitable substrate-enantiomer increases and the ee_p value falls off with the increasing turnover. Comparing ee values of two kinetic resolutions is therefore meaningful only at the same degree of conversion.

To better determine the stereo-selectivity, the notion of enantioselectivity E is therefore introduced, which describes an ability of an enzyme to distinguish between two enantiomers. The enantiomers (R and S) are competitive substrates. The ratio of the reaction rates is defined as (V_R/V_S) in Equation 2 and the specificity constants (k_{cat}/K_m) $_R$ / (k_{cat}/K_m) $_S$ as the enantiomeric ratio, E (Equation 3), which is independent of the extent of conversion.

$$\frac{V_R}{V_S} = \frac{(k_{cat}/K_m)_R \times [R]}{(k_{cat}/K_m)_S \times [S]} \quad \text{Equation 2}$$

$$E = \frac{(k_{cat}/K_m)_R}{(k_{cat}/K_m)_S} \quad \text{Equation 3}$$

In the above equations $[R]$ and $[S]$ indicate the concentration of the corresponding enantiomers (R and S) and K_m is designated as the Michaelis-Menten constant K_m , which is equal to the substrate concentration at which the reaction rate is half of its maximal value. The apparent first-order rate constant for conversion of the enzyme-substrate (ES) complex to product, k_{cat} , is called the turnover number. k_{cat}/K_m is the specificity constant and represents the apparent second-order rate constant of the enzymatic reaction. It is often used to assess the overall efficiency and specificity of enzyme reaction (Fersht 1984).

The E -value determines the enantioselectivity of the reaction (Chen et al. 1982; Chen et al. 1987). The ability of an enzyme to distinguish between enantiomers is measured by this E -value under determined reaction conditions (e.g. temperature, solvent, water activity). The E -value is therefore used instead of ee to describe the enantioselectivity of a kinetic resolution. By rule of thumb, reactions with E -values lower than 15 are normally considered inapplicable for practical purposes. When $E=15-30$, the usefulness can be regarded as moderate to good, and when it exceeds this value, excellent (Faber 2000). Moreover, the kinetics and thermodynamics of the reaction are important for calculation of the E -value. Equation 3 is used for conversion from one chiral racemic substrate to one chiral product under considering many factors: equilibrium, product inhibition, and racemization etc..

Several methods for the calculation of the E -value have been reviewed (Straathof and Jongejan 1997), as well as the problems and advantages related to each of them. ee_s and ee_p indicating the extent of conversion together with time are quantities that can be monitored for the calculation of the E -value. The methods discussed here are based on ee_s , ee_p and conversion (c) under irreversible reaction conditions (Faber and Riva 1992). The E -value can be determined using one of the following three equations (Equation 4, 5 and 6) (Chen 1982; Rakels et al. 1993).

$$E = \frac{\ln[1 - c(1 + ee_p)]}{\ln[1 - c(1 - ee_p)]} \quad \text{Equation 4}$$

$$E = \frac{\ln[(1 - c)(1 - ee_s)]}{\ln[(1 - c)(1 + ee_s)]} \quad \text{Equation 5}$$

$$E = \frac{\ln\left[\frac{1 - ee_s}{1 + ee_s / ee_p}\right]}{\ln\left[\frac{1 + ee_s}{1 + ee_s / ee_p}\right]} \quad \text{Equation 6}$$

The impact of errors of c on the E is limited in Equation 4 at low conversion, if ee_p and c are monitored. On the other hand, the effect of an error in the conversion on E is little at high conversion, using Equation 5. However, wenn an equation is used for calculation of E -value for an irreversible reaction, a faulty E -value will be achieved due to the reached equilibrium of the reaction at high conversion (Chen 1987). Equation 6 often leads to a more accurate E -value than the other two equations (Equation 4 and 5), since ee values are generally easier to be accurately determined than the conversion (c). For an accurate determination of the E , it is preferable to monitor two of the three parameters ee_s , ee_p and c during the course of the reaction. This enables the determination of E by a curve fitting method (Van Tol et al. 1991).

1.1.2.5 Immobilization of lipases

Application of immobilized enzymes provides distinct advantages over soluble enzymes in biocatalytic practice. These advantages include enhanced activity, increased selectivity, improved stability and reusability. Immobilization of lipases have been reported in many literatures (Stark and Holmberg 1989; Bosley and Peilow 1997; Ivanov and Schneider 1997; Sharma 2001). Although many applications used not immobilized lipases, a demand of an immobilized biocatalyst for synthesis and biotransformation is increasing due to the high efficiency and the recyclability of expensive enzymes. Moreover, immobilization can also enhance enzyme stability and activity.

It has been reported that adsorption or precipitation onto hydrophobic materials (Wisdom et al. 1984), adsorption in macroporous anion exchange resins (Rizzi et al. 1992), covalent attachment to functional groups (Shaw et al. 1990), entrapment in polymer gels (Telefoncu et al. 1990), microencapsulation in lipid vesicles (Balcaño et al. 1996), and sol-gel entrapment (Jaeger and Reetz 1998; Krishnakant and Madamwar 2001) can be used to immobilize lipases. The immobilization process rendered highly active, thermally and chemically stable and heterogeneous biocatalysts.

Nevertheless, adsorption onto hydrophobic materials is a simple and straightforward route for enzyme immobilization and can provide sufficient quantities of active enzymes for industrial processes. Moreover, research about distribution of enzymes on the hydrophobic carrier, poly-

(methyl methacrylate) (Lewatit VP OC 1600), and investigation of secondary structure of immobilized enzyme have been reported (Mei et al. 2003). It was found in this report that CALB (Novozyme435) was unevenly distributed in an external shell of the bead and CALB's secondary structure determined using synchrotron infrared microspectroscopy (SIRMS)-generated spectra was not altered by the immobilization.

1.1.2.6 Application of lipases in biotechnology

Lipases are quoted as being one of the most versatile enzymes by most research scientists of the world and used in a number of bioconversions. Their applications can be found in industries dealing with oils and fats, detergents, baking, cheese making, hard-surface cleaning as well as leather and paper processing (Schmid and Verger 1998; Jaeger 1999; Villeneuve 2000). Moreover, application of lipases in synthetic organic chemistry has been reported and reviewed many times (Schmid and Verger 1998; Jaeger 1999; Villeneuve 2000; Klivanov 2001; Koeller and Wong 2001; Schmid 2001).

Hydrolytic lipases have been used mostly as addition to detergents in household and industrial laundry. Moreover, enzymes can reduce the environmental load of detergent products, as firstly, they save energy by enabling a lower wash temperature to be used; secondly, they can also replace those less desirable chemicals in detergents; thirdly, they are biodegradable, leaving no harmful residues; fourthly, they have no negative impact on sewage treatment processes; and finally, they do not represent any risk for aquatic life. Lipases are also extensively used in the food industry for processing fats and oils (Sharma 2001). Another application of lipases can be found in removing the pitch from pulp produced in the paper industry. Among the most used lipases the interesting properties and great potential of CALB as industrial catalyst was described in many other reviews (Anderson 1998; Kazlauskas and Bornscheuer 1998). CALB shows some potential applications in the resolution of chiral secondary alcohols (Ohtani et al. 1998; Rotticci et al. 2001), in the production of polylactones (Uyama et al. 1997) and polyesters (Binns et al. 1998). Recently, CALB has been used successfully in one industrial process, namely, the production of isopropyl myristate, which is used as a component in cosmetics (Houde et al. 2004). Lipases are indeed one of the most versatile enzymes. In the nearly future there will be a large scale commercial exploitation of these enzymes. Enzyme sales in 1995 were estimated to be US\$30 million, wherein detergent enzymes made up 30% (Houde 2004). Lipases estimated 1000 tons are added to the

approximately 13 billion tons of detergents produced each year. A range of enzymes for various industrial purposes from Novo Nordisk is listed in **Table 1.1**.

Table 1.1: Novo Nordisk enzymes for various industrial applications.

Serial No.	Brand	Enzyme	Application
1	Lipopan [®]	Lipase	Baking industry
2	Lipozyme [®]	Lipase	Oils and fats industry
3	Novozym [®] 27007	Lipase	Pasta/Noodles
4	Palatase [™]	Lipase	Dairy industry
5	Clear-Lens [™] LIPO	Lipase	Personal care industry
6	GreaseX	Lipase	Leather
7	Lipolase [™]	Lipase	Detergent industry
8	LipoPrime [®]	Lipase	Detergent industry
9	NovoCor [™] AD	Lipase	Leather industry
10	Novozym [®] 735	Lipase	Textile industry
11	Novozym [®] 871	Lipase	Pet Food Industry

1.1.3 Cutinase

Cutinase (EC 3.1.1.74) is an enzyme which is secreted extracellularly by phytopathogenic fungi and can catalyze the hydrolysis of cutin (Purdy and Kolattukudy 1975), an insoluble polymeric structural component of the cuticle (**Figure 1.8**) covering leaves and all aerial organs of plants (Kolattukudy 1981). The fatty acids of cutin served as protector against the entry of pathogens into plants are usually C₁₆- or C₁₈- molecules and contain up to three hydroxy groups (**Figure 1.9**). It can be found that many bridges such as predominant ester bonds, peroxide bridges, and ether linkages, are present in cutins. The extracellular cutinase secreted by phytopathogenic fungi can degrade the cutin and begin the infection process. It was reported that inhibitors of cutinase could prevent fungal penetration of plants and thus prevent infection (Soliday and Kolattukudy 1983). The enzyme from several fungal sources can hydrolyze the *p*-nitrophenyl esters of hexadecanoic acid. Additionally, this enzyme is able to catalyze the hydrolysis of the ester bonds of triglycerides (Lauwereys et al. 1991) and displays a distinct stereopreference for position *sn*-3 of prochiral triacylglycerols, while *R. miehei* and *Pseudomonas* sp. lipases show some preference for position *sn*-1 (Carvalho et al. 1998). Furthermore, cutinase can hydrolyze the *R*-enantiomers in a preferential manner (Mannesse et al. 1995).

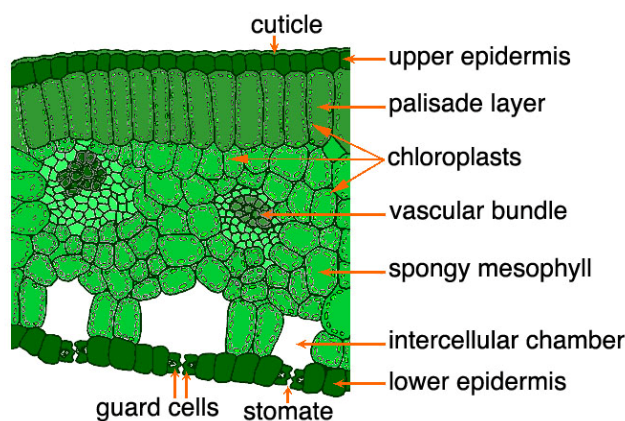


Figure 1.8: Leaf cross section. <http://extension.oregonstate.edu/mg/botany/images/fig12a-big.gif>

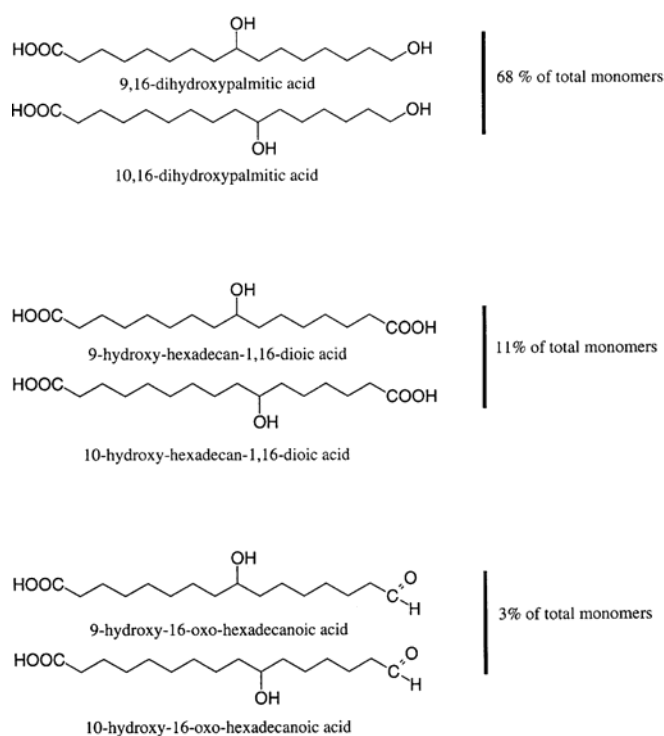


Figure 1.9: Major monomers of *Vicia sativa* cutin.

<http://www.palaeos.com/Plants/Lists/Glossary/GlossaryA.html>

1.1.3.1 Structure of cutinase

The three-dimensional (3D) structure of cutinase has been determined by X-ray crystallography (Protein Data Base (Berman 2002) entries: 1CEX, 1CUA, 1CUB, 1CUD, 1CUE and 1FFA from *Fusarium solani* (*F. solani*) and 3DCN from *Glomerella cingulata* (*G. cingulata*) (Nyon et al. 2009)). Although cutinases show large differences in size and amino acid sequence compared to lipases, these two kinds of enzyme belong to the class of serine esterases and to the superfamily of the α/β hydrolases (Carvalho 1998). Apart from sharing a

similar catalytic machinery with lipases, the cutinase show a homologous stretch (G-Y-S-Q-G) around the active Ser to the common stretch (G-Y/H-S-X-G) of lipases (Longhi et al. 1997a; Carvalho 1998). The catalytic triad S120, D175 and H188 of the cutinase is accessible to the solvent and is located at one extremity of the protein ellipsoid (Longhi 1997a). Differing from true lipases with an interfacial activation, which is necessary for lipases to display their activity due to the existence of a hydrophobic lid (or flap) covering the catalytic site in their structures, cutinases do not exhibit interfacial activation. The active site of cutinase is located at the bottom of a crevice built up by the loops 80 to 87 and 180 to 188 (Martinez et al. 1992; Martinez et al. 1993; Jelsch et al. 1998), which may constitute the interfacial binding site. Lipases need the reorientation of a few lipophilic side chains, for example L81 and L182, that play the role of a 'mini' flap (Carvalho 1998), whereas cutinase seems not to require a main-chain rearrangement when binding to interfaces. Another important feature of cutinase structure is that the oxyanion hole is preformed in cutinase instead of being induced by ligand binding and seems to be stabilized by cutinase S42 side chain (Nicolas et al. 1996).

1.1.3.2 Immobilization of cutinase

It has been reported that cutinase immobilized in different forms such as a free preparation, encapsulated in reversed micelles and immobilized on solid supports can catalyze many kinds of reactions (Carvalho 1998), which include hydrolytic (Goncalves et al. 1996; Goncalves et al. 1996a; Goncalves et al. 1999), esterification (Sereti et al. 1997; Sjursnes et al. 1998), and transesterification reactions (Parvaresh et al. 1992; Lamare and Legoy 1995; Lamare et al. 1997; Serralha et al. 1998) and for the resolution of racemic mixtures (Fontes et al. 1998). Many people reported applications of cutinase adsorbed on Accurel EP 100, a macroporous polypropylene support (Sereti 1997; Sjursnes 1998), and Accurel PA6, a macroporous polyamide support (Serralha 1998). These carriers have been proved to be suitable in active enzyme preparations. In view of the stability and reactivity, cutinase adsorbed onto a macroporous polypropylene support in supercritical CO₂ at 45°C and 130 bar displayed a considerable stability in that system (Sereti 1997).

1.1.3.3 Biotechnological application of cutinase

The biocatalytic application of cutinase has been extensively reviewed (Carvalho 1998). Cutinase has been used in many industrial applications due to its interesting properties. The

hydrolytic activity of cutinase as esterase has been intensive studied and several applications in different industrial fields have been presented (Carvalho 1998). In order to take advantage of its *in vitro* cutinolytic activity, an enzymatic preparation containing cutinase has been developed for increasing the pharmacological effect of agricultural chemicals (Genencor 1988). Furthermore, cutinases can hydrolyze soluble esters and emulsified triacylglycerols and thus be considered as a linking enzyme between esterases and lipases (Egmond and Van Bommel 1997). It has been reported that cutinases has been used in laundry and dishwashing detergent formulations (Van der Hijden et al. 1994; Egmond and Van Bommel 1997; Okkels et al. 1997). If compared with a commercial lipase, LipolaseTM, cutinase benefits the removal of triacylglycerols in a single wash process more greatly, as cutinase was able to hydrolyze the fats in the absence of calcium (Egmond and Van Bommel 1997). Cutinase can be used to degrade plastics. For example, a cutinase from *F. solani f. pisi* can hydrolyze polycaprolactone, a synthetic polyester, to water-soluble products (Murphy et al. 1996). In our work a new native cutinase from *Alternaria brassicicola* (*A. brassicicola*) was used for transesterification of 6-mercaptohexanol with methyl acrylate, which has also potential application in polymer synthesis.

1.2 Heterologous expression system for recombinant protein

1.2.1 Heterologous gene expression

The possibility of heterologous gene expression has an enormous influence on the use of proteins for industrial applications, medicine and research. While proteins were isolated with lower yields in the 1970s only from their natural sources, Itakura et al. succeeded for the first time in the heterologous *E. coli* expression of a small peptide in 1977 (Itakura et al. 1977). The heterologous expression of genes in different hosts makes, on one hand, the use of proteins possible from poorly accessible sources, such as from *Archaea*, on the other hand, it simplifies the exploration and manipulation of various biotechnologically interesting enzymes. All available expression systems are able to influence the character of the protein to be produced and challenge its applicability. For example, for a therapeutical protein the guarantee of a correct posttranslational modification is necessary to prevent an immunological shock for patients (Ballou 1976; Hayette et al. 1992). Furthermore, proteins for industrial applications must also be produced at a low price. Generally many proteins are only

functionally produced in specific hosts and some factors including codon usage preference, posttranslational modification, cellular targeting etc. are very important and thus ought not to be ignored.

1.2.2 *E. coli* expression system

The *E. coli* expression system is the first choice for high-throughput screening of CalB variants in a prokaryotic system. Compared to the published high-throughput expression system in *Saccharomyces cerevisiae* (Zhang et al. 2003; Suen et al. 2004), this system has many major advantages, which include lower costs, easier handling and the higher total amount of clones to be screened in short time scale in *E. coli*. In microtiter plates the total expression period is 48 h, whereas the *S. cerevisiae* system needs a 9-day expression period. Therefore, the *E. coli* expression system is a very notable development for the mutagenesis of CALB, which is one of the most important lipases in biotechnology.

1.2.3 *P. pastoris* expression system

1.2.3.1 Advantages of *P. pastoris* versus *E. coli* expression system

E. coli has been used as a cellular host for gene expression in a widespread way. However, production of eukaryotic proteins using this system is limited, as their derivation from eukaryotic genomes decided that they require post-translational modifications. *E. coli* as a prokaryotic organism show the inability to correctly fold the foreign protein and perform other post-translational modifications. This disadvantage limits the types of proteins that can be produced. That incorrect folding can be a result of inadequate intracellular chaperone concentrations (Cole 1996) or the reducing environment of the cytoplasm (Bardwell 1994). Therefore, *E. coli* is not generally suitable for intracellular production of proteins that contain a high level of disulfide connectivity (White et al. 1994) or proteins that require other types of posttranslational modifications which include glycosylation, disulfide isomerization, proline cis/trans isomerization, sulphation, lipidation or phosphorylation (Lueking et al. 2000).

The eukaryotic *P. pastoris* expression system offers significant advantages over *E. coli* expression system for the production of many heterologous eukaryotic proteins, while being as easy to manipulate as *E. coli* or *S. cerevisiae*. The features of this expression system are particularly suitable for target proteins that contain multiple disulfide bonds or require

glycosylation, phosphorylation, the absence of an amino-terminal methionine or oligomer formation for the correct assembly of the mature protein (Daly and Hearn 2005). It is easier, faster, and less expensive to use than other eukaryotic expression systems and generally gives higher expression levels. *P. pastoris* as yeast shares advantages on molecular and genetic manipulations with *Saccharomyces*, and ten- to hundred-fold higher heterologous protein production levels can be achieved using this expression system. These characteristics make *P. pastoris* very useful as a heterologous host.

1.2.3.2 Expression of recombinant genes in *P. pastoris*

P. pastoris (Invitrogen) is a methylotrophic yeast and can metabolize methanol as sole carbon source. The enzyme alcohol oxidase can catalyze methanol to formaldehyde and produce hydrogen peroxide, which is toxic to the cell, in a specialized cell organelle (peroxisome). The produced toxic by-products are thus kept away from the rest of the cell. Although alcohol oxidase has a poor affinity to O₂, *P. pastoris* can produce a great many of the enzyme. Heterologous gene expression in *P. pastoris* is regulated by the promoter used also for producing alcohol oxidase.

Two genes in *P. pastoris* encoding alcohol oxidase are *AOX1* and *AOX2*. The majority of alcohol oxidase activity in the cell comes from the product of the *AOX1* gene. The *AOX1* gene is expressed under the strong regulation and induction by methanol to very high levels, usually more than 30% of the total soluble protein in cells grown with methanol. It has been reported that the gene *AOX1* was isolated and the heterologous gene expression was under the control of the *AOX1* promoter (Ellis et al. 1985; Tschopp et al. 1987; Koutz et al. 1989). Although *AOX2* shows about 97% similar to *AOX1*, growth of the cells on methanol with *AOX2* is much slower than that with *AOX1*. The *AOX1* gene is expressed under the control of the level of transcription. Approximately, 5% of the polyA⁺ RNA is from the *AOX1* gene in methanol grown cells. The regulation of the *AOX1* gene contains a repression/derepression mechanism plus an induction mechanism (e. g. *GALI* gene in *S. cerevisiae* (Johnston 1987)). That means transcription is repressed by growth on glucose, even in the presence of the inducer methanol. Therefore, for optimal induction with methanol growth on glycerol is used. However, growth on glycerol alone is not sufficient to produce noticeable levels of *AOX1* expression. Methanol induced detectable levels of expression from the *AOX1* gene (Ellis 1985; Tschopp 1987; Koutz 1989). A strain with phenotypically Mut^S or Mut⁻ (Methanol utilization slow) is ascribed to the loss of the *AOX1* gene (*aox1*), and accordingly a deficiency of most of

the cell's alcohol oxidase activity. The Mut^S cells exhibit poor growth on methanol medium due to a reduction in the cells' ability to metabolize methanol. The Mut⁺ (Methanol utilization plus) cells show the ability of wild type strains to metabolize the sole carbon source, methanol. Two kinds of heterologous expression in *P. pastori*, either intracellular or secreted, are available. The presence of a signal sequence at the N-terminal end of the protein to target it to the secretory pathway is required for secretion. In spite of the successful application of the native secretion signal present at some heterologous proteins, the secretion signal sequence (α factor prepro peptide) from the *S. cerevisiae* has been verified to be the most success (Cregg et al. 1993; Scorer et al. 1993). As secreted proteins the heterologous protein produced in the medium shows the great advantage including the vast majority of the total protein in the medium and thus serving as the first purification-step of the protein (Barr *et al.*, 1992).

Glycosylation occurred at the recognized glycosylation sites (Asn-X-Ser/Thr) in the protein's primary sequence may happen when expression of heterologous gene in *P. pastoris*. However, there is no hyperglycosylate in *P. pastoris*, in comparison to *S. cerevisiae*. Both *S. cerevisiae* and *P. pastoris* have a majority of N-linked glycosylation of the high-mannose type; however, it has been reported that glycosylated proteins produced in *P. pastoris* showed much shorter oligosaccharide chains than those in *S. cerevisiae* (Tschopp 1987; Grinna and Tschopp 1989). Very little O-linked glycosylation is observed in *P. pastoris*. Glycoproteins generated in *P. pastoris* may show less problems than that produced in *S. cerevisiae* due to the similarity of the glycoprotein structure with that of higher eukaryotes (Cregg 1993).

P. pastoris x-33 (Yang and Hew 2001) used in this study is a wild-type stain with Mut⁺ phenotype. The pPICZ α A vector contains the ZeocinTM resistance *Sh ble* gene (*Streptoalloteichus hindustanus* bleomycin resistance gene) to allow selection of the plasmid using ZeocinTM, and therefore, selection of positive transformants in *E. coli* and *P. pastoris*. pPICZ α A encodes the α factor signal sequence from *S. cerevisiae* for secretion of recombinant proteins into the medium. The expression of recombinant genes results from the control of the *AOX1* promoter, which is induced by methanol and repressed by glucose and glycerol.

1.3 Modification of the enzyme properties

The natural function of enzymes almost never complies with the specific conditions required in industrial processes. The enzymatic reaction therefore must be optimized in order to obtain the desired yield, high activity and stability under process conditions, desired substrate specificity and high regio- and stereoselectivity. Molecular biological methods have conferred the opportunity to improve the properties of enzymes when they do not meet the process requirements. To modify an enzyme, in the past few years, rational protein design and directed evolution have emerged as effective alternative methods to optimize biocatalytic reactions (Bornscheuer et al. 2002). These two general strategies for protein engineering are shown in **Figure 1.10**.

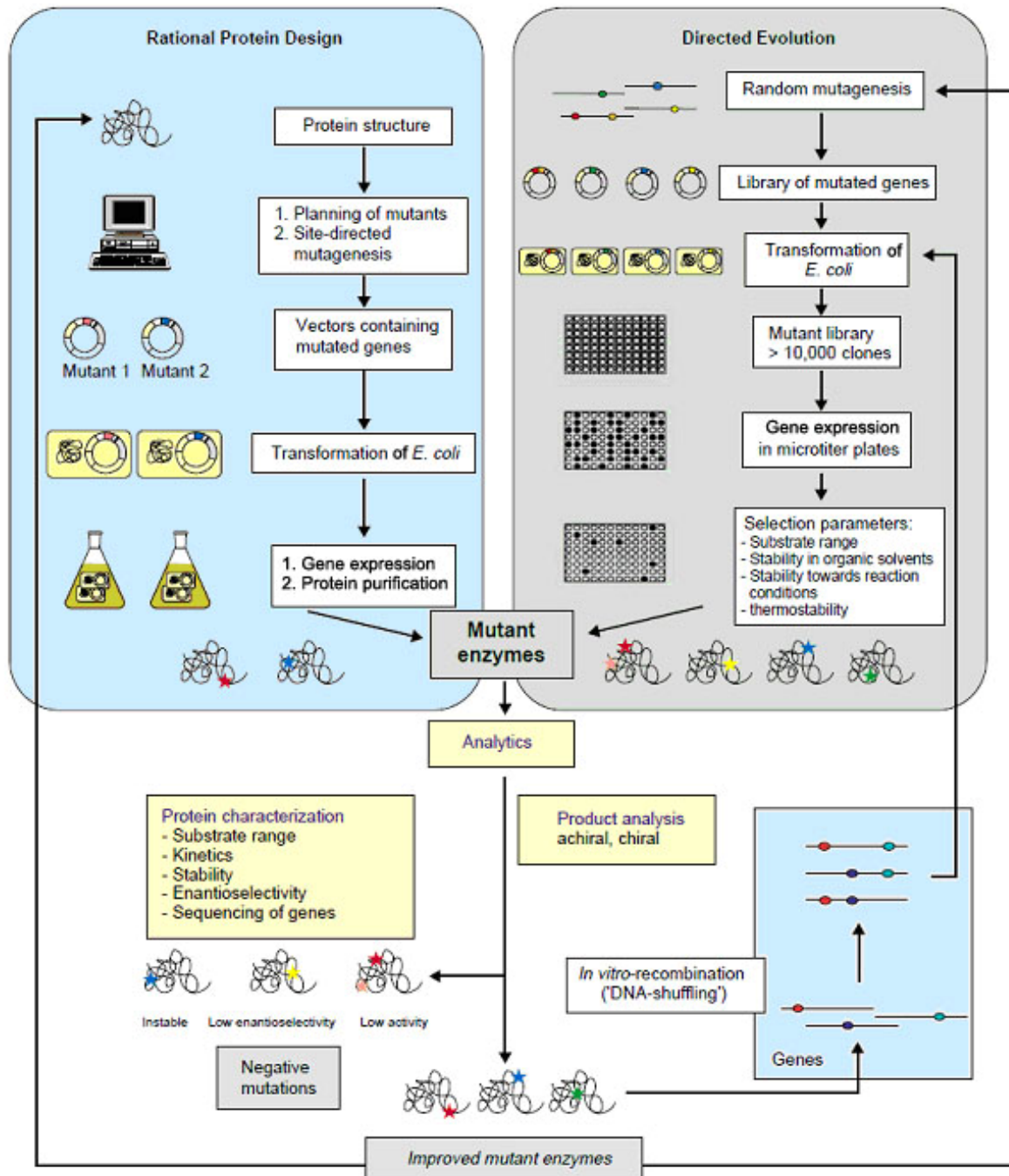


Figure 1.10: Comparison of directed evolution and rational protein design Modified from the literature (Bornscheuer and Pohl 2001). Directed evolution starts with generation of gene mutation libraries by random mutagenesis, which are then expressed in host cells. The corresponding libraries are usually screened in microtiter plates using a range of selection parameters. Rational design mutants are modified on the basis of their structure by bioinformatic tools and fulfilled by site-directed mutagenesis. After transformation of host cells, the variant is expressed, purified and analyzed. Both protein engineering approaches are possible to be repeated or combined until biocatalysts with desired properties are generated.

1.3.1 Directed evolution

Directed evolution including error-prone PCR (epPCR), saturation mutagenesis, and/or DNA shuffling has become popular methods for developing biocatalysts (Brakmann and Schwienhorst 2004; Svendsen 2004; Reetz et al. 2005). It has been reported that evolutionary approaches can be used to engineer biomolecules (Spiegelman et al. 1965; Eigen and Gardiner 1984).

Widely used in directed evolution experiments are epPCR, which introduces random errors into DNA sequences during PCR under mutagenic reaction conditions (e.g. imbalanced nucleotides or by addition of Mn^{2+} or Mg^{2+} to the reaction mixture) (Leung et al. 1989; Cadwell and Joyce 1992), yielding randomly mutated products. Spee et al. reported that the mutation rate may be influenced by addition of nucleotide analogues such as 8-oxo-dGTP or dITP (Spee et al. 1993). Furthermore, DNA shuffling have been reported as a method for *in vitro* recombination (Stemmer 1994a; Stemmer 1994b) and used to improve biocatalysts (Reetz and Jaeger 1999). In addition, there were also some successful examples about saturation mutagenesis (Miyazaki and Arnold 1999; Walbot 2000; DeSantis et al. 2003; Zheng et al. 2004). DeSantis et al. reported that this mutagenesis technique effects the combinatorial saturation of each amino acid in the protein to each of the other 19 amino acids through the gene site saturation mutagenesis. And it combined with a novel high-throughput mass spectroscopy assay; a number of improved variants of a nitrilase were identified (DeSantis 2003).

The random mutagenesis by the error-prone PCR technique very rarely creates more than one change per codon. As a consequence not all the amino acids can be introduced at a given position, possibly preventing the creation of an improved variant. Random methods often find improved enzyme variants with mutations far from the active site. Enzymes have most of their amino acids far from the active site and random mutagenesis will consequently target those amino acids with a higher frequency. That explains why few variants with mutations close to the active-site are found, even if such mutations affect the performance of the enzyme to a larger extent (Park et al. 2005).

1.3.2 Rational protein design

Rational protein design is rapidly emerging as a powerfull approach to improve the enzyme. The prerequisite of rational protein desigh is the availability of the structure of the enzyme

and knowledge about the relationships between sequence, structure and mechanism or function (Bornscheuer and Pohl 2001). The rapid increasing number of sequences stored in public data bases make this approach popular than before. Moreover, the success rate increases if more information about the enzyme is available, such as reaction mechanism, catalytic residues, active-site conformation, and substrate specificity. Through rational protein design, amino acid substitutions are often chosen by sequence comparison with homologous sequences depending on the purpose of the mutagenesis. One or a few amino acids which may affect the property are substituted by other amino acids through site-directed mutagenesis to create one or a few mutants. After expression of the mutants, the enzyme variants are characterized to ascertain the success of the optimization of the catalyst. On the other hand, using bioinformatic tools such as molecular modeling, it has been possible to predict how to increase the activity, selectivity and the stability of enzymes, even if there are no structural data available and the structure of a homologous enzyme is used as a model. Some basic knowledge about this method and successful application have been published (Kazlauskas 2000; Bornscheuer and Pohl 2001; Magnusson 2005).

An example of rational redesign is a very stable mutant of a thermolysin-like protease from *Bacillus stearothermophilus* created by this method (Van den Burg et al. 1998). In order to create rigidifying mutations such as Ala to Pro and Gly to Ala as well as one disulfide bridge, eight amino acids were mutated. When the mutations were selected, thermostable variants were used as models. The half-life at 100°C increased from less than half a minute for the wild-type to 170 min for the rationally designed mutant. While the activity at 37°C remained as high as that of the wild-type protease, the stability also increased towards denaturing agents. The stabilizing effect of the rigidifying mutations was explained by reduced entropy of the denatured enzyme. More recently the active-site of a rationally redesigned lipase for catalysis of Michael-type additions was explored (Carlqvist et al. 2005). In addition, creating space for large secondary alcohols (Magnusson 2005a) and the increased enantioselectivity with temperature by rationally redesign of *C. antarctica* lipase B were reported (Magnusson 2005b).

1.3.3 Combination of directed evolution and rational protein design

Although the positions of mutations are often different to a great extent, directed evolution and rational design are both applicative to producing desired mutant enzymes for protein engineering. On one hand, mutations created by directed evolution are far away from the place where the reaction takes place, as was shown for improved enantioselectivity (Liebeton

et al. 2000) and altered substrate specificity (Bornscheuer et al. 1999) of hydrolases. On the other hand, by rational design those amino acid residues which are close to the active site, the binding pocket etc. and appear 'logical' to the researcher, examining the three-dimensional structure, can be modified to alter the trait of the enzyme or even to generate a new enzymatic activity (Mouratou et al. 1999). In order to create an improved biocatalyst within the requested industrial timelines for economic applications and increasing our understanding of structure/function relationships, more studies have to be performed by more combinations of both protein engineering tools.

Many successful example of the use of directed evolution and rational protein design was reviewed (Bornscheuer and Pohl 2001). A successful example was reported by researchers at Novo Nordisk (Bagsvaerd, Denmark). A targeted heme peroxidase from *Coprinus cinereus* was used as a dyetransfer inhibitor in laundry detergent (Cherry et al. 1999). Incubation under conditions mimicking those in a washing machine (e.g. pH 10.5, 50°C, 5-10 mM peroxide) was performed, which is followed by screening for improved stability through measuring residual activity. Mutants were obtained by epPCR (out of 64,000) and by rational design as well. For both methods position E239 to be crucial for success was identified by sequencing of the best variants. Saturation mutagenesis showed that replacement with Gly, as predicted by computer- modeling, afforded the best performance. Subsequent *in vivo* shuffling resulted in dramatic improvements, giving a mutant with 174 times the thermal stability and 100 times the oxidative stability of the wild-type peroxidase.

More recently, a new practical method (CAST: combinatorial active-site saturation test) combining the features of rational design and combinatorial amino acid randomization at focused sites has been developed for solving the long-standing problem of wide substrate acceptance of enzymes (Reetz 2005). With difference from previous focused libraries (Yang et al. 2002; Brakmann and Schwienhorst 2004), a complete set of pairs of amino acids around the bound substrate is considered in this method. This helps to systematically create relatively small libraries of mutants, the screening of which by currently available assays yields positive hits and consequently the identification of the critical regions around the active site which are crucial for substrate acceptance. In our work combination of these two methods was also performed; besides site-directed mutagenesis, rational design was improved by saturation mutagenesis library based on promising positions suggested by bioinformatic tools, which was referred to the first part of our work.

Moreover, for mutagenesis approaches and protein engineering, the gene encoding the enzyme of interest, a suitable (usually microbial) expression system, and a sensitive detection

system are prerequisites. For lipase detection and assay, methods have been reviewed in detail (Beisson et al. 2000).

1.4 Acrylation

Acrylation is a means to introduce cross-linking functionality into target compounds. Traditional chemical processes for producing acrylate esters employ high temperatures frequently leading to polymerization of acrylic double bonds. To avoid these undesired reactions polymerization inhibitors and acid catalysts have been introduced (Tetsuya Ohru et al. 1975) allowing for reactions at 80 to 100°C. Enzymatic processes conducted at moderate temperatures might be beneficial in acrylation reactions as additives can be omitted, energy saved, selectivity and tolerance of functional groups enhanced as well as product quality and purity improved. Selectivity of enzymes is an advantage if there are several reactive functionalities (hydroxyls, amines, thiols) in the molecule of interest. A few groups reported the application of lipases in acrylation reactions during the last two decades. First reports originate from Hajjar using a lipase from *Chromobacterium viscosum* (Hajjar et al. 1990). Subsequent work employed CALB (Novozym 435) for transesterification of methyl acrylate (Warwel et al. 1996) or for direct esterification of acrylic acid (Park et al. 2004). The industrial interest in acrylation is emphasized by patents in the field originated from chemical companies like e. g. BASF (Hauer et al. 2003). In view of the eco-friendly production of monomer or direct polymer compound by biochemical method using enzymes from microorganism, the corresponding investigations promise thus a broad prospect in industrial application.

1.4.1 Acrylation of hydroxypropylcarbamate

The acrylated ester of hydroxypropylcarbamates (hpc) studied in the first part of our work is difficult to catalyze by classic chemical methods using acid catalysts as mentioned above; in particular, it is not possible to achieve a colorless product. However, the low amount of pigment is indispensable for a potential application as reactive cross-linker in the clear lacquer. Although this ester is already commercially available and used in e.g. automotive industry as a monomer for the manufacture of protective lacquer-coatings, the chemical process should be replaced by a biotechnological process using *C. antarctica* lipase B up to now. During the synthesis of hydroxypropylcarbamate-acrylate (hpca) (**Figure 1.11**) through transesterification a

mixed kinetic is observed. A fast synthesis is followed by a slow period to complete the reaction. This is due to the fact that hydroxypropylcarbamate is a mixture of primary and secondary alcohols. The reaction with one enantiomer of the secondary alcohol is probably hindered.

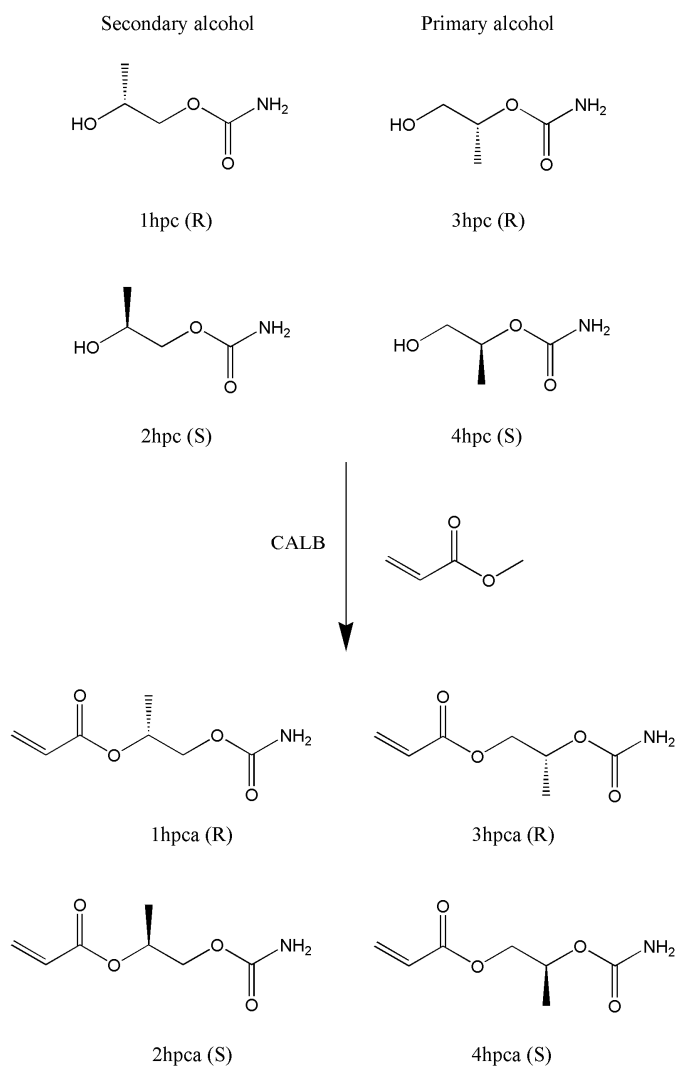


Figure 1.11: Transesterification of hydroxypropylcarbamates with methyl acrylate catalyzed by CALB. Abbreviations hpc for the hydroxypropylcarbamate regio- and stereoisomers and hpca for the acrylated hpc are used (R: *R*-configuration; S: *S*-configuration).

1.4.2 Acrylation of 6-mercaptohexanol

Methyl acrylate can be polymerized to polyacrylate which is an acrylic resin used in an emulsified form for lacquer, textile finishes, adhesives and, mixed with clay, to gloss paper; The side chain with various groups (e.g. thio or amino groups) in polyacrylate will lead to a

wide variety of physicochemical characters, which can satisfy different industrial requirements. Therefore, investigation about introduction of these side chains in polymers through esterification or transesterification is very interesting for industrial application.

However, there were some difficulties from our preparative experiments in the hydrolysis or esterification of the polymers catalyzed by enzyme. Investigation of such esterification or transesterification was thus carried out with monomer (methyl acrylate) firstly. In the second part of our study, the transesterification (**Figure 1.12**) of 6-mercaptohexanol with methyl acrylate (i.e. acrylation of 6-mercaptohexanol) was catalyzed by cutinase and lipase.

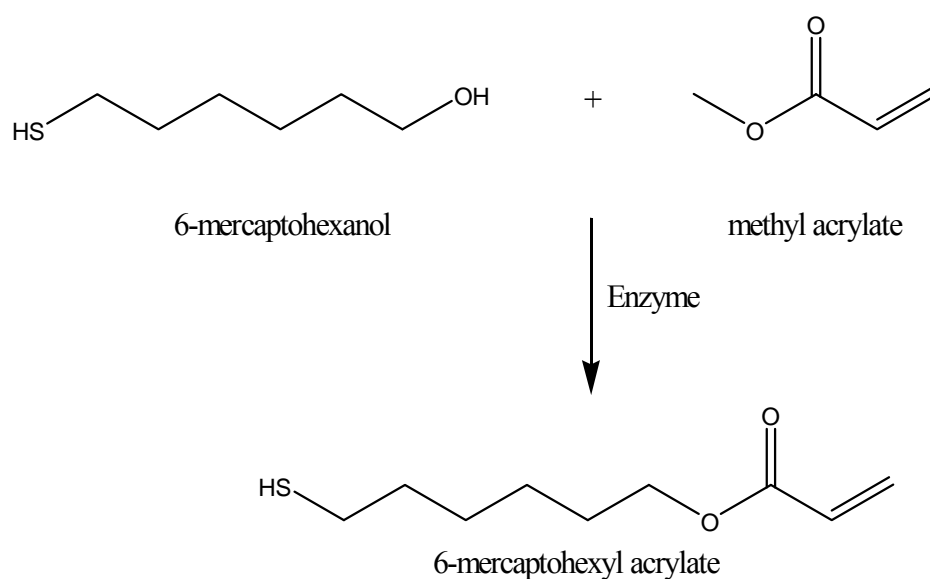


Figure 1.12: Transesterification of 6-mercaptohexanol with methyl acrylate catalyzed by enzyme.

1.5 Goals of this work

Improved acrylation of hydroxypropylcarbamate with methyl acrylate by rational protein design of *C. antarctica* lipase B

After screening of well-known enzymes for enzyme catalyzed transesterification of hydroxypropylcarbamate (hpc: 1hpc, 2hpc, 3hpc and 4hpc) with methyl acrylate by BASF, CALB exhibited the highest activity under the tested α/β -hydrolases. However, the wild-type CALB can not reach full conversion in short time. For industrial purposes it is necessary to increase the activity of the wild-type enzyme and at the same time decrease the enantioselectivity for full conversion of all *R* and *S* enantiomers. It is therefore anticipated that through our strategy including directed evolution and rational protein design CALB can show more activity towards the substrates (hpc), which is a mixture of secondary and primary alcohols containing *R* and *S* enantiomer respectively (**Figure 1.11**). For rational protein design

promising positions had to be identified by molecular modeling and substitutions realized by site-directed mutagenesis as well as constructed saturation mutagenesis libraries. For library screening purpose CALB variants were expressed in *E. coli* (Liu 2006). This expression system is more suitable for high-throughput requirements in terms of expression time and number of clones. But for a high expression level of recombinant protein *P. pastoris* (Cereghino and Cregg 2000) was selected as an ideal expression host of CALB. Plasmid DNAs had to be isolated from those *E. coli* clones with improved performance in enzyme activity and sequenced. *P. pastoris* had to be transformed with those plasmids and the corresponding transformants characterized with respect to activity in tributyrin hydrolysis, hydroxypropylcarbamates acrylate (hpcA) hydrolysis and stereoselectivity in hydrolysis of 1-phenylethylpropionate. In respect of acrylation of hydroxypropylcarbamate with methyl acrylate, lyophilized and immobilized CALB was supposed to be used as an almost water-free reaction system since the presence of water in reaction would disturb the conversion. Beside identification of appropriate mutants, a suitable carrier for catalyzer also plays an important role in reaction. It was found that CALB showed activity towards the substrate only by immobilization on hydrophobic carriers, e.g. on MP1000. Therefore, hydrophobic carriers MP1000 and HP20L had to be prepared for transesterification.

Cloning, expression and characterization of a cutinase (pCUTAB1) from *A. brassicicola* for transesterification of methyl acrylate with 6-mercaptohexanol

In order to find an enzyme which is able to catalyze transesterification of polyacrylate and amino- or mercaptoalcohol, screening of an enzyme library was performed by BASF. They found that a cutinase from *Humicola insolens* (*H. insolens*) showed the highest activity for such reaction. However, this cutinase is already patented and thus not economical for industrial applications. Therefore, our work was to find a cutinase, which shows homology to the *H. insolens* cutinase (Hi_Cutinase) and exhibits also activity for such reaction. However, work with polymers showed some practical difficulties in our preparative experiments. Transesterification of methyl acrylate as monomer with 6-mercaptohexanol was thus investigated primarily in our work. For seeking a proper enzyme, firstly, a homologous protein had to be found by sequence alignments. Secondly, this corresponding new gene had to be cloned and expressed in *P. pastoris*. Besides the following characterization of this protein, the transesterification of 6-mercaptohexanol with methyl acrylate also had to be analyzed using immobilized form of enzymes and compared with other possible enzymes like lipase CALB wild-type and variants.

2 Materials and Methods

2.1 Materials

2.1.1 Instruments

Instruments	Company
Agarose gel electrophoresis	
DNA Sub™ Cell , Mini Sub™ DNA Cell, Mini Sub™ Cell GT	BioRad
Video Copy Processor P66E	Mitsubishi
BWM 9X Monitor	Javelin Electronics
UV-lamp table	NEG-Biotech
Centrifuges	
Eppendorf Centrifuge 5417 C/5417 R (rotor F-45-30-11), Eppendorf Centrifuge 5810 R (rotor A-4-62)	Eppendorf, Hamburg, Germany
Sorvall® RC-5C PLUS (rotor SS-34)	Thermo Electron ORPORATION
Dispersion tools	
Ultra-turrax T25, ULTRA-TURRAX® T18 basis	Janke & Kunkel, Labortechnik, IKA®-WERK GMBH & CO.KG,
DNA sequencing	GATC Biotech AG, Konstanz, Germany
Electroporation	
Gene Pulser®, Pulse Controller	BioRad, Hercules, USA
Evaporation system	
Genevac Ez-2 & Ez-2 ^{Plus}	GENEVAC LTD. IPSWICH ENGLAND
GC/MS-QP2010	Shimadzu
Incubator	
Shaker for microtiter plates: 2-storey top frame, Incubator Hoods	Edmund Bühler GMBH, Hechingen, Germany
HT-Incubator shaking incubators	Infors AG, Bottmingen, Switzerland
WTE incubators	Binder, Tuttlingen, Germany
Thermomixer 5436/Comfort Heidolph REAX 3 orbital	Eppendorf, Hamburg, Germany

Materials and Methods

shaker	Heidolph, Kelheim, Germany
water bath (FIONS C1, B3)	Haake, Karlsruhe, Germany
cryostat RMS, RM6	MGW Lauda, Hannoversch-Muenden, Germany
Microscopy	
Mikroskop Axiolab	CarlZeiss
Microwave oven	
Micro-Chef FM A935	Moulinex
PCR-cycler	
Master Cycler Gradient	Eppendorf
Robocycle Gradient 40	Stratagene [®] , Amsterdam, Netherlands
pH-Meter	
Digital pH Meter pH525	WTW, Weilheim, Germany
pH-Stat	
Impulsomat 614, pH-Meter 620, Dosimat 665, Dosino 800, Titrande 842, Stirrer 801, pH-Meter 6.0262.100, and additional items.	Metrohm Ltd., Filderstadt, Germany
Programm for Titration with automation: tiamo [™]	
Program Version 1.X, Metrohm 8.101.0401	
Pipette	
0.5-10, 10-100, 100-1000, 500-2500, 500-5000 µl pipettes, 30-300 µl multichannel pipettes, multistepper pipettes	Eppendorf, Hamburg, Germany
Polyacrylamide gel electrophoresis (PAGE)	
Minigel-Twin G42	Biometra [®] , Goettingen, Germany
Power Pac 3000, power Pac 300 Model 583 Gel Dryer	BioRad, München, Germany
Protein purification	
Äkta explorer	Amersham Bioscience, Freiburg, Germany
Rotor	
F-45-30-11, A-4-62	Eppendorf, Hamburg, Germany
SS-34	Sorvall, Langenselbold, Germany
Scales	
Basic MC1 Research RC 210 D	Sartorius, Goettingen, Germany
Precision Advanced	OHAU [®] , Florham Park, N.J.,

	USA
Sonifier	
Sonifier 250	Branson, Dietzenbach, Germany
Sonorex Super RK 514 H	Brandelin, Germany
Spectrophotometer	
Ultraspec 3000 UV/Visible Spectrophotometer	Amersham Biotech, Freiburg, Germany
Ultrafiltration	
Amicon 8050, 80200	Millipore, Bedford, USA
Thermomixer	
Thermomixer 5436	Eppendorf, Hamburg, Germany
Vacuum concentrator	
SpeedVac Concentrator 5310	Eppendorf, Hamburg, Germany
Vortex	
Vortex Genie 2	Scientific Industries

2.1.2 Consumables

Consumables	Company
filter paper	Biorad, Hercules, USA
Sequi-Blot™ PVDF membrane	
Zeta-Probe® GT Genomic Tested Blotting Membrane	
pipette tips, 0.5, 1.5, 2.0 ml reaction tubes	Eppendorf, Hamburg, Germany
PS microplate 96 well	Greiner Bio-one, Frickenhausen, Germany
pipette tips, 15, 50 ml conical tubes	Greiner, Nuertingen, Germany
ultrafiltration membranes (10 kDa, 44.5 mm, 63.5 mm)	Millipore, Bedford, USA
sterile filters	Millipore, Molsheim, France

2.1.3 Databases and programs

Application/URL	Database/Programme
<i>Sequence query</i>	
http://www.ebi.ac.uk/embl/	EMBL Data Base

Materials and Methods

http://www.ncbi.nlm.nih.gov/Database/index.html	NCBI Data Base
<i>Sequence alignment</i>	
http://bips.u-strasbg.fr/fr/Documentation/ClustalX/	ClustalX
http://igs-server.cnrs-mrs.fr/Tcoffee/tcoffee_cgi/index.cgi	T-Coffee
<i>Structure search</i>	
http://www.rcsb.org/	Protein Data base
Expasy.org/spdbv	SwissPDBViewer
<i>Patent search</i>	
http://gb.espacenet.com/	Europe's network of patent databases
<i>Sequence similarity search</i>	
http://www.ncbi.nlm.nih.gov/blast/Blast.cgi	BLAST
<i>sequence and structure of hydrolase</i>	
http://www.led.uni-stuttgart.de/	Lipase Engineering Database
<i>Signal peptide cleavage site prediction</i>	
http://www.cbs.dtu.dk/services/SignalP/	SignalP 3.0 server
<i>N-Glycosylation sites prediction</i>	
http://www.cbs.dtu.dk/services/NetNGlyc/	The NetNglyc 1.0 server
<i>Protein hydropathy plot</i>	
http://www.vivo.colostate.edu/molkit/hydropathy/	hydropathy scale
<i>Oligonucleotide design and analysis tools</i>	
http://eu.idtdna.com/analyzer/applications/oligoanalyzer/default.aspx	OligoAnalyzer 3.1 from Integrated DNA Technologies
<i>Codon usage search</i>	
http://www.kazusa.or.jp/codon/	Codon Usage Database
<i>Homology Protein Modelling</i>	
http://swissmodel.expasy.org/	SWISS-MODEL
<i>Computer analysis of DNA sequences and the deduced amino acid sequences</i>	
http://products.invitrogen.com/ivgn/en/US/adirect/invitrogen?cmd=catProductDetail&productID=12605103	Vector NTI Advance 10.3 from Invitrogen Corporation. Software SeqMan™ II and Clone Manager Version 7 for Windows 95
<i>Visualization of Protein 3 D Structure</i>	
http://pymol.sourceforge.net/	PyMOL™ 0.99 rc1, DeLano

Scientific LLC. (DeLano
2002)

2.1.4 Chemicals

Chemicals	Company
Accurel microporous polymers MP 1000 (<1500 μm)	Akzo
PAGE-PLUS Concentrate	Amresco, Solon, USA
HP20L, hydroxypropylcarbamate (Carbalink) hydroxypropylcarbamate acrylate	BASF AG, Ludwigshafen, Germany
BioRad protein assay kit, Precision Plus Protein™ all Blue Standard	BioRad Laboratories, Richmond, USA
magnesium chloride, magnesium sulfate anhydride, manganese chloride, PageRuler™ Unstained Protein Ladder	Fermentas, St. Leon-Rot
agar, ammonium chloride, ammonium hydroxide, ammonium peroxy-disulphate (APS), ammonium sulphate, ampicillin sodium salt, bromphenol blue, calcium chloride dehydrate, cobalt chloride, Coomassie Brilliant Blue R-250, diethyl ether, N,N'- dimethyl formamide (DMF), dimethyl sulphoxide (DMSO), di-potassium hydrogen phosphate, di- sodium hydrogen phosphate dehydrate, ethanol, ethidiumbromide, ethyl butyrate, ethyl caprylate, ethylenediamine tetra-acetic acid (EDTA), formamide, glycine, gum arabic, hydrochloric acid, isopropyl- β -D- thiogalactoside (IPTG), lysozyme from hen egg white, magnesium chloride hexahydrate, magnesium sulphate anhydrous, manganese chloride, 2-mercaptoethanol, methyl acetate, methyl propionate, methyl butyrate, methyl caproate, methyl caprylin, methyl decanoate, methyl laurate, methyl myristate, 3-(morpholino) propanesulfonic acid (MOPS), nickel chloride, olive oil, 1-phenylethylpropionate, potassium acetate, potassium chloride, potassium dihydrogen phosphate, <i>p</i> -nitrophenol (<i>p</i> NP), <i>p</i> NP butyrate (<i>p</i> NPB), <i>p</i> NP	Fluka Chemie, Buchs, Switzerland

palmitate (<i>p</i> NPP), rubidium chloride, sorbitol, sodium acetate anhydrous, sodium chloride, sodium dihydrogen phosphate, sodium dodecylsulfate (SDS), sodium hydroxide, sodium molybdat-dihydrat, sodium salt hydrate, tetramethylethylenediamine (TEMED), tryptone, yeast extract, zinc sulphate heptahydrate	
agarose, standard for agarose gel (1 kb, 1 kb plus ladder), urea	Gibco BRL GmbH, Eggenstein , Germany
ZeoZin™	Invitrogen, Leek, Niederlande
manganese sulphate monohydrate, water HPLC-pure	Merck, Darmstadt, Germany
desoxynucleotide triphosphate (dNTPs, 100 mM)	Promega, Madison, USA
acetic acid 100%, acetone, glycerol, n-hexane, methanol, tris-(hydroxymethyl)-aminomethane (Tris), Tween 20	Roche, Mannheim, Germany
Roti®-Phenol/Chloroform, complete™, Roti®-Mark Standard	Roth, Karlsruhe, Germany
Casein, Triton-X-100, 16-Hydroxyhexadecanoic acid	Sigma-Aldrich, Taufkirchen, Germany

2.1.5 Enzymes

Enzyme	Company
<i>Taq</i> DNA polymerase	Eppendorf, Hamburg, Germany
Calf intestinal alkaline phosphatase (CIAP), RNase-Free DNase, <i>DpnI</i> , <i>EcoRI</i> , <i>HindIII</i> , <i>NdeI</i> , <i>NotI</i> and <i>SacI</i> restriction enzyme, <i>pfu</i> DNA polymerase, <i>Taq</i> DNA polymerase, T4 DNA ligase	Fermentas, St. Leon-Rot, Germany
Lysozyme, proteinase K	Fluka Chemie, Buchs Schweiz
Super Script™ III Reverse transcriptase, RNase OUT™ recomb. RNase Inhibitor	Invitrogen
QuikChange® Multi enzyme blend	Stratagene Products Division, Agilent Technologies, United States and Canada
RNaseH, Reverse Transcriptase	QIAGEN, Hilden, Germany
Lyticase	Sigma

2.1.6 Oligonucleotides and plasmids

Primers	Application and Sequence (5' to 3')
	<i>Sequencing of CALB in pColdIII construct</i>
pCold_fw	ACGCCATATCGCCGAAAGG
pCold_rev	GGCAGGGATCTTAGATTCTG
	<i>Subcloning of CALB from PUC18 vector in pColdIII vector</i>
CALB_NdeI_fw ^a	CGATTCATATGCTACCTTCCGGTTCGGACC
CALB_EcoRI_rev ^a	CCTTAAGAATTCTCAGGGGGTGACGATGCC
	<i>Subcloning of CALB from pColdIII vector in pPICZαA</i>
CALB_EcoRI_fw ^a	GATGAATTCACTACCTTCCGGTTCGGACC
CALB_NotI_rev ^a	TTTTCTTTTGGCGCCGCTCAGGGGGTGACGATGCC
	<i>saturation mutagenesis at position L277, L278 and L281</i>
CALB_SM277_278_281_fw ^a	GGTCGCCCGGGCTGCGNNBNNBGCGCCGNNBGTGCAG CCATCGTGGCG
CALB_SM277_278_281_rev ^a	CGCCACGATGGCTGCAGCVNNCGGCGCVNNVNNCGCAG CCGCGGCGACC
	<i>saturation mutagenesis at position W104</i>
CALB_W104X_fw ^a	CAAGCTTCCCCTGCTCACCNNTCCCAGGGTGGTCTGG
CALB_W104X_rev ^a	CCAGACCACCCTGGGAWNNGGTGAGCACGGGAAGCTTG
	<i>saturation mutagenesis at position L278</i>
CALB_L278X_fw ^a	GCTGCGCTCNNKGCGCCGGCGGCTGCAGCCATC
CALB_L278X_rev ^a	GCCGCCGGCGCMNNGAGCGCAGCCGCGGCGACC
	<i>Site-directed mutagenesis</i>
CALB_W104F_fw ^a	CTCACCTTTTCCCAGGGTGG
CALB_W104F_rev ^a	CTGGGAAAAGGTGAGCACG
CALB_T42A_fw ^a	ACCGGCGCTACAGGTCC
CALB_T42A_rev ^a	CCTGTAGCGCCGGTTC
CALB_T42AS47A_fw ^a	ACCGGCGCTACAGGTCCACAGGCATTCGACTCG
CALB_T42AS47A_rev ^a	GTCGAATGCCTGTGGACCTGTAGCGCCGGTTC
CALB_S47A_fw ^a	CACAGGCATTCGACTCG
CALB_S47A_rev ^a	TCGAATGCCTGTGGACC
CALB_L278A_fw ^a	GCTGCGCTCGCAGCGCCGGCGGCTGCAGCCATC
CALB_L278A_rev ^a	GCCGCCGGCGCTGCGAGCGCAGCCGCGGCGACC
CALB_L278V_fw ^a	TGCGCTCGTAGCGCCGGCGGCTG
CALB_L278V_rev ^a	CGGCGCTACGAGCGCAGCCGC

Materials and Methods

	<i>Sequencing of gene in pPICZαA</i>
5' AOX	GACTGGTTCCAATTGACAAGC
3' AOX	GCAAATGGCATTCTGACATCC
	<i>Cloning of CUTAB1 in pPICZαA</i>
<i>CUTAB1_EcoRI_fw</i> ^a	CCGGCAGAATTCATGATGAACCTCAACTTGTTACTCTC
<i>CUTAB1_NotI_rev</i> ^a	CATTGCGGCCGCCTATGCTGAGTC
Plasmids	Reference/Company
pColdIII	TaKaRa BIO EUROPE, Japan (Goldstein et al. 1990)
pPICZαA	Invitrogen, Leek, Niederlande (Cereghino and Cregg 2000)

^a Restriction enzyme sites or site of mutagenesis are underlined. N is designated as A, T, C or G; B as C, G or T, V as G, C or A, W as A or T; K as G or T; M as A or C.

2.1.7 Strains

Species	Strain	Genotype/Features	Company
<i>Escherichia coli</i>	DH5α	F ⁻ φ80 <i>lacZ</i> Δ <i>M15</i> Δ(<i>lacZYA-argF</i>)U169 <i>deoR recA1 endA1 hsdR17</i> (r _k ⁻ , m _k ⁺) <i>phoA supE44 λ</i> ⁻ <i>thi-1 gyrA96 relA1</i>	Clontech, Heidelberg, Germany
<i>Escherichia coli</i>	Origami [®] B	F ⁻ <i>ompT hsdS_B</i> (r _B ⁻ m _B ⁻) <i>gal dcm lacY1 aphC gor522::Tn10 trxB</i> (Kan ^R , Tet ^R)	Novagen, Darmstadt, Germany
	XL10-Gold ultracompetent cells	Tet ^r Δ(<i>mcrA</i>)183 Δ(<i>mcrCB-hsdSMR-mrr</i>)173 <i>endA1 supE44 thi-1 recA1 gyrA96 relA1 lac Hte</i> [F' <i>proAB lacI^qZΔM15 Tn10</i> (Tet ^r) Amy Cam ^r]	Stratagene Products Division, Agilent Technologies, United States and Canada
<i>Pichia pastoris</i>	X-33	wild-type	Invitrogen, Leek, Niederlande
<i>Alternaria brassicicola</i>	DSM 62008	wild-type	DSMZ, Braunschweig, Germany

2.1.8 Commercial Kits

Kit	Company
QIAquick [®] Gel Extraction Kit	QIAGEN, Hilden, Germany
QIAquick [®] PCR Purification Kit	
Plasmid Midi Kit	
RNasy [®] Plant Mini Kit	
Super Script [™] III RT	Invitrogen
QuikChange [®] Site-Directed Mutagenesis Kit	Stratagene Products Division, Agilent Technologies, United States and Canada
QuikChange [®] Multi Site-Directed Mutagenesis Kit	
GenElute [™] Plasmid Miniprep Kit	Sigma-Aldrich, Taufkirchen, Germany

2.1.9 Commonly used buffer and media

Luria-Bertani Medium (LB-Medium)

Tryptone	10 g/l
Yeast Extract	5 g/l
NaCl	5 g/l

Autoclave for 20 minutes. Let cool to ~55°C and add desired antibiotics at this point. Store at room temperature or at +4°C.

LB-Agar Plates

LB-Medium	
Agar	15 g/l

Autoclave for 20 minutes. Let cool to ~55°C and add desired antibiotics at this point. Pour into 10 cm petridishes, store at +4°C.

LB-Tributylin-Agar Plates

LB-Medium	
Agar	15 g/l
Tributylin	1%

Homogenize for 10 min using Ultraturrax (24 000 rpm). Autoclave for 20 minutes. Let cool to ~ 55°C and add desired antibiotics at this point. Pour into 10 cm petridishes, store at +4°C.

Yeast Extract Peptone Dextrose Medium (YPD)

Yeast extract	10 g/l
Peptone	20 g/l
H ₂ O	800 ml
Autoclave for 20 minutes. Add 200 ml sterile 10% D-glucose stock solution	

YPDS + Zeocin™ Agar Plates

Yeast extract	10 g/l
Peptone	20 g/l
Sorbitol	182.2 g/l
Agar	15 g/l
H ₂ O	800 ml
Autoclave for 20 minutes. Add 200 ml sterile 10% D-glucose stock solution. Cool solution to ~60°C and add 1.0 ml of 100 mg/ml Zeocin™. Store YPDS plates containing Zeocin™ at +4°C in the dark. The shelf life is one to two weeks.	

Buffered Glycerol-complex Medium (BMGY)

Yeast extract	10 g/l
Peptone	20 g/l
H ₂ O	800 ml
Autoclave for 20 minutes. Cool to room temperature, then add the following and mix well.	
1 M potassium phosphate buffer, pH 6.0 (autoclaved)	100 ml
10% Glycerol (autoclaved)	100 ml
Store media at +4°C. The shelf life of this solution is approximately two months.	

Buffered Methanol-complex Medium (BMMY)

Yeast extract	10 g/l
Peptone	20 g/l
H ₂ O	900 ml
Autoclave for 20 minutes. Cool to room temperature, then add the following and mix well.	
1 M potassium phosphate buffer, pH 6.0 (autoclaved)	100 ml
Store media at +4°C. The shelf life of this solution is approximately two months.	
Methanol (add before use)	0.5% (v/v)

Corn Meal Medium

Corn meal	50 g/l
H ₂ O	800 ml
Leave overnight in the refrigerator. Heat at 60°C for 1 h. Filter and make up volume to 1 l. Autoclave for 20 minutes on liquid cycle. Store media at +4°C.	

Corn Meal Agar Plates

Corn meal	50 g/l
H ₂ O	800 ml
Leave overnight in the refrigerator. Heat at 60°C for 1 h. Filter and make volume up to 1 l.	
Agar	10 g/l
Heat to dissolve agar, then autoclave. Store agar plates at +4°C.	

Modified CZapek's medium (Trail and Koeller 1993; YAO and Köller 1994)

NaNO ₃	0.6 g/l
K ₂ HPO ₄	0.6 g/l
MgSO ₄ (anhydrous)	0.2 g/l
KCl	0.2 g/l
FeSO ₄ ·7H ₂ O	0.01 g/l
H ₂ O	to 1000 ml
Autoclave for 20 minutes. Cool to room temperature. Store at +4°C.	

2.1.10 Stock solutions

Stock solution	Amount
Ampicillin	100 mg/ml
Zeocin™	100 mg/ml
IPTG	1 M
Dissolve appropriate amount in water and filter sterilize. Store at -20°C.	
Glycerol	10%
Mix 100 ml of glycerol with 900 ml of water. Sterilize either by filtering or autoclaving. Store at room temperature. The shelf life of this solution is greater than one year.	
D-glucose	10%
Dissolve 100 g of D-glucose in 1000 ml of water. Autoclave for 20 minutes or filter sterilize. The shelf life of this solution is approximately one year.	
Potassium phosphate buffer, pH 6.0	1 M
Combine 132 ml of 1 M K ₂ HPO ₄ , 868 ml of 1 M KH ₂ PO ₄ and confirm that the pH = 6.0±0.1 (if the pH needs to be adjusted, use phosphoric acid or KOH). Sterilize by autoclaving and store at room temperature. The shelf life of this solution is greater than one year.	

2.2 Methods

2.2.1 Molecular biological methods

2.2.1.1 Purification of total RNA from filamentous fungi

In order to get corresponding mRNA of cutinase pCUTAB1, conidia of *A. brassicicola* obtained from 5-day-old cultures grown on corn meal agar or the corn meal medium was added to 100 ml modified Czapek's medium supplemented with 25 mg cutin monomer (16-hydroxyhexadecanoic acid (Trail and Koeller 1993; Fan and Köller 1998)). The culture was incubated at room temperature for 24 h or 36 h without shaking; the culture was harvested by centrifugation at 20800 × g for 1 min. For purification of total RNA and the following cloning and expression of *CUTAB1* in *P. pastoris*, 100 mg cell pellet from the centrifugation was frozen at -80°C for a few minutes, put in liquid nitrogen, grinded to powder, and the following steps were carried out according to the RNasy[®] Plant Mini Kit (QIAGEN) protocol.

2.2.1.2 Isolation of plasmid DNA from *E. coli* and DNA sequencing

Minipreparation for small amount plasmid isolation

This method based on alkaline lysis (Birnboim and Doly 1979) allows isolation of highly pure plasmid DNA for sequencing or enzymatic digestion. Spin Miniprep kits from Qiagen or Sigma were used. After complete lysis of the cells with SDS, the RNA is hydrolyzed with NaOH and RNaseI. Plasmid DNA after denaturation by NaOH is immediately renatured after addition of neutralization buffer whereas genomic DNA is precipitated. After centrifugation, the plasmid DNA in the supernatant is purified by ion-exchange chromatography.

For a typical plasmid minipreparation 2 ml overnight culture was harvested by centrifugation. Plasmid DNA isolation from the resulting cell pellet was performed according to the protocol of the manufacturer.

Midipreparation for large amount plasmid isolation

In order to isolate large amount of highly pure plasmid DNA, a midipreparation was performed. This method is also based on alkaline lysis, followed by an ion-exchange chromatography and an isopropanol precipitation.

For each midipreparation, 50 ml overnight culture was harvested by centrifugation. The Midiprep kit from Qiagen was used. The plasmid DNA isolation was carried out according to the protocol of the manufacturer.

DNA sequencing

After mini-preparation of DNA, 30 μ l sample with plasmid DNA (30-100 ng/ μ l) was sequenced by GATC Biotech AG.

2.2.1.3 Quantification of RNA or DNA

The RNA or DNA concentration can be determined by spectrophotometric measurement at 260 nm and 280 nm. The adsorption (OD) at 260 nm can be used to calculate the concentration of nucleic acid in the sample. An OD of 1 corresponds to 50 μ g/ml for double stranded DNA, 37 μ g/ml for single stranded DNA and 40 μ g/ml for RNA. Proteins in general have considerably lower A_{280} than nucleic acids on an equivalent weight basis. Thus, even a small increase in the A_{280} relative to A_{260} (or a lowering of the A_{260}/A_{280} ratio) can indicate severe protein contamination. The ratio of A_{260}/A_{280} gives an estimate of the purity of the DNA. Pure DNA and RNA preparations have a ratio of ~ 1.8 and 2.0 respectively. If there is contamination with protein or phenol, the ratios will be lower than 1.8.

2.2.1.4 Polymerase chain reaction

The polymerase chain reaction (PCR) was used for amplification of the specific DNA fragments of the known sequences (Mullis et al. 1986). Two oligonucleotides are used as primers to determine the DNA fragment to be amplified. The DNA template is denatured by heating to break the hydrogen bonds between the DNA strands. When the solution cools to the annealing temperature, which was dependent on the length of synthetic primer and calculated by OligoAnalyzer 3.1 (2.1.3), the primers bind to their target sequence, and DNA polymerase extends the annealed primers by joining the free nucleotide bases to the primers. For most DNA polymerase, 1000 bp are synthesized within 1 min. The product of the last reactions can be used as template for the next amplification. Therefore, the reaction is repeated, resulting in an exponential increase of the desired DNA product.

Standard protocol for PCR-amplification

Component of Standard PCR	Volume
10 x polymerase buffer	5 μ l
dNTPs (mixture, 2.5 mM of each one)	4 μ l
Template DNA (20-200 ng/ μ l)	2 μ l
Sense-primer (5' \rightarrow 3') (10 pmol/ μ l)	2 μ l
Antisense-primer (3' \rightarrow 5') (10 pmol/ μ l)	2 μ l
DNA-polymerase (2 U/ μ l)	1 μ l
MgCl ₂ (25 mM)	2 μ l
dd H ₂ O	32 μ l
Total volume	50 μ l

Temperature Program of Standard PCR

Step	Temperature ($^{\circ}$ C)	Time (min)	Cycle
Denaturation	95	4	1
Denaturation	95	1	} 25
Annealing	50	1	
Extension	72	1	
Final extension	72	4	1

2.2.1.5 cDNA synthesis

Reverse transcriptase, a RNA-dependent DNA polymerase (QIAGEN), can synthesize cDNA *in vitro* from a mRNA template. Just like other polymerases, a short double-stranded fragment is needed at the 3' end of the mRNA, which acts as a starting point for the polymerase. Therefore a short complementary synthetic oligonucleotide (oligo dT primer) is added to the mRNA template to form a polyT-polyA hybrid with the polyA-tail, which is present at the 3' end of most eukaryotic mRNAs. A complementary DNA is synthesized to the mRNA template by the reverse transcriptase, together with all 4 deoxynucleotide triphosphates, magnesium ions and at neutral pH.

For cDNA synthesis in our case, 5 μ l (0.75 μ g) RNA with a concentration of 146 μ g/ml was mixed with 1 μ l 50 mM Oligo (dT)₁₂₋₁₈. dd H₂O was added to the mixture to a total volume of 13 μ l. This solution was incubated at 65°C for 5 min, on ice for 1 min, and then centrifuged briefly at 20800 \times g. The following components were added to this solution.

Component*	Volume
5 x First-Strand Buffer	4 μ l
0.1 M DTT	1 μ l
RNase OUT™ Recomb. RNase Inhibitor	1 μ l
SuperScript III RT (Reverse Transcriptase)	1 μ l

* All components were supplied with SuperScript III RT. Reverse Transcriptase (Invitrogen).

The total mixture was gently pipetted up and down, incubated at 50°C for 30-60 min, and then 15 min at 70°C. In order to remove RNA, 1 μ l *E. coli* RNaseH was added to this mixture and incubated at 37°C for 20min.

PCR for *CUTABI* synthesis from cDNA

CUTABI was synthesized from cDNA according to the above stated principle of standard PCR. The only difference was the use of singlestranded DNA.

Protocol of PCR for *CUTAB1* synthesis from cDNA

Component	Volume
10 x polymerase buffer	5 μ l
dNTPs (mixture, 2.5 mM of each one)	2 μ l
cDNA (120 ng/ μ l)	2 μ l
Sense-primer (5'→3') (10 pmol/ μ l)	2 μ l
Antisense-primer (3'→5') (10 pmol/ μ l)	2 μ l
<i>Pfu</i> DNA-polymerase (2 U/ μ l)	1 μ l
MgCl ₂ (25 mM)	1.5 μ l
dd H ₂ O	34.5 μ l
Total volume	50 μ l

Temperature Program

Step	Temperature (°C)	Time (min)	Cycle
Denaturation	95	2	1
Denaturation	95	1	} 35
Annealing	55	1	
Extension	72	2	
Final extension	72	4	1

2.2.1.6 Mutagenesis by PCR

2.2.1.6.1 Error-prone PCR

Error-prone PCR (epPCR) is a technique used to generate variants with random mutations (Leung 1989; Cadwell and Joyce 1992). Normally *Taq* polymerase is used because of its naturally high error rate, with errors biased towards AT to GC changes. Error-prone PCR reactions commonly contain higher concentrations of MgCl₂ than in basic PCR, in order to stabilize non-complementary basepairs. Using unequal dNTPs and an addition of MnCl₂ and dITP increases the error-rate in PCR. Therefore, a plasmid carrying the *CALB* gene was used as DNA template. Original *Taq*-polymerase buffer was used. The components of the reaction were mixed together according to the following recipe.

Component	Volume
10 x polymerase buffer	5 μ l
dNTPs *	4 μ l
Template DNA (20-200 ng/ μ l)	1 μ l
Sense-primer (5' \rightarrow 3') (100 pmol/ μ l)	1 μ l
Antisense-primer (3' \rightarrow 5') (100 pmol/ μ l)	1 μ l
<i>Taq</i> DNA-polymerase (2 U/ μ l)	1 μ l
MgCl ₂ (25 mM)	3 μ l
MnCl ₂ (5 mM)	0.5 μ l
dITP (5 mM)	0.5 μ l
dd H ₂ O	33 μ l
Total volume	50 μ l

* Unequal mixture of dATP, dGTP, dCTP and dTTP: end concentration of 0.8 mM

The PCR reaction was carried out in a thermal cycler using the following program.

Temperature Program			
Step	Temperature ($^{\circ}$ C)	Time (min)	Cycle
Denaturation	95	4	1
Denaturation	95	1	} 30
Annealing	50	1	
Extension	72	1.5	
Final extension	72	4	1

2.2.1.6.2 Single site-directed mutagenesis (QuikChange[®])

Single site-directed mutagenesis (**Figure 2.1**) is a method in which a mutation is created at a defined position in a DNA molecule with known sequence. It is carried out by using PCR. Usually plasmids containing a wild-type gene are used as template and two synthetic complementary oligonucleotide primers containing the desired mutation. Because the newly synthesized DNA strands are based on the primers, a mutated plasmid is produced. To avoid unexpected mutations in the plasmid, a polymerase with proofreading ability e.g. *Pfu* polymerase is used in the PCR. In order to remove wild-type plasmids, the PCR product is treated with *DpnI*, which digests specifically methylated DNA. DNA isolated from several *E. coli* strains, e.g. DH5 α , is methylated, in contrast to the PCR synthesized DNA.

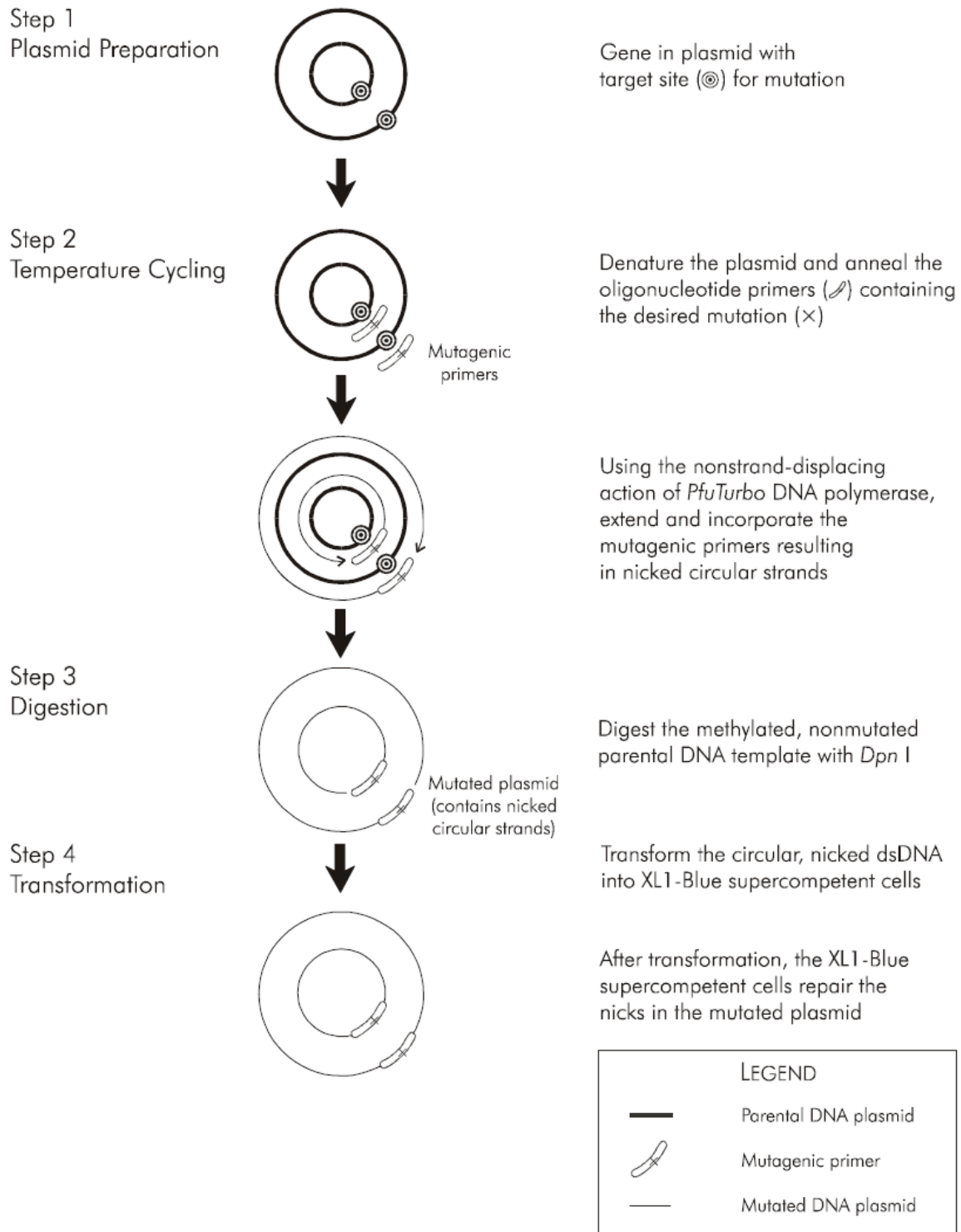


Figure 2.1: Overview of the QuikChange[®] Site-Directed Mutagenesis method (from instruction of QuikChange[®] Multisite-directed Mutagenesis Kit).

For site-directed mutagenesis, plasmid DNA was used as template DNA. The PCR components of the reaction mixture were pipetted together according to the following recipe.

PCR Component for Quik Change [®] PCR	Volume
10 x PCR buffer	5 µl
dNTPs (mixture, 2.5 mM of each one)	4 µl
1. PCR-primer (5'→3') (10 pmol/ µl)	2 µl
2. PCR-primer (3'→5') (10 pmol/ µl)	2 µl
Template DNA (20-200 ng/ µl)	2 µl
<i>Pfu</i> DNA-polymerase (2 U/µl)	1 µl
MgCl ₂ (25 mM)	2 µl
dd H ₂ O	33 µl
Total volume	50 µl

The PCR reaction was carried out in a thermal cycler using the following program.

Temperature Program for Quik Change [®] PCR			
Step	Temperature (°C)	Time (min)	Cycle
Denaturation	95	2	1
Denaturation	95	1	} 16-20 ^c
Annealing	48 ^a	1	
Extension	72	7-11 ^b	
Final extension	72	4	1

^a The annealing temperature was dependent on the length of synthetic primer and calculated by OligoAnalyzer 3.1 (2.1.3).

^b The synthesis time was based on the size of the plasmid. *Pfu* DNA- polymerase needs 2 min per 1000 bases.

^c The cycle times were based on the kind of the desired mutation. For one base change, 16 cycles were needed, on the other hand, 20 cycles for single-change of amino acids.

2.2.1.6.3 Sequential introduction of mutations

PCR was performed as the above stated single site-directed mutagenesis (QuikChange[®]) using the template (pColdIII_*CALB_wild-type*) and the primers (*CALB_W104X_fw* and *CALB_W104X_rev*). PCR products were treated with *DpnI* for 3 h. After electroporation of the PCR products in Origami[®] B competent cells, the plasmid mixture

(pColdIII_CALB_W104X) was extracted from the overnight culture in 5 ml LB medium with 100 µg/ml ampicillin diluted from stock solutions (2.1.10). PCR was performed again using the plasmid mixture (pColdIII_CALB_W104X) as template and primers (L278X). After electroporation of the PCR products in Origami[®] B and cultivation on tributyrin LB agar plates with ampicillin, colonies with halos were picked in microtiter plate and random 10 colonies were sequenced after plasmid extraction.

2.2.1.6.4 Multi site-directed mutagenesis (QuikChange[®])

The QuikChange[®] Multi Site-Directed Mutagenesis Kit offers a rapid and reliable method for site-directed mutagenesis of plasmid DNA at up to five different sites simultaneously. A single mutagenic oligonucleotide is required to mutagenize each site, using a double-stranded DNA template following the one-day, three-step procedure outlined in **Figure 2.2**. This technique allows oligo-mediated introduction of site-specific mutations into virtually any double-stranded plasmid DNA.

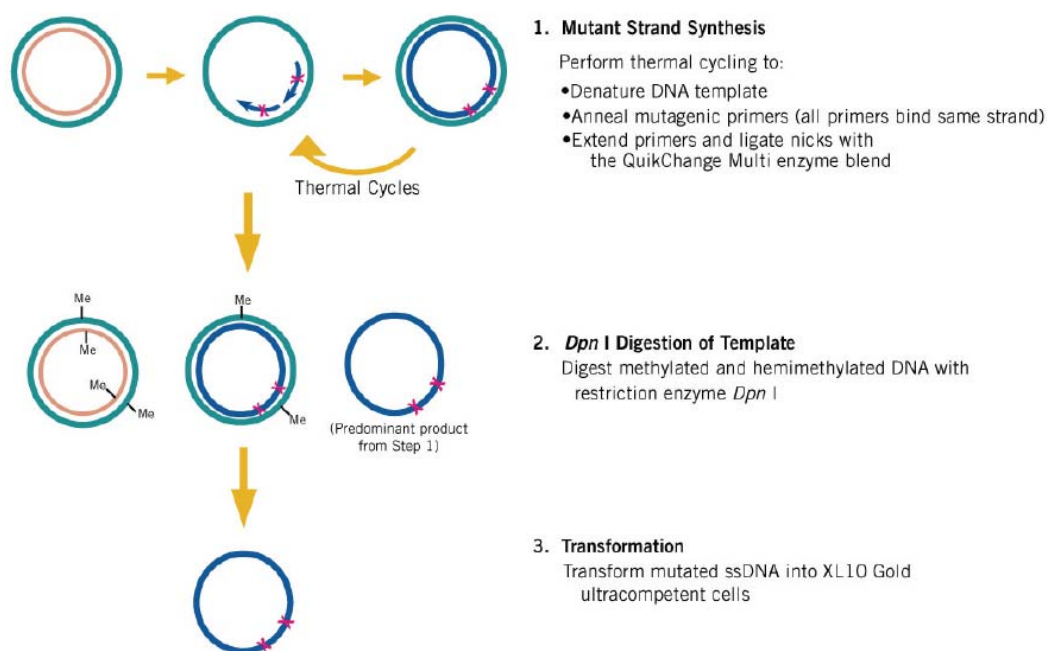


Figure 2.2: Overview of the QuikChange[®] Multi Site-Directed Mutagenesis method (from instruction of QuikChange[®] Multisite-directed Mutagenesis Kit).

PCR Component for Multi-site QuikChange [®] PCR	Volume
10 x QC-Multi reaction buffer	2.5 µl
dNTP Mix ^a	1 µl
W104X primer (5'→3') (10 pmol/ µl)	1 µl
L278X primer (3'→5') (10 pmol/ µl)	1 µl
Template DNA (pColdIII_ <i>CALB_wild-type</i>) (243 ng/ µl)	0.5 µl
QuikChange [®] Multi enzyme blend (2.5 U/µl)	1 µl
dd H ₂ O	18 µl
Total volume	25 µl

^a The composition of the reaction buffer and of the dNTP mix in the Kit is proprietary.

The PCR reaction was carried out in a thermal cycler using the following program.

Temperature Program for Multi-site QuikChange [®] PCR			
Step	Temperature (°C)	Time (min)	Cycle
Denaturation	95	1	1
Denaturation	95	1	30
Annealing	55	1	
Extension	65	12	
Final extension	65	12	1

2.2.1.7 Colony PCR

The colony PCR is performed after a transformation to screen colonies containing the desired plasmid. Primers are used to generate a PCR product of expected size. Thus, any colony which gives rise to an amplification product of the expected size is likely to contain the desired DNA sequence.

2.2.1.7.1 Bacterial Colony PCR

Colony PCR mixture was prepared on ice as in the following recipe, always adding polymerase last. After beginning PCR program, the block was heated to 95°C, and then “PAUSE” was pressed. Colonies were selected and numbered on the bottom side of the plate. To each cold PCR tube lid containing a 25 µl PCR reaction, in which a small amount of colony was added. The mixture was pipetted up and down. After good mixing, the mixture

was twirled in the tube. This was done for all colonies to be analyzed, the plate was covered with microseal film and the reaction was proceeded by pressing “PAUSE” again.

PCR mixture	Volume
10 x polymerase buffer	2.5 μ l
dNTPs (mixture, 2.5 mM of each one)	1 μ l
Sense-primer (5'→3') (10 pmol/ μ l)	1 μ l
Antisense-primer (3'→5') (10 pmol/ μ l)	1 μ l
<i>Taq</i> DNA-polymerase (2 U/ μ l)	0.2 μ l
dd H ₂ O	19.3 μ l
+ Colony	
Total volume	25 μ l

PCR Program			
Step	Temperature (°C)	Time (sec)	Cycle
Denaturation	95	180	1
Denaturation	95	40	} 25
Annealing	50	60	
Extension	72	240	
Final extension	72	60	1

2.2.1.7.2 Yeast Colony PCR

10 μ l of a *P. pastoris* culture was placed into a 1.5 ml microcentrifuge tube. For relatively dense cultures, 1 μ l of the culture was diluted with 9 μ l water. Alternatively, a single colony was picked and resuspended in 10 μ l of water. 5 μ l of a 5 U/ μ l solution of lyticase was added and the mixture was incubated at 30°C for 10 min. The sample was frozen at -80°C for 10 min or immersed in liquid nitrogen for 1 min. A 50 μ l PCR mixture was set up for a hot start PCR as the following:

PCR mixture	Volume
10 x polymerase buffer	5 μ l
dNTPs (mixture, 2.5 mM of each one)	1 μ l
5' AOX1 primer (10 pmol/ μ l)	1 μ l
3' AOX1 primer (10 pmol/ μ l)	1 μ l
dd H ₂ O	34 μ l
MgCl ₂ (25 mM)	2 μ l
Cell lysate	5 μ l
Total volume	50 μ l

This PCR mixture was placed in the thermocycler and incubated at 95°C for 5 minutes. 1 μ l of a 5 U/ μ l solution of *Taq* polymerase was added. The reaction was performed using the following program.

PCR Program			
Step	Temperature (°C)	Time (min)	Cycle
Denaturation	95	1	} 30
Annealing	48	1	
Extension	72	3	
Final extension	72	1	1

2.2.1.8 DNA digestion with restriction endonucleases

Double-stranded DNA was digested by restriction endonuclease at specific positions, known as recognition sequences. Many restriction enzymes produce sticky ends of DNA molecules, which can be further ligated by T4 ligase to other DNA molecules with the same sticky ends. 5 μ l 10 x restriction enzyme buffer was mixed with 0.1-5 μ g purified DNA and 2 U restriction endonuclease, and then water was added to a final volume of 50 μ l and mixed gently. The reaction mixture was then incubated at 37°C for 1 h. To inactivate the restriction endonuclease, the reaction mixture was incubated at 80°C for 20 min. Afterwards, the digested DNA was purified by agarose gel extraction. The following tables show typical reaction mixtures for digestion of pPICZ α A and insert.

Component of vector digestion	Volume
DNA (20-200 ng/ μ l)	20 μ l
10 x O-buffer	5 μ l
<i>EcoR</i> I (1-10 U/ μ l)	2 μ l
<i>Not</i> I (1-10 U/ μ l)	2 μ l
dd H ₂ O	21 μ l
Total volume	50 μ l

Component of insert digestion	Volume
All PCR product	30 μ l
10 x O-buffer	5 μ l
<i>EcoR</i> I (1-10 U/ μ l)	2 μ l
<i>Not</i> I (1-10 U/ μ l)	2 μ l
dd H ₂ O	11 μ l
Total volume	50 μ l

2.2.1.9 Dephosphorylation of DNA

The 5' phosphate group of the linearized vector was removed using calf intestinal alkaline phosphatase (CIAP) to prevent self ligation of digested plasmids. This treatment was used to decrease vector background in cloning. 1 U CIAP was added into the reaction mixture following digestion of vector with restriction endonucleases and incubated at 37°C for 1 h. After dephosphorylation, the reaction mixture was incubated at 65°C for 20 minutes to denature CIAP. The DNA was then purified by agarose gel extraction to remove undigested plasmid, salts and proteins for further usage.

2.2.1.10 Ligation of DNA with T4 DNA ligase

The T4 DNA ligase can catalyze the formation of a phosphodiester bond between juxtaposed 5'-phosphate and 3'-hydroxyl termini in duplex DNA or RNA with blunt or cohesive-end termini. This ligase repairs single-strand nicks in duplex DNA, RNA or DNA/RNA hybrids but has no activity on single-stranded nucleic acids (Rossi et al. 1997; Cherepanov and de Vries 2001). The T4 DNA ligase requires ATP as cofactor.

For ligation, digested and purified vector - and insert-DNA were mixed together at different ratios as shown in the following table. 2 μ l ligase buffer, which contain 10 mM ATP (10 x),

1 μ l T4 ligase (1 U/ μ l) and water, were added to the mixture with a final volume of 20 μ l and was incubated at room temperature for 1 h.

Component of ligation	Approach 1.	Approach 2.
Vector (e.g. pPICZ α A)	200 ng	100 ng
Insert	600 ng	1000 ng
T4 ligase buffer (10 x)	2 μ l	2 μ l
T4 ligase (1 U/ μ l)	2 μ l	2 μ l
dd H ₂ O	8 μ l	5 μ l
Total volume	20 μ l	20 μ l

2.2.1.11 Agarose gel electrophoresis of DNA

Agarose gel electrophoresis of DNA was performed as described previously (Sambrook et al. 2001). A mechanism similar to sifting objects through a sieve was used in the electrophoresis. In the case of DNA-based gel electrophoresis, an electric field allowed pushing negatively charged DNA molecules through a gel matrix towards the anode is used. Numerous parameters including the concentration of agarose, voltage, conformation of DNA and size of DNA can affect the migration behavior. Under the same conditions, larger DNA molecules move more slowly than smaller or supercoiled DNA because of stronger frictional drag. Ethidium bromide, a fluorescent dye, causes retardation of DNA, because ethidium bromide intercalates and uncoils DNA.

Ethidium bromide was added to the warm liquid agarose gel solution (1 μ l 1% solution to 10 ml agarose). The warm agarose gel solution was stirred to disperse ethidium bromide and then filled into a gel rack with a comb, which was removed after the gel has cooled down and gelled. The gel with the rack was put into a chamber and then covered with 1 x TAE buffer. 1 kb DNA ladder (molecular weight marker) was loaded into the first gel slot. DNA samples were mixed 1:1 with DNA loading-buffer and loaded into the rest gel slots. Electrophoresis was performed at 120 V for 20 – 30 min. The gel was examined by ultraviolet light and documented.

Buffer	Compound	Amount
50 x TAE buffer	Tris	242 g
	Acetate acid	57.1 ml
	0.5 M EDTA, pH 8.5	100 ml
	ddH ₂ O	add to 1000 ml
1% Agarose gel solution	Agarose	4 g
	1 x TAE buffer	400 ml
	Agarose was boiled in a microwave oven with 1 x TAE buffer until the agarose dissolved. The agarose gel solution was cooled and stored at 60°C.	
6 x loading buffer	Glycerol	30% (w/v)
	Bromphenol blue	0.2% (w/v)
	EDTA, pH 7.5	25 mM
	ddH ₂ O	add to 2 ml

2.2.1.12 Isolation of DNA from agarose gel

For isolation of a desired DNA fragment after PCR or restriction enzyme digestion, an agarose gel electrophoresis was carried out. The band corresponding to the desired DNA fragment was cut using a scalpel on a UV-lamp table. To avoid damage of DNA by UV, this step should be done very quickly. The DNA fragment was extracted as described in the manual of QIAquick Gel Extraction kit. The QIAquick system utilizes the selective binding properties of DNA on silica-gel membranes in the presence of high salt concentrations.

2.2.2 Microbiological Methods

2.2.2.1 Methods for *E. coli*

2.2.2.1.1 Storage and cultivation of *E. coli* strains

For long-term storage, one volume of sterile 87% glycerol was added to equal volume of overnight culture of *E. coli* in LB medium with appropriate amount of antibiotic. The mixture was homogenized by vortexing and stored at -80°C. To recover the bacteria, an inoculum from the glycerol stock was streaked with a sterile inoculation needle onto a LB agar plate containing appropriate antibiotics.

To prepare a pre-culture, a single colony was picked from a LB agar plate, inoculated in 5 ml liquid LB medium containing 100 µg/ml ampicillin or 25 µg/ml Zeozin™ and grown at 37°C, with shaking at 180 rpm overnight.

2.2.2.1.2 Transformation of *E. coli* by heat shock (Mandel and Higa 1970)

Rubidium chloride method for preparation of *E. coli* competent cells

Buffer:

Compound of TfbI	Amount	Final Concentration (mM)
Potassium acetate	0.588 g	30
Rubidium chloride	2.42 g	100
Calcium chloride (2H ₂ O)	0.294 g	10
Manganese chloride (4 H ₂ O)	2.0 g	50
Glycerol	30 ml	15% (v/v)
ddH ₂ O	add to 200 ml	

pH 5.8 with diluted acetic acid. Sterilize by filtering.

Compound TfbII	Amount	Final Concentration (mM)
MOPS	0.21 g	10
Calcium chloride	1.1 g	75
Rubidium chloride	0.121 g	10
Glycerol	15 ml	15% (v/v)
ddH ₂ O	add to 100 ml	

pH 6.5 with diluted NaOH. Sterilize by filtering.

1) Preparation of *E. coli* competent cells

After transfer of 1 ml overnight culture of *E. coli* into 100 ml LB medium, the cells were incubated at 37°C and with shaking at 180 rpm to an OD₆₀₀ 0.4-0.6. The cells were chilled on ice for 15 min and centrifuged at 4°C and 3220 × g for 5 min. The supernatant was discarded. After resuspension of the cells in 40 ml pre-chilled TfbI gently by pipetting up and down, the cell solution was incubated on ice for 15 min and then centrifuged again at 4°C and 3220 × g for 5 min. The supernatant was discarded. The pellet was gently resuspended in 4 ml prechilled TfbII. For long-term storage, cells were aliquoted (100 µl or 200 µl), frozen in liquid nitrogen and stored at -80°C.

2) Transformation

1 µl plasmid DNA (50-100 ng of DNA) or 20 µl ligation mixture were added to an aliquot of competent *E. coli* cells and mixed gently. After incubation on ice for 30 min, this cell mixture was put on water bath at 42°C for 1 min, then immediately incubated on ice 1-2 min. 800 µl LB medium were added to the cell mixture which was incubated further at 37°C, with shaking at 180-200 rpm for 1 h. The transformed cells were centrifuged at $3220 \times g$ for 2 min and the supernatant was discarded. The pellet was resuspended in the remaining supernatant and spread on a pre-warmed LB-agar plate containing the appropriate antibiotic. The plate was incubated at 37°C overnight for formation of colonies.

2.2.2.1.3 Transformation of *E. coli* by electroporation (Neumann et al. 1982)

Medium:

Component of SOB Medium	Concentration (g/l)
Tryptone	20
Yeast extract	5
Sodium chloride	0.6
Potassium chloride	0.5
dd H ₂ O	Add to 1000 ml

Autoclave for 20 minutes on liquid cycle. Store media at +4°C.

Component of SOC Medium	Amount
SOB	1000 ml
1 M Glucose	20 ml
Sterilize by filtering with 0.2 µm membrane	
	MgCl ₂ 20.3 g
2 M magnesium buffer	MgSO ₄ 24.7g
	dd H ₂ O add to 5 ml
Sterilize by filtering with 0.2 µm membrane	

SOC media were prepared by adding 20 ml of 1 M sterile glucose and 5 ml of 2 M magr buffer to the SOB media. Store media at +4°C.

1) Preparation of electrocompetent cells

Electrocompetent cells were prepared for transformation according to the method described previously (Dower et al. 1988). 100 ml of LB media were inoculated with 1/100 volume of a

fresh overnight culture which had been incubated overnight at 37°C, with shaking at 180 rpm. The culture was incubated at 37°C and with shaking at 200 rpm until the OD₆₀₀ reached 0.4 (about 2 h). Cells were then harvested by centrifugation at 4°C, 3220 × g for 5 min. The pellet was firstly washed with 50 ml sterile ice cold ddH₂O, centrifuged at 4°C, 3220 × g for 10 min, then with 25 ml of sterile ice cold 10% (v/v) glycerol and centrifuged 4°C, 3220 × g for 10 min. Afterwards, the cells were resuspended in 10 ml of sterile ice-cold 10 % (v/v) glycerol and centrifuged again at 4°C, 3220 × g for 10 min. The corresponding pellet was resuspended in 10% (v/v) glycerol with a final volume of 250 µl. The cell concentration should be about 2-3 × 10¹⁰ cells /ml. The cells were aliquoted (50 µl) and frozen in liquid nitrogen, and could be stored at -80°C for at least 6 months under these conditions.

2) Electroporation

The eletroporation was carried out using a Gene Pulser (Bio-Rad). 25 µl of ice-cold, fresh cells were mixed with 1 to 2 µl of DNA (50-100 ng of DNA), incubated on ice for 15-30 min and transferred into an ice-cold cuvette. Cells were pulsed at 25 µF, 2.5 kV and 200 Ω. After pulsing, 1 ml of warm recover medium (SOC) was added to the cells and transferred in a fresh, sterile 2 ml warm tube. The cell suspension was incubated at 37°C and with shaking at 180 rpm for 30-60 min and then transferred in 5 ml LB medium. 50 µl of the cell suspension were spread on LB-agar plates containing appropriate antibiotics. The cell suspension in LB medium was further incubated at 37°C, with shaking at 180 rpm for overnight, and then the tubes were centrifuged at 4°C, 20800 × g for 1 min to collect all the cells. The pellet was dissolved in 80 µl of SOC medium and spread (or spread after 1:1000 dilution) on LB-agar plates containing appropriate antibiotics.

2.2.2.1.4 Expression of recombinant lipase in *E. coli*

Expression of recombinant lipase in *E. coli* in shake flasks

E. coli Origami B cells were transformed with pColdIII constructs. Cells were grown at 37°C and with shaking at 180 rpm in 100 ml LB medium with 100 µg/ml ampicillin up to an optical density of 0.4-0.6 at 600 nm. Subsequently, cultures were chilled on ice for 30 min, and lipase expression was induced by adding IPTG (final concentration 1 mM). Cells were grown for an additional 24 h at 15°C and with shaking at 180 rpm, harvested by centrifugation and disrupted by sonification.

Expression of recombinant lipase in *E. coli* in microtiter plates (MTPs)

For library screening purpose CALB variants were expressed in *E. coli* (Liu et al. 2006). Expression of CALB in the *E. coli* cytoplasm was based on the pColdIII vector system (TAKARA BIO INC., Japan). The purified PCR product was used to transform Origami B cells by electroporation. 50 μ l cell suspensions were plated on LB agar plates supplemented with appropriate concentration of ampicillin and tributyrin. After overnight incubation at 37°C and then 5-24 h at 16°C, colonies showing halos and therefore producing an active lipase were picked into 96-well MTPs containing 200 μ l LB medium with 100 μ g/ml ampicillin and 5% (v/v) DMSO in each well. This so-called master plate was incubated further at 37°C, with shaking at 400 rpm overnight, and then stored at -80°C.

20 μ l cell suspensions from each well of the master plate containing active CALB variant was transferred in a new 96-well microtiter plate with 150 μ l LB medium and 100 μ g/ml ampicillin for expression. This expression plate was incubated at 37°C and with shaking at 400 rpm until an optical density of 0.4-0.6 at 37°C was reached. Cells were chilled on ice for 30 min, and the lipase expression was induced by adding IPTG up to a final concentration of 1 mM. After 24 h incubation at 15°C, with shaking at 200 rpm shaking, cells were harvested by centrifugation and disrupted by lysozyme.

2.2.2.1.5 Disruption of *E. coli* cells

Disruption by sonification

After harvest of the cells by centrifugation, they were resuspended in 20 ml 50 mM potassium phosphate buffer pH 7.5 containing 1 mM PMSF. The cells were disrupted by sonication using a Sonifier 250 sonicator. The cell suspension was put on ice and sonicated for 1 min with output 40 W, 40% work interval and 1 min break. This process was repeated 5 times. The cell extract was centrifuged at 38729 g and 4°C for 20 min. The cell lysate was carefully removed in a new tube.

Disruption by lysozyme for expression in microtiter plate (MTP)

E. coli cell pellets in MTPs were lysed by adding 50 μ l lysis buffer (1 mM sodium phosphate, pH 6.0, 1 mg/ml lysozyme; DNase 2% (v/v)). Lysates were incubated for 10 min at 37°C, with shaking at 300 rpm, and chilled on ice for 30 min. After incubation for 1 h at -80°C, lysates were thawed at room temperature, and cell debris was removed by 30 min centrifugation at 3220 \times g and 4°C.

2.2.2.2 Methods for *P. pastoris*

2.2.2.2.1 Storage and cultivation of *P. pastoris* strains

To store cells for months to years, a single colony of each strain was cultured overnight in YPD. The cells were harvested and suspended in YPD containing 15% glycerol at a final OD₆₀₀ of 50-100 (approximately 2.5-5.0 x 10⁹ cells/ml). Cells were frozen in liquid nitrogen and then stored at -80°C.

The cultivation of *P. pastoris* was carried out in YPD Medium. Therefore 10 ml of YPD was inoculated with a single colony of the *P. pastoris* strain from a YPDS agar plate and propagated overnight at 28-30°C in a shaking incubator (180-200 rpm). For selection of recombinant cells Zeozin™ with a final concentration of 100 µg/ml was added.

2.2.2.2.2 Transformation of *P. pastoris*

1) Preparation of electrocompetent cells

Five milliliter of *P. pastoris* strain was incubated in YPD medium in a 50 ml conical tube at 30°C overnight. 500 ml of fresh medium was inoculated in a 2 liter flask with 0.1-0.5 ml of the overnight culture. Let to grow overnight again to an OD₆₀₀ = 1.3-1.5. The cells were centrifuged at 1500 g for 5 min at +4°C. The pellet was resuspended with 500 ml of ice-cold (0°C) sterile water. The cells were then centrifuged three times more at 1500 g for 5 min at +4°C. After each centrifugation the pellet was resuspended consecutively in 250 ml of ice-cold (0°C) sterile water, 20 ml of ice-cold (0°C) 1 M sorbitol and in the end in 1 ml of ice-cold (0°C) 1 M sorbitol for a final volume of approximately 1.5 ml. The cells were kept on ice and used for the following transformation.

2) Electroporation

Eighty microliter of the competent *P. pastoris* cells were mixed with 5-10 µg of linearized DNA (in 5-10 µl sterile water) in 1.5 ml microcentrifuge tube and incubated on ice for 5 min. (Note: For circular DNA, use 50-100 µg) The mixture was carefully transferred into an ice-cold (0°C) 0.2 cm electroporation cuvette. The cells were pulsed, according to the manufacturer's instructions for *P. pastoris* (*P. pastoris* expression Kit of Invitrogen), with 1500V, 25µF and 200Ω. Immediately 1 ml of ice-cold 1 M sorbitol was added to the cuvette. The cuvette contents were transferred to a sterile 15 ml conical tube. This was incubated at 30°C without shaking for 1 to 2 h. After that, 10, 25, 50, 100 and 200 µl were respectively spread on YPDS plates containing 100 µg/ml Zeocin™. Plating at low cell densities, efficient

Zeocin™ selection was favored. Plates were incubated from 3 to 10 days at 30°C until colonies formed.

2.2.2.2.3 Expression of recombinant lipase in *P. pastoris*

A single colony was inoculated in 10 ml of BMGY Medium with Zeocin™ in a 50 ml baffled flask. The culture was grown at 28-30°C in a shaking incubator (250-300 rpm) until culture reached an OD₆₀₀ = 5-15 (approximately 16-24 h). This means that cells were then in log-phase growth. The cells were harvested by centrifuging at 2500 g for 5 minutes at room temperature. After decanting the supernatant, the cell pellet was resuspended to an OD₆₀₀ of 1.0 in BMMY medium to induce gene expression (approximately 100-200 ml). The culture was placed in a 1 liter baffled flask and further grown in an incubator. 100% methanol was added to a final concentration of 0.5% (v/v) every 24 h to maintain induction. Each time when methanol was added, 1 ml of the culture was transferred to a 1.5 ml microcentrifuge tube. These samples were used to analyze expression levels and the optimal time for the harvest was determined accordingly. The samples were centrifuged at 20800 × g in a tabletop microcentrifuge for 2-3 minutes at room temperature. The time points of the harvest were as following: 0 h, 6 h, 12 h, 24 h (1 day), 36 h, 48 h (2 days), 60 h, 72 h (3 days), 84 h, and 96 h (4 days). To analyze protein secretion, the supernatant was transferred to a separate tube. The cells and supernatants were separately stored at -80°C until ready to assay. After 3-5 days expression, the cells were harvested by centrifuging at 3220 × g and 4°C for 10 min. The supernatant was transferred to a new conical tube for assay and stored at 4°C.

2.2.2.3 Methods for *A. brassicicola*

2.2.2.3.1 Cultivation of *A. brassicicola*

An ampoule with stain *A. brassicicola* from DSMZ was opened and the dried culture was resuspended in 1 ml liquid corn meal medium. One drop of the suspension was streaked onto a corn meal agar plate or in 100 ml corn meal medium and incubated at 30°C for 3-5 days. For long-term storage strains were stored in 50% glycerol at -80°C.

2.2.2.3.2 Expression of a cutinase from *A. brassicicola*

Conidia of *A. brassicicola* obtained from 5-day-old cultures grown on corn meal agar or corn meal medium (washed with modified Czapek's medium) were inoculated in 100 ml modified Czapek's medium supplemented with 25 mg cutin monomer (16-Hydroxyhexadecanoic acid (Trail and Koeller 1993; Fan and Köller 1998)). After a few days cultivation, the cells were harvested by centrifuging at $20800 \times g$ for 1 min. The supernatant was analyzed by *p*NPP assay.

For expression of *CUTAB1* in *P. pastoris*, the cutinase was incubated in the same way as for the expression of recombinant lipase in *P. pastoris* (2.2.2.2.3) after cloning of *CUTAB1* in pPICZ α A.

2.2.3 Biochemical methods

2.2.3.1 Concentration of protein

Samples with low protein concentrations were concentrated by ultrafiltration using Amicon[®] Stirring Cells or Centricon[®] Centrifugal Filter Devices from Millipore YM 10 filters according to the instructions supplied by manufacturer. Amicon Ultrafiltration Stirred Cells were supplied with Millipore Ultrafiltration Membranes (10 kDa).

2.2.3.2 Determination of protein concentration

Protein concentration in the aqueous solution was determined with a Protein Assay Kit from Bio-Rad (Bradford 1976). The assay is based on the principle that the absorbance maximum for an acidic solution of Coomassie Brilliant Blue G-250 (CBBG) shifts from 465 nm to 595 nm when binding to proteins at arginine, tryptophan, tyrosine, histidine, and phenylalanine residues occurs. Apart from the hydrophobic interaction, ionic interactions stabilize also the anionic form of the dye, causing a visible color change. The assay is monitored at 595 nm in a spectrophotometer. As the samples are to be assayed, protein standards were prepared in the same buffer. As standard bovine serum albumin (BSA) with concentrations of 0, 10, 20, 30, 40, 50 $\mu\text{g/ml}$ were used in the assay ($<50 \mu\text{g/ml}$).

Each sample consisted of 800 μl of one of the protein standard solutions or unknown samples mixed with 200 μl Dye (CBBG) stock solution in a 1.5 ml plastic cuvette. After intensive

mixing, the samples were incubated 5 min at room temperature. The absorbance at 595 nm was measured by Pharmacia Biotech Ultraspec 3000 Spectrophotometer.

2.2.3.3 Sodium dodecyl sulphate - polyacrylamide gel electrophoresis

The Sodium dodecyl sulphate – polyacrylamide gel electrophoresis (SDS-PAGE) is used to separate proteins according to their molecular weight to check for the purity and the molecular weights of the proteins. SDS denatures and binds to the proteins. Therefore, the SDS gel electrophoresis of samples having identical charge to mass ratios results in fractionation by size (Shapiro et al. 1967; Weber and Osborn 1969; Laemmli 1970). Proteins migrate to the anode in an electric field. Polyacrylamide gel works here as a molecular sieve, big molecules run slower through the gel than small molecules due to stronger frictional drag. Proteins extracted from the crude solution and from various purification steps were analyzed by SDS-PAGE.

Buffer	Compound	Amount
4 x Lower Tris buffer	Tris	36.34 g
	SDS	0.8 g
	H ₂ O	add to 200 ml
	The pH value was adjusted to 8.8 with HCl.	
4 x upper Tris buffer	Tris	12.11 g
	SDS	0.8 g
	H ₂ O	add to 200 ml
	The pH value was adjusted to 6.8 with HCl.	
Staining solution	Coomassie Brilliant Blue	1 g
	Glacial acetic acid	100 ml
	Methanol	300 ml
	H ₂ O	600 ml
Destaining solution	Methanol	300 ml
	Glacial acetic acid	100 ml
	H ₂ O	600 ml
5 x running buffer	Tris	15 g/l
	Glycine	72 g/l
	SDS	10% (w/v)
	The pH value was adjusted to 8.3 with HCl	

Materials and Methods

Buffer	Compound	Amount
2 x loading buffer	Tris/HCl (pH 6.8)	100 mM
	Glycerol	20% (v/v)
	SDS	4% (w/v)
	β -mercaptoethanol	10% (w/v)
	Bromophenol blue	0.02% (w/v)
5 x loading buffer	Tris/HCl (pH 6.8)	320 mM
	Glycerol	50% (v/v)
	SDS	10% (w/v)
	β -mercaptoethanol	25% (w/v)
	Bromophenol blue	0.1% (w/v)
SDS gel	Compound	Amount
Stacking gel (3.9%)	4 x Upper Tris	1.0 ml
	Acrylamide bisacrylamide 30% (v/v)	0.52 ml
	H ₂ O	2.47 ml
	Ammonium persulfate 10% (w/v)	40 μ l
	TEMED	4 μ l
Resolving gel (12.5%)	4 x Lower Tris	2.00 ml
	Acrylamide bisacrylamide 30% (v/v)	3.33 ml
	H ₂ O	2.67 ml
	Ammonium persulfate 10% (w/v)	40 μ l
	TEMED	4 μ l

After fitting together two glass plates, the resolving gel was poured into the gap between the glass plates. Isopropanol was loaded over the gel to ensure a flat surface and to exclude air. Isopropanol was washed off with water after the gel had polymerized. The stacking gel was poured onto the polymerized resolving gel and a comb was inserted in the stacking gel solution (optimal polymerization for overnight at 4°C). Followed by the polymerization of the stacking gel, the comb was removed and the gel was put in an electrophoresis chamber, which was filled with electrophoresis buffer. The protein samples were mixed with one volume of twofold SDS loading buffer (Sambrook 2001) or with ratio of 1:4 of 5 x Loading buffer, and heated for 5 min at 95°C. After cooling to RT the samples and the standard protein marker (Roti[®]-Mark Standard or Precision Plus Protein[™] all Blue Standard) were loaded in the wells.

The electrophoresis per gel was carried out at 10 mA for 10 min and 25 mA for approximately 60 min. Followed by electrophoresis, the gel was put in the staining solution on a shaker overnight and destained three times with destaining solution. Finally the gel was dried at 80°C in vacuum between filter paper and cellophane foil to be stored.

Precision Plus Protein™ all Blue Standard MW (kDa)	PageRuler™ Unstained Protein Ladder	Roti®-Mark standard (ROTH)	MW (kDa)
250	200	Myosin, beef	212
150	150	β-Galactosidase, rec. <i>E.coli</i>	118
100	120	Serumalbumin, beef, glycosylated	66
75	100	Ovalbumin, chicken, glycos.	43
50	85	Carbonic anhydrase	29
37	70	Trypsin inhibitor, soja	20
25	60	Lysozyme, chicken	14
20	50		
15	40		
10	30		
	25		
	20		
	15		
	10		

2.2.3.4 Densitometric analysis

Protein solutions containing different amounts of the protein of interest were separated by SDS-PAGE. The gels were stained with Coomassie brilliant blue R-250, dried and finally scanned. For the densitometric analysis Scion Image software (<http://www.scioncorp.com>) was used. This method is very useful for estimation of the fraction of the protein of interest when the protein has not been purified.

2.2.3.5 Purification of recombinant pCUTAB1

After expression of *CUTAB1* in *P. pastoris*, the supernatant was concentrated using Amicon concentrator. 0.5 ml concentrated pCUTAB1 (15 mg/ml) solution was mixed with 0.5 ml 1 M ammonium sulfate. The diluted pCUTAB1 solution was purified in a single step under native

condition using a 1 ml HiTrap™ Phenyl FF (low sub) column and a chromatography system (ÄKTA). The protein was eluted from the column with 20 mM potassium phosphate buffer pH 8.0.

2.2.3.6 Biochemical characterization

2.2.3.6.1 pH-stat assay

For the determination of hydrolase activity of the crude extract or purified enzymes pH-stat assay (Peled and Krenz 1981) was used. For the pH-stat assay 20 ml aliquots of a substrate emulsion (200 mM of tributyrin, 2% (w/v) gum arabic in water) were added to the thermostated reaction chamber of the pH-stat, preheated to different temperatures (25°C, 30°C, 35°C, 40°C, 45°C and 50°C). After addition of enzyme the pH was automatically kept constant at appointed pH 7.5 or 8 by addition of 0.01 M NaOH solution. The NaOH consumption, which is proportional to the conversion, was recorded and used for calculation of the activity. One unit of hydrolase activity was defined as 1 μmol of fatty acid released by enzyme per min under assay conditions. The specific activity was calculated by the following equation.

$$A = \frac{c_{NaOH}}{M_{enzyme}} \times \left(\frac{\Delta y}{\Delta x} \right)$$

A	[U/mg]	specific activity
c_{NaOH}	[mol/l]	molar NaOH concentration
M_{enzyme}	mg	amount of enzyme
$\Delta y/\Delta x$	[ml/min]	slope

2.2.3.6.2 Spectrophotometric assay

The lipolytic activity of the crude extract and purified enzymes was measured spectrophotometrically towards *p*-nitrophenyl (*p*NP) esters (e.g. *p*-nitrophenyl butyrate (*p*NPB) and *p*-nitrophenyl palmitate (*p*NPP)). In the spectrophotometric assay 2-4 μg of the protein was added to a Tris-HCl buffer containing 0.5% (v/v) Triton X-100, 0.1% aqueous gum arabic and 0.1 M Tris-HCl pH 8 in a total volume of 900 μl in a 1.5 ml cuvette. The cuvette was placed in the jacket holder of Pharmacia Biotech Ultraspec 3000 spectrophotometer. The different reaction temperatures were maintained by a circulation water bath. After the solution of the reaction was thermal equilibrated (5 min), 100 μl 6.5 mM

*p*NP ester sonically dispersed in 2-propanol was added to initiate the reaction. The reaction progress was monitored by reading of absorbance at 410 nm that accompanied release of *p*-nitrophenol from hydrolysis of *p*NP esters. The specific activity was calculated by the following equation. One unit of the activity was defined as the amount of enzyme that released 1 μmol of *p*-nitrophenol per min under assay conditions. The molar extinction coefficient ϵ of the *p*-nitrophenol depended on pH was determined via a calibration curve (Figure 2.3).

$$A = \frac{\Delta E}{\epsilon \times d \times c_{enzyme}}$$

A	[U/mg]	specific activity
ΔE	[min^{-1}]	slope at 410 nm
ϵ	[$\text{M}^{-1} \text{cm}^{-1}$]	molar extinction coefficient
d	[cm]	cuvette diameter (e.g. 1 cm)
c_{enzyme}	[mg/l]	concentration of enzyme

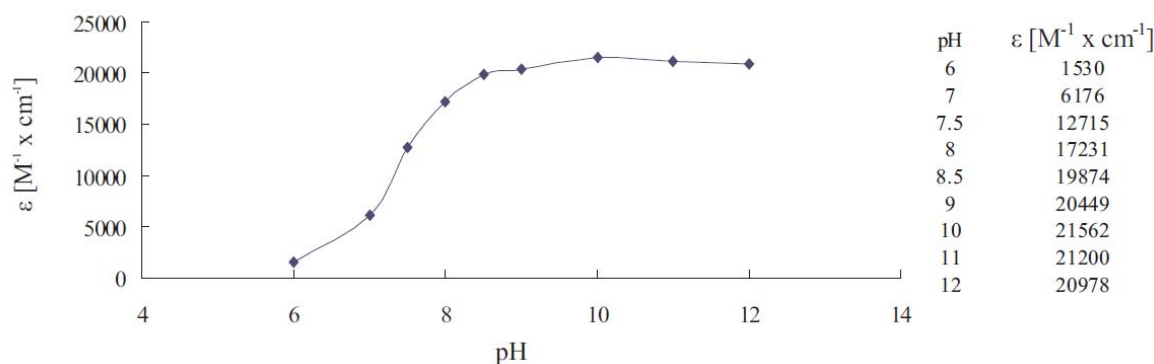


Figure 2.3: Molar extinction coefficient ϵ of *p*NP depending on pH. To initiate the reaction, 100 μl 0.05 mg/ml *p*NP dispersed in 2-propanol was added to 900 μl Tris-HCl buffer containing 0.5% (v/v) Triton X-100, 0.1% aqueous gum arabic and 0.1 M Tris-HCl with different pH values ranging from pH 6-12 in a total volume of 1 ml in a 1.5 ml cuvette. The value of the molar extinct coefficient ϵ [$\text{M}^{-1} \times \text{cm}^{-1}$] of *p*NP was calculated according to the following equation:

$$\epsilon = \frac{E \times M}{d \times c_{pNP}}$$

ϵ	[$\text{M}^{-1} \times \text{cm}^{-1}$]	molar extinction coefficient
E		absorbance at 410 nm
M	[g/mol]	molecular mass
d	[cm]	cuvette diameter (e.g. 1 cm)
c_{pNP}	[mg/l]	concentration of <i>p</i> NP

2.2.3.6.3 Substrate specificity of pCUTAB1

For the determination of substrate specificity of pCUTAB1, 5% (v/v) triglycerides, including tributyrin, tricaprylin, triolein, olive oil, and fatty acid methyl as well as ethyl esters, including methyl acetate, methyl propionate, methyl butyrate, ethyl butyrate, methyl caproate, methyl caprylin, ethyl caprylin, methyl decanoate, methyl laurate and methyl myristate were emulsified with 2% (w/v) gum arabic as stabilizer in water. For solid substrates at room temperature, such as tripalmitin and tristearin, 1% (w/v) substrate with 2% (w/v) aqueous gum arabic was used. The activities were determined by the pH-stat assay.

2.2.3.6.4 Temperature and pH optima of pCUTAB1

The temperature and pH optima of pCUTAB1 were determined by measuring the activity towards 8 mM *p*NPP spectrophotometrically (2.2.3.6.2). The temperature optimum was determined after 5 min incubation of the enzyme at a given temperature (25°C, 30°C, 35°C, 40°C, 45°C or 50°C) at pH 8 in Tris-HCl buffer containing 0.5% (v/v) Triton X-100, 0.1% aqueous gum arabic, 0.1 M Tris-HCl and water. The pH optimum was measured after 5 min incubation of the protein at room temperature and 40°C in the above Tris-HCl buffer within a pH range from 6 to 12. In each measurement 2-4 µg of concentrated pCUTAB1 were used.

2.2.3.6.5 Temperature and pH stability of pCUTAB1

In order to determine the temperature stability of pCUTAB1, many samples including 2-4 µg enzyme in each one were incubated at pH 8 in Tris-HCl buffer containing 0.5% (v/v) Triton X-100, 0.1% aqueous gum arabic, 0.1 M Tris-HCl pH X (Buffer B) and water at 40°C for 5 days. The activity of each incubated sample towards *p*NPP was measured every 30 min in the first 2 h and then every hour until 4 h (2.2.3.6.2). The pH stability of pCUTAB1 was investigated by incubating the samples, including 2-4 µg enzyme in each sample, in the buffer B at pH 8. The remaining activity of each sample including pCUTAB1 was measured spectrophotometrically for 1 min (2.2.3.6.2).

2.2.3.6.6 Kinetic measurements

The kinetic constants K_m and V_{max} for the hydrolysis of *p*NPP were calculated from the enzyme concentration dependent activities in the standard spectrophotometric assay (2.2.3.6.2)

at pH 8 and Lineweaver-Burk plots using a least-squares best fit to the Michaelis-Menten equation. In the spectrophotometric assay 10 μ l enzyme solution containing 2-4 μ g pCUTAB1 was added to 890 μ l Tris-HCl buffer containing 0.5% (v/v) Triton X-100, 0.1% aqueous gum arabic and 0.1 M Tris-HCl pH 8 in a 1.5 ml cuvette. After adding 100 μ l *p*NPP with different concentration, the reaction was initiated. The concentration of *p*NPP sonically dispersed in 2-propanol ranged from 0.3 mM to 8 mM. All values were determined in triplicate and were corrected for the autohydrolysis of the substrates. The deviations for all data were between $\pm 1.0\%$ and $\pm 5.0\%$.

2.2.4 Immobilization of enzyme

For measurement of activity of enzyme in organic solvents, the enzyme was immobilized on hydrophobic carriers MP1000 and/or HP20L. Therefore the supernatant from the expression of recombinant gene in *P. pastoris* was concentrated until a protein concentration of 3-15 mg/ml was reached using Amicon[®] Stirring cells with a Millipore Ultrafiltration Membrane (10 kDa). Protein concentration was determined by the Bradford method using the BioRad kit according to the manufacturer's instructions. Hydrophobic carriers were degreased using 100% ethanol. Subsequently the protein was immobilized on the supporter using 1.7 ml (≈ 5 mg) concentrated enzyme (e.g. concentration 3 mg/ml) and 500 mg MP1000. After the protein solution (1.7 ml) was diluted in 38.3 ml buffer A containing 25% ethanol and 75% 50 mM potassium-phosphate buffer at appropriate pH (e.g. for CALB pH 6-6.5) which was in the range of the isoelectric point (pI) of the protein, 500 mg degreased MP1000 was added to the diluted enzyme solution. The mixture was stirred at 6°C for 40 h. Immobilized enzyme was recovered by filtration and washed three times with buffer A. The carrier-bound enzyme was dried after a few hours until over night at room temperature in fume hood.

2.2.5 Assay systems

2.2.5.1 Screening of lipase activity with tributyrin agar plate assay

E. coli Origami B Cells were grown on LB agar plates containing 1% emulsified tributyrin and an appropriate antibiotic. After cell growth at 37°C for 24 h, plates were incubated at 15 °C (for pColdIII expression) or room temperature for expression. The appearance of clear

zones (halos) around colonies resulting from hydrolysis of tributyrin was taken as a positive indication of lipolytic activity.

2.2.5.2 Hydrolysis assay for hpca

For measurement of activity of an enzyme towards the target product (acrylated hydroxypropylcarbamate (hpca)), a new assay was developed. This high-throughput activity assay was based on hydrolysis of hpca and simultaneous spectrophotometrical detection of the protons released in this reaction using the pH-indicator bromocresol purple. This indicator displays a color change from pH 6.8 (purple) to pH 5.2 (yellow). Moreover, the activity of enzyme can be measured by a decrease of absorption at 581 nm.

20 μ l cell lysate of *E. coli* was added to 180 μ l of 1 mM sodium-phosphate buffer pH 6.0 supplemented with 0.5% (v/v) hpca and 60 μ g/ml bromocresol purple in a 96-well MTP. The reaction was carried out at room temperature and the reaction progress was followed for 10 min by tracking the absorption decrease at 581 nm using a SpectraMax 386 PC MTP-spectrophotometer.

The same assay was used to characterize CALB variants expressed in *P. pastoris*. 100 μ l cell lysate was then added to 900 μ l of 1 mM sodium-phosphate buffer pH 6.0 supplemented with 0.5% (v/v) hpca and 60 μ g/ml bromocresol purple in 1 ml PS cuvettes. The reaction progress was followed for 10 min by tracking the absorption decrease at 581 nm using a Pharmacia Ultrospec 3000 spectrophotometer.

2.2.5.3 Analysis of the enantioselectivity of lipases by gas chromatography

In order to investigate the preference of *R* or *S* enantiomer of an enzyme, the enantioselectivity of the enzyme was measured by gas chromatography. 3 ml supernatant of CALB from expression in *P. pastoris* was mixed with 3 ml 100 mM sodium phosphate buffer pH 7.5, and 44.25 μ l 1-phenylethylpropionate was added to the mixture. 1 ml samples were taken at different time points and extracted with 300 μ l isoctane. After 1 min centrifugation at $20800 \times g$, 200 μ l organic phase was dried with Na_2SO_4 and then analyzed directly by GC. Enantiomers of substrate and product were separated on a Fisons instruments GC 8000 series equipped with a 50 m cyclodex β -F/P column using H_2 as carrier gas. The column oven was programmed as follows: 1) 100°C for 40 min 2) 100°C to 175°C at 10°C min^{-1} . Retention times of 1-phenylethylpropionate enantiomers were: (+) 46.8 min, (-) 47.1 min; retention

times of phenylethanol enantiomers were: (+) 40.7 min, (-) 42.7 min. Products were identified by authentic standards. Product formation was calculated from the peak area ratios.

2.2.5.4 Analysis of activity of lipase and cutinase by GC/MS

For measurement of the transesterification activity of lipase and cutinase in organic solvents, 10 μl samples were withdrawn in 500 μl diethylether to be analyzed by GC/MS. All experiments were done in triplicate. The control experiments were carried out without enzyme.

Acrylation of hydroxypropylcarbamate (hpc) by lipase CALB

The transesterification of methyl acrylate with hpc was catalyzed by immobilized CALB. 10 μl hpc (mixture of two pairs of enantiomers primary:secondary = 1:1) were converted with 1 ml methyl acrylate (11 mmol) and 5-13 mg carrier immobilized by CALB variants (about 50 μg) in a screw-capped vial under continuous shaking at 400 rpm and 40°C in a horizontal shaker. The reaction product methanol was removed from the reaction by addition of 300 mg 4Å molecular sieve to shift the reaction equilibrium to the products.

Acrylation of 6-mercaptohexanol by lipase CALB and cutinase pCUTAB1

Unless stated otherwise, methyl acrylate (500 μl = 6 mmol) and 6-mercapto-1-hexanol (10 μl = 75 μmol) were placed in a screw-capped vial with about 10 mg carrier (about 50 μg enzyme). Methyl acrylate was used as a solvent and substrate. The reaction mixture was incubated at room temperature (22°C) with continuous shaking speed at 400 rpm in a horizontal shaker.

GC/MS analysis

To determine the degree of conversion in the transesterification reactions, samples were analyzed on a Shimadzu GC/MS-QP2010 equipped with a FS-Supreme column (30 m long, internal diameter 0.25 mm, film thickness 0.25 μM) using helium as carrier gas at a linear velocity of 30 cm s^{-1} . MS-settings were: interface at 270°C, ion source at 200°C, start time at 4 min, MS-scan frequency (TIC-mode) 2 s^{-1} .

Arylation of hpc:

The column oven was programmed as follows: 1) 40°C for 1 min 2) 40°C to 250°C at 15°C min^{-1} 3) 250°C to 300°C at 30°C min^{-1} 4) 300°C for 5 min. The retention times in the acrylation of hpc were: methyl acrylate 3.2 min, 1hpc und 2hpc 7.7 min, 3hpc und 4hpc 8.3 min and hpca 9.8 min. Products were identified by authentic standards.

Arylation of 6-mercaptohexanol:

The column oven was programmed as follows: 1) 70°C for 1 min 2) 70°C to 280°C at 15°C min⁻¹ 3) 280°C to 310°C at 30°C min⁻¹ 4) 310°C for 2 min. The retention times in the acrylation of 6-mercaptohexanol were: methyl acrylate 3.2 min, 6-mercaptohexanol 6.78 min and 6-mercaptohexyl acrylate 8.97 min. Products were identified by NMR (work of Sabine Eiben).

The percentage conversion was calculated based on the following equation.

$$\text{Conversion (\%)} = [A_{\text{product}} / (A_{\text{product}} + A_{\text{substrate}})] \times 100\%$$

Where A_{product} = peak area of product, while $A_{\text{substrate}}$ = peak area of substrate.

3 Results

3.1 Improved acrylation of hydroxypropylcarbamate by rational protein design of *C. antarctica* lipase B

BASF have screened some well-known enzymes for transesterification (**Figure 1.11**) of hydroxypropylcarbamate (hpc: 1hpc, 2hpc, 3hpc and 4hpc) with methyl acrylate. The results showed that the CALB had the highest activity among all the screened enzymes. However, the wild-type CALB does not catalyze full conversion in an acceptable time scale. For industrial purposes, it was necessary to increase the activity of the wild-type enzyme. It was therefore anticipated that through our strategy, including directed evolution and rational protein design (**Figure 3.1**), CALB will show higher activity towards the substrate (hpc), which is a mixture of primary and secondary alcohols containing *R* and *S* enantiomer respectively (**Figure 1.11**). For rational protein design as shown in **Figure 3.1**, promising positions were identified by the molecular modeling and the substitutions were realized by the site-directed mutagenesis and constructed saturation mutagenesis library. For library screening, CALB variants were expressed in *E. coli* (Liu 2006). This expression system is more suitable for high-throughput requirements in terms of expression time and number of clones. However, *P. pastoris* (Cereghino and Cregg 2000) was selected as an ideal expression host of CALB for the higher expression level of the recombinant gene. Plasmid DNAs were isolated from those *E. coli* clones with improved performance in enzyme activity and were sequenced (by GATC, Konstanz, Germany). *P. pastoris* was transformed with those plasmids and the transformants were characterized with respect to activity in tributyrin hydrolysis, hydroxypropylcarbamates acrylate (hpc) hydrolysis and stereoselectivity in hydrolysis of 1-phenylethylpropionate. With respect of acrylation of hpc with methyl acrylate, lyophilized and immobilized CALB were used as an almost water-free reaction system since the presence of water in reaction can disturb the conversion. Apart from the identification of appropriate mutants, a suitable carrier for the enzyme also plays an important role in the reaction. It was shown that CALB showed only activity towards the substrate after immobilization on hydrophobic carriers, e.g. on MP1000. Therefore, hydrophobic carriers MP1000 and HP20L were prepared for the following transesterification studies.

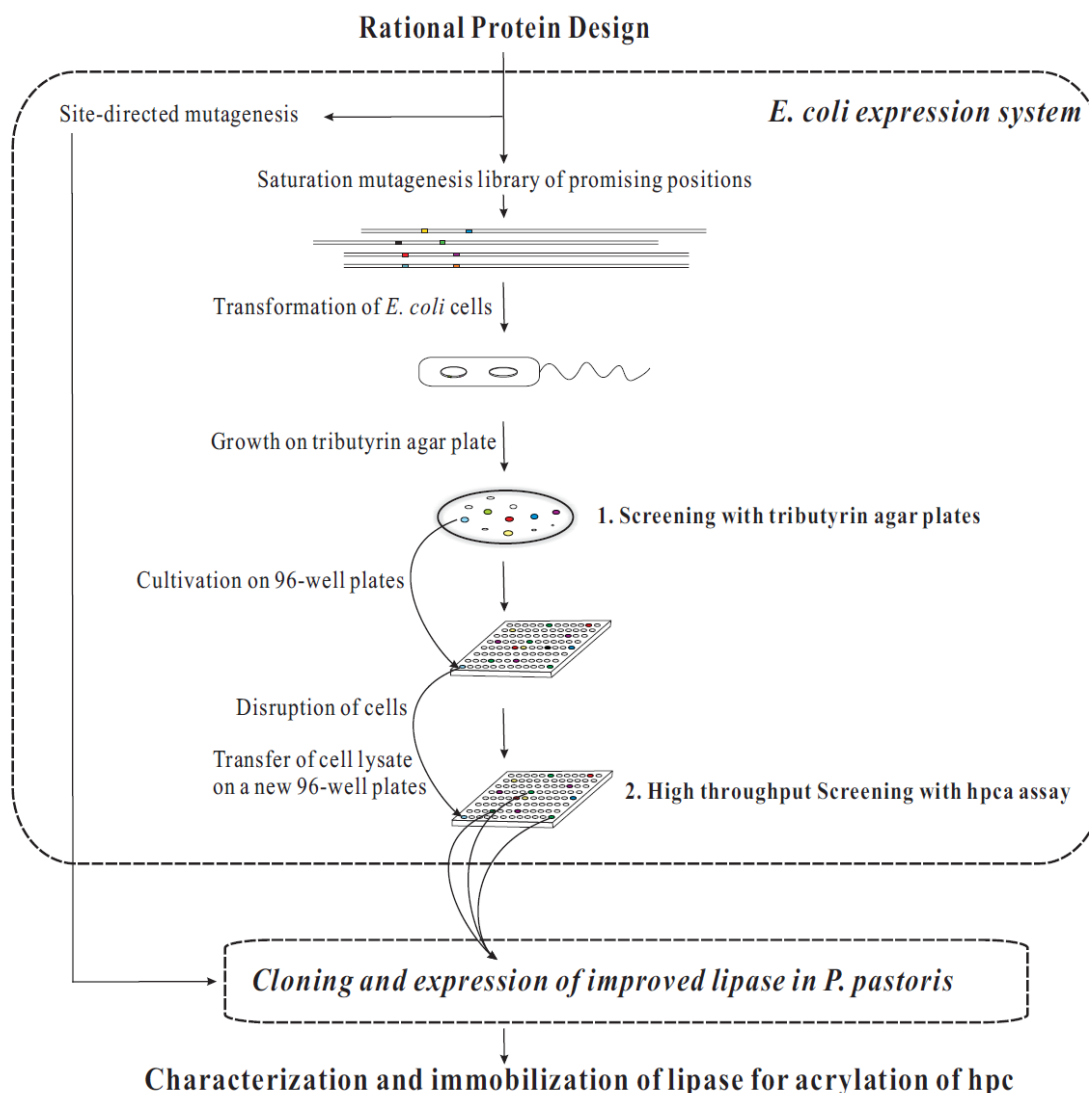


Figure 3.1: Overview of strategy from rational protein design to improved CALB variants for acylation of hpc with methyl acrylate.

3.1.1 Rational protein design by molecular modeling

In order to increase the activity of CALB, positions around the active site have been investigated by molecular modeling by Peter Trodler. In docking of the primary and the secondary alcohols in the active site of CALB, the *S*-enantiomer of the secondary alcohol (2hpc) was identified as the bottleneck in this reaction (**Table 3.1**) (Trodler 2008). Possible positions of 1hpc, 2hpc, 3hpc and 4hpc in the binding pocket (**Figure 3.2**) and All productive binding modes of the covalently bound transition state were determined by docking (Trodler 2008). The slowest reacting enantiomer was identified by the highest docking score to be 2hpc, the *S*-enantiomer of the secondary alcohol. Based on rational design, the mutations of center positions in the binding pockets were expected to increase the size of

the stereospecificity pocket and thereby increase the binding ability of 2hpc (**Figure 3.3**) (Troddler 2008), and finally to reach full conversion, which could not be achieved using the wild-type CALB in short time.

The position L278 (**Figure 3.6**) identified by docking was supposed to be a key position for increasing the activity of CALB. Thus, a substitution of Leu by Tyr, Phe, Val and Ala at position 278 was suggested to increase the volume of the binding pocket. The effect of the mutations at position 278 was theoretically analyzed by molecular dynamics simulations (Troddler 2008). After short MD simulations of 600 ps, the distance d ($H_{NE2} - O_{alc}$) between the hydrogen atom of the catalytic His and the oxygen of the alcohol moiety was selected as geometrical parameter. 2hpc was identified again as slow reacting enantiomer by the longest distance d ($H_{NE2} - O_{alc}$) after MD simulation. The mutant L278A was supposed to show a higher activity in acrylation of hpc by a shorter distance d ($H_{NE2} - O_{alc}$) (**Table 3.2**) (Troddler 2008). Therefore, mutants (L278Y, L278F, L278V and L278A) constructed by site-directed mutagenesis at position 278 were investigated in the following experiments. Moreover, as the positions 277, 278 and 281 in a long α -helix form the entrance to the active site of CALB, a combination of mutations at those positions was believed to change the size of the entrance for the substrate hpc. Therefore, it was suggested to construct a saturation mutagenesis library at positions 277, 278 and 281.

In view of a combination of many mutations, which have the highest activity, selectivity or stability in each position, may not lead to an expected improvement. Therefore, construction and screening of a multi-site saturation mutagenesis library seemed to be a suitable method to uncover mutually increasing and positive effects of mutations at different positions. Thus, a two-site saturation mutagenesis library (L278X/W104X, X indicated any one of 20 amino acids) was suggested, based on the positions of L278 (**Figure 3.6** and **Figure 3.7**), the key position for increasing activity, and W104 (**Figure 3.6** and **Figure 3.7**), having a significant impact on the stereoselectivity of CALB reported by Patkar (Patkar et al. 1998). Patkar et al. reported that mutant W104H was created to introduce more space in the active site and the increased space was very likely to reduce enantiomeric selectivity of the enzyme.

Furthermore, the residues 42, 47 and 104 (**Figure 3.7**) constitute the medium binding pocket (stereospecificity pocket) for secondary alcohols and have been reported to show low flexibility, while the large binding pocket for secondary alcohols showed higher flexibility (Troddler et al. 2008). For enlarging the medium binding pocket for 2hpc and lowering the stereoselectivity of CALB, substitution of T42 and S47 with smaller amino acids (e.g. Ala) as well as W104 with Phe should create more space in the active site. Mutants T42A, S47A,

T42A/S47A and W104F were thus suggested and investigated further. Additionally, in view of searching a best mutant with the highest activity and the lowest stereoselectivity for the acrylation of hpc, mutants from a combination of S47A with the best mutants from screening of the saturation mutagenesis library (L278X/W104X) should also be constructed.

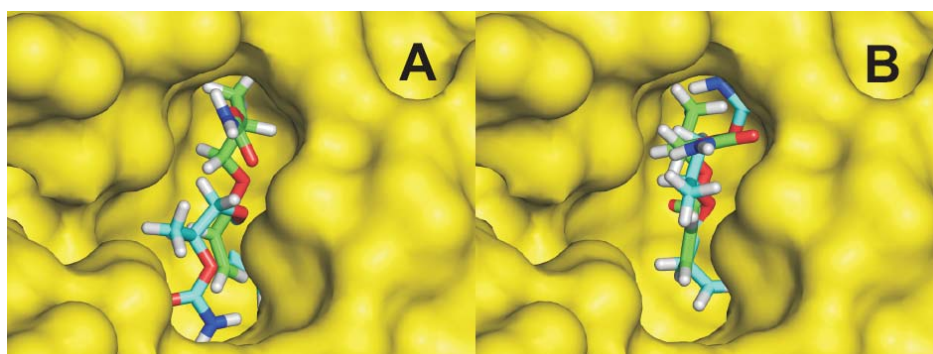


Figure 3.2: (A) Positions of primary alcohols 3hpc (green) and 4hpc (blue) and (B) secondary alcohols 1hpc (green) and 2hpc (blue) in the binding pocket of CALB wild-type (Troedler 2008).

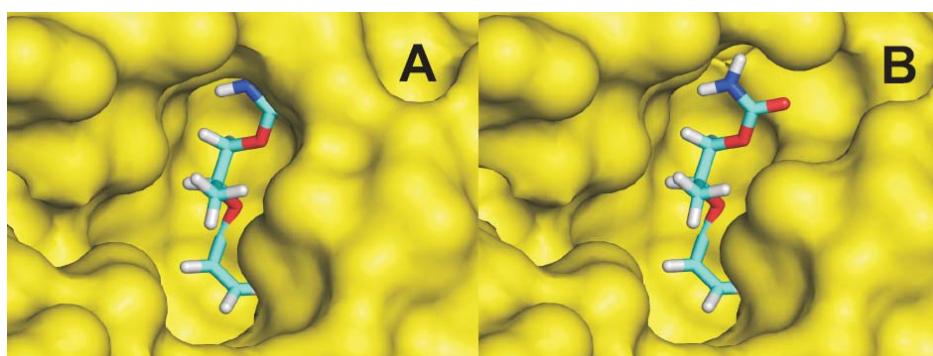


Figure 3.3: (A) Orientation of the slowly reacting *S*-enantiomer of the secondary alcohol (2hpca) in the wild-type and (B) in the mutant L278A (Troedler 2008).

Table 3.1: Docking scores determined by Peter Troedler (Troedler 2008) of 1hpca, 2hpca, 3hpca and 4hpca in CALB wild-type.

Substrate	found Conformations	Scoring
1hpca	79	- 3.89
2hpca	37	- 3.47
3hpca	58	- 4.69
4hpca	42	- 4.65

Table 3.2: Distance $d(H_{NE2}-O_{alc})$ determined by Peter Trodler (Trodler 2008) of 1hpca, 2hpca, 3hpca and 4hpca in a productive mode in CALB wild-type and mutant L278A.

	1hpca ^a	1hpca ^b	2hpca ^a	2hpca ^b	3hpca ^a	4hpca ^a
$d(H_{NE2}-O_{alc})$	2.1	2.0	2.4	2.1	2.0	1.9

^a in CALB wild-type. ^b in CALB mutant L278A.

3.1.2 Expression of *CALB* in the *E. coli* for library screening

3.1.2.1 Summary of functional expression of *CALB* in the *E. coli* cytoplasm

Functional expression of *CALB* in *E. coli* has been described previously (Liu 2006), therein we reported for the first time the functional expression of lipase B from the yeast *C. antarctica* (*CALB*) in the *E. coli* cytoplasm. The enzyme possessing three disulfide bonds has been functionally expressed in the strain Origami[®] B. Expression under the control of a *lac* promoter yielded 2 U/mg activities, whereas expression of a thioredoxin-*CALB* fusion protein yielded 17 U/mg activities. The native enzyme was most efficiently expressed under control of the *cspA* promoter (11 U/mg). Coexpression of different chaperones resulted in a strong increase in active protein formation (up to 61 U/mg). A codon-optimized synthetic variant of *CALB* did not show significant effects on functional protein yield. Functional *CALB* expression was not only achieved in shake flasks but also in microtiter plate scale. Therefore, this *CALB* expression system is suitable for high-throughput applications, including the screening of large gene libraries as those derived from directed evolution experiments.

3.1.2.2 Optimization of transformation efficiency for library creation

For library creation, PCR (2.2.1.6.3 and 2.2.1.6.4) was performed using plasmid (pColdIII_ *CALB_wild-type*) and degenerate primers (2.1.6: *CALB_W104X* and *CALB_L278X*). The PCR-product was digested using the enzyme *DpnI* and transformed using a chemical method (2.2.2.1.2) in Origami[®] B used as a good expression host for *CALB* (Liu 2006). However, the number of colonies on tributyrin LB agar plates with appropriate antibiotic was less than five colonies, although the total pellet from 1 ml culture was plated onto one plate, indicating the very low transformation efficiency when using competent cells Origami[®] B. Therefore, competent *E. coli* DH5 α with high transformation efficiency was applied for chemical transformation. The number of transformants was not considerably increased either,

4-10 colonies per plate were obtained. Electroporation (2.2.2.1.3) was therefore carried out using Origami[®] B and DH5 α as competent cells. The transformation efficiency for both cells was significantly increased, more than 1000 colonies per plate using 100 μ l cell cultures of Origami[®] B and more than 3000 colonies per plate of DH5 α have been observed. As a good expression system for *CALB* (Liu 2006), Origami[®] B was then selected for application in our work.

3.1.2.3 Increasing mutagenesis efficiency of library

After electroporation (2.2.2.1.3) of Origami[®] B competent cells with the PCR-product using the plasmid (pColdIII_ *CALB_wild-type*) and the degenerate primers (2.1.6: *CALB_W104X* and *CALB_L278X*), the quality of the library was checked by the percentage of mutants. For reaching high mutagenesis efficiency at both positions (W104X and L278X), sequential introduction of mutations (2.2.1.6.3) was performed. **Figure 3.4** shows the consecutive two-round PCR products (pColdIII_ *W104X* and pColdIII_ *L278X/W104X*) in 1% agarose gel. Clear bands of linearized PCR products can be observed at about 5.3 kb corresponding to the size of pColdIII_ *CALB*. After transformation with 1 μ l PCR products, ten colonies were sequenced. 50% of total colonies had mutations at position W104X and 60% at L278X, and only about 30% were observed to own mutations at both sites (**Table 3.3**).

In order to increase the mutagenesis efficiency, QuikChange[®] Multi Site-Directed Mutagenesis Kit (Stratagene) was applied, which provides high mutagenesis rate in several defined positions in one step. **Figure 3.4** (C) shows the PCR product of pColdIII_ *CALB_W104X/L278X* in 1% agarose gel when using this PCR method (2.2.1.6.4) and the plasmid (pColdIII_ *CALB_wild-type*) as well as the degenerate primers (2.1.6: *CALB_W104X* and *CALB_L278X*). Although the band of the linearized PCR product (pColdIII_ *CALB_W104X/L278X*) is not very distinct, 1 μ l PCR product was enough to create sufficient colonies for the library. Beside Origami[®] B, XL10-Gold[®] Ultracompetent Cells in the Kit was used as competent cells for electroporation (2.2.2.1.3). Ten colonies from each kind of competent cells were sequenced to check the mutation ratio at positions W104X and L278X. The results are summarized in **Table 3.3**. The single site mutations of W104X or L278X for Origami[®] B occurred in 70% and 50% of the clones respectively, and that for XL10-Gold[®] Ultracompetent Cells both were present in 90% of the clones. There were 3 colonies from Origami[®] B containing plasmid with mutations at both positions W104X and L278X, and 8 colonies from XL10-Gold[®] Ultracompetent Cells, i.e. 30% and 80% of the

clones were mutated at both positions in each kind of competent cells. The total amounts of mutants from Origami[®] B and XL10-Gold[®] Ultracompetent Cells are 90% and 100% respectively (**Table 3.3**). Although sequencing of only 10 colonies is not highly representative, it indicated that the mutagenesis efficiency was highly improved by that method (2.2.1.6.4). For library creation, the double-stranded plasmid DNA was prepared from the transformants of XL10-Gold[®] Ultracompetent Cells and then transformed again in Origami[®] B, as the Origami[®] B was a better expression system for *CALB* (Liu 2006).

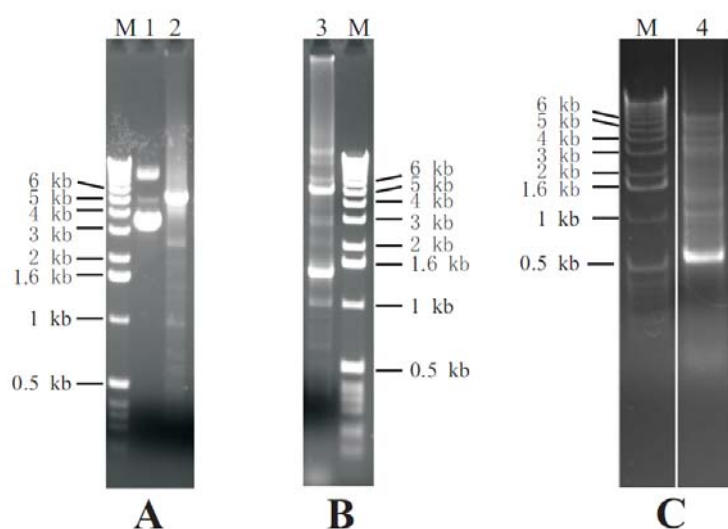


Figure 3.4: PCR products of sequential introduction of mutations (2.2.1.6.3) (A) using the plasmid (pColdIII_*CALB_wild-type*) and the degenerate primer (2.1.6: *CALB_W104X*) and (B) using the plasmid (pColdIII_*CALB_W104X*) and the degenerate primer (2.1.6: *CALB_L278X*) and (C) of two-site saturation mutagenesis created by the QuikChange[®] Multi Site-Directed Mutagenesis Kit (Stratagene) (2.2.1.6.4) using the plasmid (pColdIII_*CALB_wild-type*) and the degenerate primers (2.1.6: *CALB_W104X* and *CALB_L278X*). The linearized PCR products are 5.3 kb. M corresponds to 1 kb DNA ladder. 1: circularized template pColdIII_*CALB_wild-type*; 2: pColdIII_*CALB_W104X*; 3: pColdIII_*CALB_L278X/W104X* from sequential introduction of mutagenesis; 4: pColdIII_*CALB_L278X/W104X* from QuikChange[®] Multi Site-Directed Mutagenesis Kit.

Table 3.3: Comparison of the mutagenesis efficiency in Origami[®] B and XL10-Gold[®] Ultracompetent Cells.

	Sequential introduction of mutations	QuikChange [®] Multi Site-Directed Mutagenesis Kit	
	Origami [®] B	Origami [®] B	XL10-Gold [®] Ultracompetent Cells
W104X	50%	70%	90%
L278X	60%	50%	90%
W104X and L278X	30%	30%	80%
Mutations in 10 colonies	60%	90%	100%

3.1.2.4 Development and validation of a high-throughput assay for the created library

In order to screen mutant libraries for acrylated hpc (hpca) (**Figure 1.11**) and to characterize individual mutants, an assay (2.2.5.2) based on the hydrolysis of hpca was developed. This setup allows online monitoring of the reaction progress. In order to validate the assay, the wild-type *CALB* was expressed in *E. coli* Origami[®] B cells in microtiter plates. Using different amounts of CALB lysate, the maximum velocity (V_{max}) of corresponding reactions was in proportion to the amount of CALB used in the respective well. **Figure 3.5** shows that the correlation between the V_{max} and the concentrations with a double increasing series for CALB wild-type. This system was used in the following experiments to screen the mutant libraries and for characterization of mutated enzymes expressed by *P. pastoris*.

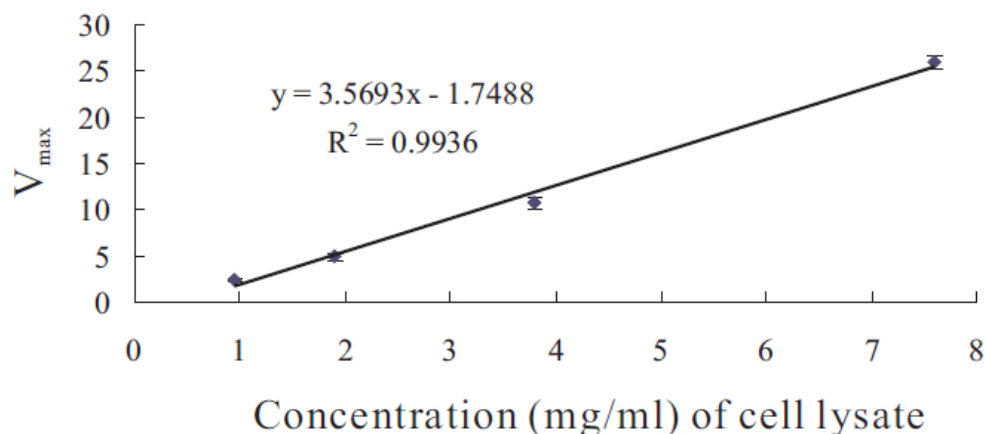


Figure 3.5: Validation of hpca assay (2.2.5.2) using 4 different concentrations (0.9, 1.9, 3.8 and 7.6 mg/ml) of wild-type CALB lysate from expression in *E. coli* Origami[®] B with a double fold serial dilution. The original concentration of cell lysate of wild-type CALB was 7.6 mg/ml, which was diluted 3 times and created the 4 different concentration of cell lysate. V_{max} indicated the activity ($\Delta A_{581} \cdot \text{min}^{-1}$) in the hpca hydrolysis and was defined as the absorption change (mili units) at 581 nm per minute. The deviations of the measurements were less than 5%. R^2 called the correlation coefficient indicates the strength of a linear relationship between two variables and judges the reliability of the regression straight line.

3.1.3 Modification of enzyme properties

3.1.3.1 Directed evolution using epPCR

Error-prone PCR (epPCR) can introduce random copying errors by adding different ratio of Mn^{2+} and/or Mg^{2+} to the reaction mixture of PCR. It has been proven to be useful to generate randomized libraries of nucleotide sequences (Cadwell and Joyce 1992). Therefore, we applied this method into our work to generate mutants with a higher activity towards hpc than wild-type CALB. After transformation of Origami[®] B and first screening with the tributyrin LB agar plates with appropriate amount of ampicillin, the number of colonies with clear halos, i.e. with active lipase, was too low to meet the quantitative need of a library for screening of a specific active lipase, leading to limited applicability of this library, although a mutant L278P with higher activity towards tributyrin than wild-type CALB was found.

3.1.3.2 Site-directed mutagenesis

In order to determine and compare the activity of CALB mutants at position 278 (Figure 3.6),

different mutations (L278Y, L278F, L278V and L278A) with progressively increasing sizes of the binding pocket for the secondary alcohol compared to the wild-type CALB were introduced separately through site-directed mutagenesis using pPICZ α A_CALB_wild-type as template (Trodler 2008). The protein variants were expressed in *P. pastoris* after transformation of *P. pastoris* using pPICZ α A_CALB_L278Y, _L278F, _L278V and _L278A respectively, the activities of the concentrated crude enzymes were measured and are summarized in **Table 3.4**. The increase of the size of the binding pocket was accompanied by a significant increase in the rate of hydrolysis of tributyrin, resulting in three to six fold higher activities as compared to the wild-type of CALB. Especially substitution of L278 by Ala had the strongest effect on the activity.

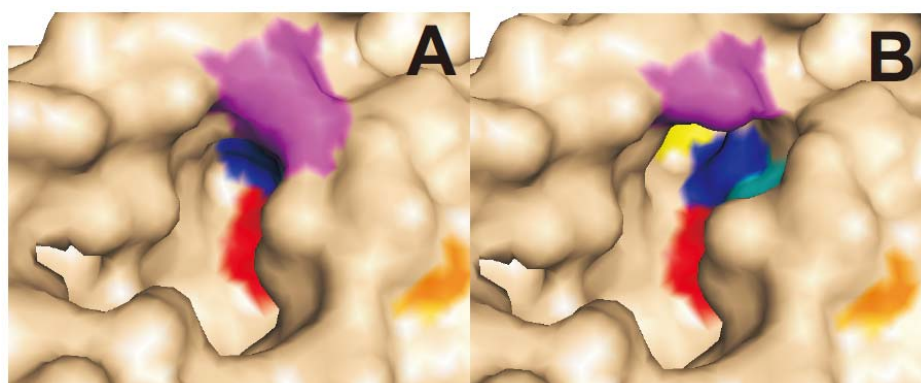


Figure 3.6: (A) Solvent accessible surface of the wild-type and (B) the mutant L278A/W104F/S47A. The residues of catalytic triad (S105, D187 and H224) were colored in red, orange and cyan respectively. The residue at position L278 was marked in purple, W104 in blue and S47 in yellow.

Table 3.4: Activity (Trodler 2008) of different CALB variants expressed in *P. pastoris* in tributyrin hydrolysis.

CALB variant	wild-type	L278Y	L278F	L278V	L278A
Activity (U/mg) ^a	740	710	2630	3573	4390

^a 1 U was defined as 1 μ mol/min in the hydrolysis of tributyrin. The deviations in the activity measurements were <5%.

For increasing the stereoselectivity pocket constituted by T42, S47 and W104 (**Figure 3.7**), mutants T42A, S47A, T42A/S47A and W104F suggested by the molecular modeling (3.1.1) were realized by site-directed mutagenesis (2.2.1.6.2). All those mutants were cloned (3.1.4.1), expressed and characterized in *P. pastoris*, described in the next chapter.

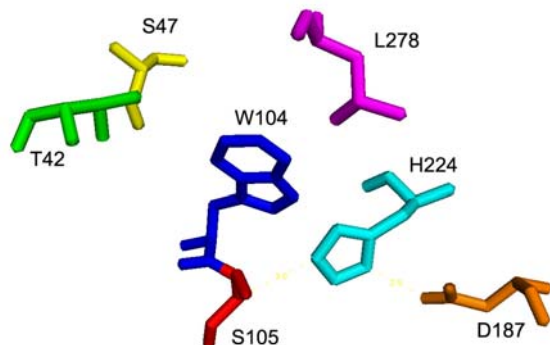


Figure 3.7: Residues around the CALB active site and stereoselectivity pocket. The residues of catalytic triad (S105, D187 and H224) were colored in red, orange and cyan respectively. The residue at position L278 was marked in purple, W104 in blue, T42 in green and S47 in yellow.

3.1.3.3 Saturation mutagenesis at positions L277, L278 and A281

For creation of the saturation mutagenesis library at positions 277, 278 and 281, the amino acid at each position should be substituted by the other 19 amino acids through saturation mutagenesis in which pColdIII_CALB_wild-type as template and degenerate primers (2.1.6) were used in the PCR (2.2.1.6.2). In the degenerate primers (2.1.6: CALB_SM277_278_281_fw and CALB_SM277_278_281_rev), NNB-codons were used at the positions 277, 278 and 281. Here, “N” is designated as “A”, “T”, “C” or “G” nucleotide, while “B” indicates “C”, “G” or “T” for reducing appearance of the stop codon and the number of colonies to be screened. After transformation by heat shock (2.2.2.1.2) with all PCR products (pColdIII_CALB_L277X_L278X_A281X) into Origami[®] B cells, colonies with clear halos on the LB-agar plates were transferred into the wells with LB medium and appropriate amount of ampicillin of the microtiter plates. Library L277X_L278X_A281X with about 400 colonies was thus constructed and screened using the hpca assay (2.2.5.2). A candidate with the highest activity, 76 $\Delta A_{581} \cdot \text{min}^{-1}$ ($\Delta A_{581} \cdot \text{min}^{-1}$ was defined as the absorption decrease (mili units) at 581 nm per minute), was sequenced and the result showed that the mutant was L278A. Due to the low transformation efficiency using the Origami[®] B competent cells and the chemical method, the number of the colonies statistically did not cover total mutants at positions 277, 278 and 281. Even so, L278A was proved to be the best mutant for the hpca hydrolysis

among the variants which had been screened. In the *hpcA* hydrolysis assay, the more yellow color of the corresponding reaction was proportional to the higher activity measured by the cell lysate of CALB variants. E.g. the corresponding color change resulted from the *hpcA* hydrolysis catalyzed by the cell lysate from the negative control pColdIII, positive control pColdIII_CALB_wild-type and the mutant pColdIII_CALB_L278A are presented in **Figure 3.8**. The purple of the pColdIII corresponds the activity of $2 \Delta A_{581} \cdot \text{min}^{-1}$, the orange of the pColdIII_CALB_wild-type of $28 \Delta A_{581} \cdot \text{min}^{-1}$ and the yellow of the pColdIII_CALB_L278A of $76 \Delta A_{581} \cdot \text{min}^{-1}$ respectively.



Figure 3.8: Photo representation after 30 min reaction in the microtiter plate of the *hpcA* hydrolysis catalyzed by the cell lysate of the empty vector pColdIII, CALB wild-type and mutant L278A. Purple indicates no activity, yellow indicates higher activity.

3.1.3.4 Two-site saturation mutagenesis library (L278X/W104X)

For creation of a two-site saturation mutagenesis library (L278X/W104X) PCR (2.2.1.6.4) was performed using the plasmid (pColdIII_CALB_wild-type) and the degenerate primers (2.1.6: CALB_W104X and CALB_L278X). Due to the low transformation efficiency using the Origami[®] B competent cells transformed by the chemical method (2.2.2.1.2, 3.1.2.2 and 3.1.3.3), the PCR product was transformed using XL10-Gold[®] Ultracompetent Cells in the QuikChange[®] Multi Site-Directed Mutagenesis Kit and then Origami[®] B cells as competent cells by the electroporation method (2.2.2.1.3) verified to improve the transformation (3.1.2.2) and mutagenesis efficiency (3.1.2.3). The library (L278X/W104X) was thus constructed using the QuikChange[®] Multi Site-Directed Mutagenesis Kit.

Sequencing of 20 clones out of 4000 of the library comprising 1400 members with halo on tributyrin plates, revealed that at both positions 90% of the plasmids carried the respective mutations, it could be thus expected that nearly 95% of possible combinations of mutations at positions 278 and 104 were covered by this library.

Screening of the library with the *hpcA* assay (2.2.5.2) resulted in identification of the mutant L278A, showing the highest activity ($76 \Delta A_{581} \cdot \text{min}^{-1}$) and three times higher activity than that of the wild-type ($28 \Delta A_{581} \cdot \text{min}^{-1}$) in the hydrolysis of *hpcA* (**Table 3.5**). Additionally, the activity ($58 \Delta A_{581} \cdot \text{min}^{-1}$) of the double mutant L278A/W104F was also increased in the

hydrolysis of hzca which was two times higher than the wild-type (**Table 3.5**). Both mutants were also selected for further characterization. Moreover, mutants L278E, L278C and W104Y also showed higher activity in the hzca assay than the wild-type CALB in a different degree. The color change due to the hzca hydrolysis catalyzed by these mutants was photographed and displayed in **Figure 3.9**. It can be seen that along with the increasing hydrolysis activity towards hzca the color is more yellow, i.e. more protons were released in the reaction. The wild-type shows only low activity in the assay (**Table 3.5**) and the corresponding color is deep orange (**Figure 3.9**). A negative control in **Table 3.5**, using the empty pColdIII vector, shows no detectable activity and therefore the corresponding color is purple.

Table 3.5: Comparison of hzca hydrolysis (2.2.5.2) measured by following the decrease in absorption at 581 nm of the pH indicator bromocresol purple. CALB wild-type and mutants were expressed in *E. coli* using the pColdIII vector. The deviations in the activity measurements were <5%.

	pColdIII ^a	wild-type ^a	W104Y ^a	L278E ^a	L278C ^a	L278A ^a	L278A/W104F ^a
$\Delta A_{581} \text{ min}^{-1b}$	2	28	35	42	39	76	58

^a Cell lysate from *E. coli* transformed with the empty vector pColdIII and pColdIII with *CALB_wild-type*, *L278E*, *L278C*, *W104Y*, *L278A* and *L278A_W104F* respectively.

^b $\Delta A_{581} \text{ min}^{-1}$ was defined as the absorption change (mili units) at 581 nm per minute.

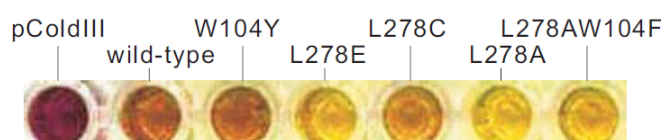


Figure 3.9: Color change of the pH indicator bromocresol purple due to the hzca hydrolysis catalyzed by *E.coli* cell lysate of CALB wild-type and the mutants. Color changing from purple to yellow indicates an increase of the corresponding activity of CALB variants.

3.1.4 Expression of *CALB* variants in *P. pastoris* and characterization

3.1.4.1 Subcloning of *CALB* variants into *P. pastoris*

For expression of *CALB* variants in *P. pastoris*, the gene *CALB* was subcloned from pColdIII_*CALB* into pPICZ α A vector (Invitrogen) (**Figure 3.10**). First, it was polymerized using the template (pColdIII_*CALB_wild-type*) and the primers (2.1.6: *CALB_EcoRI* and *CALB_NotI*). After digestion (2.2.1.8) of the PCR product with restriction endonucleases *EcoRI* and *NotI*, *CALB* was ligated (2.2.1.10) with the empty pPICZ α A vector digested with the same restriction endonucleases and then pPICZ α A_*CALB* was constructed after successful transformation of DH5 α and validation by sequencing. For secretion of the recombinant *CALB* variants into the medium by *P. pastoris* (2.2.2.2.3), α factor from *S. cerevisiae* was fused with the *CALB* gene under the control of 5'*AOXI* promoter, which is induced by methanol.

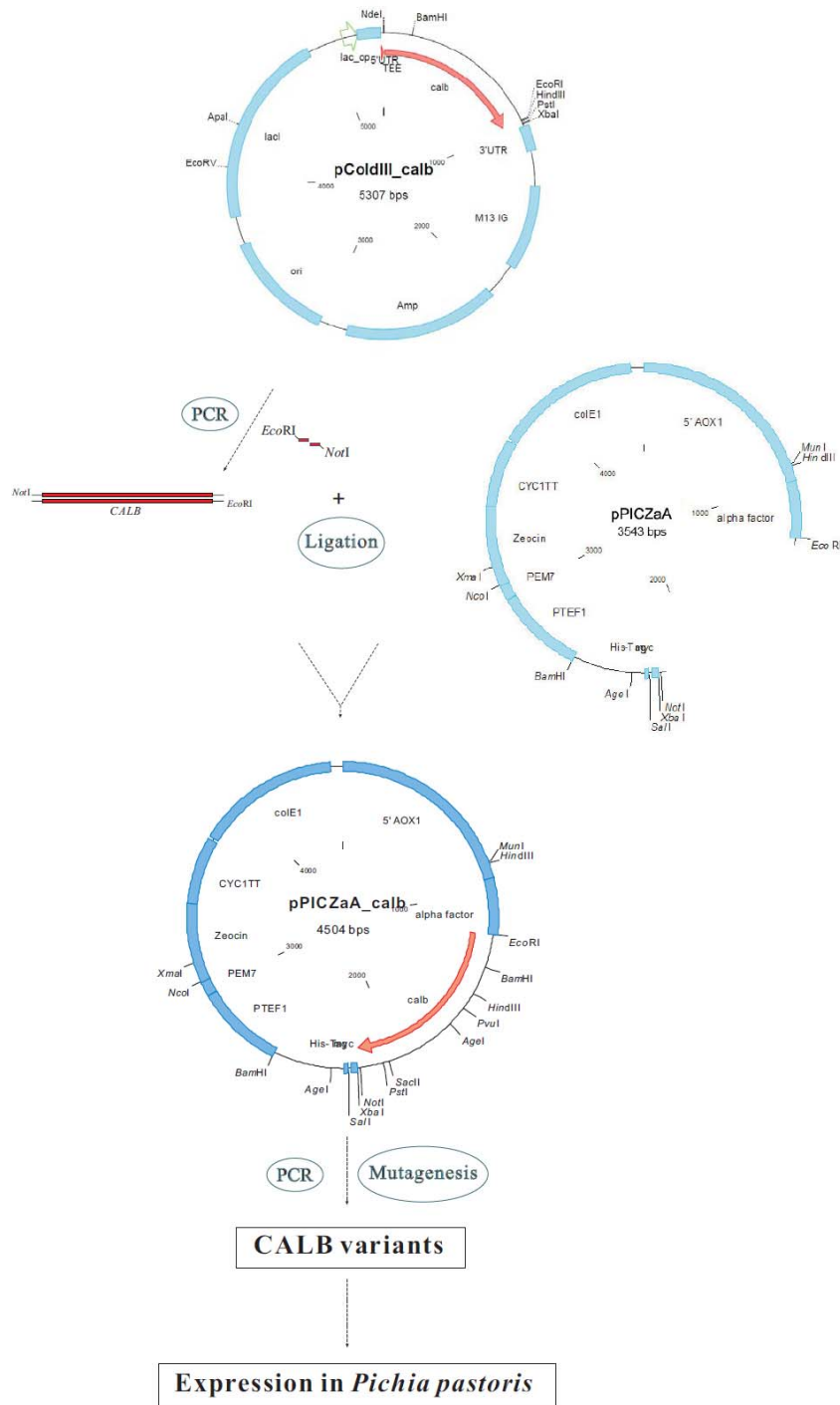


Figure 3.10: Overview of subcloning from pColdIII_CALB into pPICZαA_CALB, mutagenesis and expression of CALB variants in *P. pastoris*.

After subcloning (Figure 3.10) of *CALB* wild-type from pColdIII into pPICZαA that arose from our early projects (Rusnak 2004; Liu 2006), mutants T42A, S47A, T42A/S47A and W104F (3.1.3.2) were realized by site-directed mutagenesis (2.2.1.6.2) using the template (pPICZαA_CALB_wild-type) and the primers (2.1.6: *CALB_T42A*, *CALB_S47A*,

CALB_T42AS47A and *CALB_W104F* respectively). After successful transformation (2.2.2.2.2) of *P. pastoris*, the effect of these mutants T42A, S47A, T42A/S47A and W104F on activity and stereoselectivity through expression (2.2.2.2.3) in *P. pastoris* were investigated and described below. Mutants L278A and L278V were also constructed by site-directed mutagenesis (2.2.1.6.2) using the template (pPICZ α A_*CALB_wild-type*) and the primers (2.1.6: *CALB_L278A*, or *_L278V*). **Figure 3.11** shows a clear band of a PCR product using primers (*CALB_S47A_fw* and *CALB_S47A_rev*) in 1% agarose gel. The size of this band is about 4.5 kb and matches the expected size of linearized pPICZ α A_*CALB_S47A*. The other PCR products using other primers containing different mutations have the same size as pPICZ α A_*CALB_S47A*. Moreover, from the *E. coli* library screening, the mutant L278A/W104F showed higher activity than the wild-type and a possibly decreased stereoselectivity. For investigation of the single effects of positions W104 and S47 on hpcA formation, mutations L278A/S47A and L278A/W104F/S47A were constructed through site-directed mutagenesis (2.2.1.6.2). In order to get double mutations (*L278A/W104F* and *L278A/S47A*), sequential introduction of site-directed mutagenesis (2.2.1.6.3) was carried out. The first PCR was performed using pPICZ α A_*CALB_wild-type* as template and primers with *L278A* mutations, and the second round of PCR using pPICZ α A_*CALB_L278A* as template and primers (2.1.6) containing *W104F* or *S47A* mutations. The mutant *L278A/W104F/S47A* was also constructed using the site-directed mutagenesis PCR (2.2.1.6.2) using the template pPICZ α A_*CALB_L278A/W104F* and the primer with *S47A* mutation (2.1.6).

After transformation (2.2.2.1.2) of DH5 α and mutation validation by sequencing following *CALB* variants: T42A, S47A, T42A/S47A, W104F, L278A, L278V, L278A/W104F, L278A/S47A and L278A/W104F/S47A, were obtained. Through successful transformation (2.2.2.2.2) using those pPICZ α A_*CALB_variants* into *P. pastoris*, these variants were inserted into the genome of *P. pastoris*.

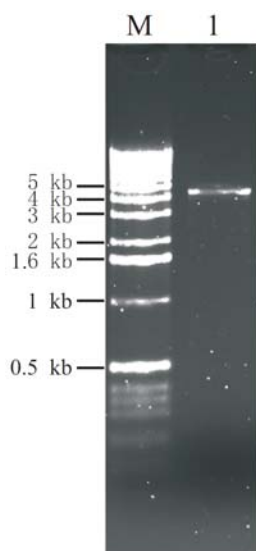


Figure 3.11: PCR product of linearized plasmid (pPICZ α A_CALB_S47A) using QuikChange[®] Site-Directed Mutagenesis Kit (Stratagene). The linearized PCR product is 4.5 kb. M corresponds to 1 kb DNA ladder. 1: pPICZ α A_CALB_S47A.

3.1.4.2 Expression of *CALB* variants in *P. pastoris*

The flow chart from subcloning of *CALB* gene to its expression in *P. pastoris* is illustrated in **Figure 3.10**. For expression of *CALB* variants in *P. pastoris*, six-ten transformants of each *CALB* variants were selected and cultured in 50 ml BMMY medium under the induction of 0.5% (v/v) methanol in shake flasks (2.2.2.2.3). One candidate with the highest specific activity towards tributyrin was cultured further in 200 ml BMMY medium under the induction of 0.5% (v/v) methanol in shake flasks. As a negative control, *P. pastoris* containing the empty vector was also cultivated and showed no activity. Expression and secretion of *CALB* wild-type and mutants L278A, L278V, L278A/W104F, L278A/W104F/S47A into the supernatant was analyzed by SDS-PAGE. A major band of 36 kDa is observed (**Figure 3.12**) and corresponds to the recombinant *CALB* secreted by *P. pastoris* (Rotticci-Mulder et al. 2001). Moreover, *CALB* variants T42A, S47A, T42A/S47A, W104F and L278A/S47A were also expressed in *P. pastoris*. The concentration of total protein in the supernatant was 110-200 mg/l. The expression level of these recombinant *CALB* variants was similar.

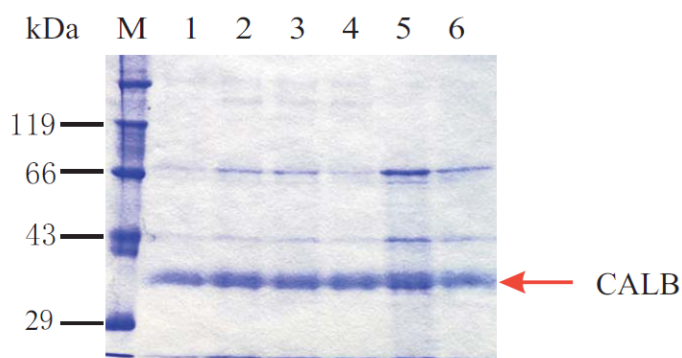


Figure 3.12: Coomassie blue stained SDS-PAGE analysis of recombinant CALB wild-type and variants produced in *P. pastoris*. The analysis was performed on a 12% SDS-PAGE. 2-4 μg of the total proteins of each supernatant of CALB variants cultivation was loaded onto each lane. M indicates protein molecular weight standards (Roti[®]-Mark STANDARD, ROTH). Lane 1: L278V; Lane 2: L278A/W104F/S47A; Lane 3: L278A/W104F; Lane 4: L278A; Lane 5: wild-type (4 μg) and Lane 6: wild-type (2 μg). Recombinant CALB is indicated by a red arrow.

3.1.4.3 Characterization of CALB variants

More than 50% of the protein in the supernatant of the recombinant *P. pastoris* strains was CALB as quantified by densitometric analysis using the program Scion Image (2.2.3.4). Nevertheless, samples of CALB wild-type and mutants had to be concentrated by the Amicon concentrator[™] (10 kDa membrane) (2.2.3.1), due to the high requirements of protein for immobilization. The specific activities of these lipases towards tributyrin and hpca are summarized in **Table 3.6**. L278A shows the highest activity (4390 U/mg) towards tributyrin and is 6 fold more active than the wild-type. Moreover, the specific activities of L278V, L278A/S47A, L278A/W104F, L278A/W104F/S47A, and S47A are all higher than the wild-type. However, T42A, T42A/S47A and W104F, in contrast to wild-type, exhibit a slightly lower activity towards tributyrin. Furthermore the CALB variants: L278A, L278A/S47A, L278A/W104F, L278A/W104F/S47A, show a higher hydrolysis activity towards hpca (2.2.5.2) in scale of 1 ml cuvette than the wild-type. Moreover, the enantioselectivity of CALB variants was measured using 1-phenylethylpropionate as substrate and analyzed by gas chromatography (Fisons instruments GC 8000) (2.2.5.3) and the corresponding results are shown in **Table 3.6** and compared in the following by the effects of amino acid positions.

Results

Table 3.6: Characterization of CALB variants expressed by *P. pastoris*.

CALB variant	Activity to tributyrin [U/mg] ^a	Activity to hpca [ΔA ₅₈₁ min ⁻¹ mg ⁻¹] ^b	E ^c
wild-type	740 ± 30	89 ± 3	> 300
T42A	494 ± 14	n.d. ^d	205
S47A	850 ± 29	64 ± 3	> 300
T42A/S47A	536 ± 16	n.d. ^d	216
W104F	500 ± 18	26 ± 1	30
L278V	3573 ± 171	n.d. ^d	n.d. ^d
L278A	4390 ± 204	195 ± 8	95
L278A/W104F	1770 ± 29	130 ± 3	4
L278A/S47A	1800 ± 55	207 ± 9	80
L278A/W104F/S47A	1618 ± 67	223 ± 11	5

^a Reaction mixture contained 5% (v/v) tributyrin emulsified in 2% aqueous gum arabic, water, and enzyme (concentrated sample of CALB cultivation) in a total volume of 20 ml. Rate of hydrolysis was determined at pH 7.5 and at room temperature by continuous titration of the liberated acids with a pH-stat (2.2.3.6.1). Activity expressed as units per milligram. One unit of hydrolase activity was defined as 1 μmol of acids released by enzyme per min under assay conditions.

^b Activity expressed as ΔA₅₈₁ per min in the hpca hydrolysis (2.2.5.2), ΔA₅₈₁ was defined as the absorption change at 581 nm.

^c Enantioselectivity (E) determined in hydrolysis of 1-phenylethylpropionate (2.2.5.3) and calculated according to the following equation (1.1.2.4.3):

$$E = \frac{\ln\left[\frac{1 - ee_s}{1 + ee_s / ee_p}\right]}{\ln\left[\frac{1 + ee_s}{1 + ee_s / ee_p}\right]}$$

^d n.d.: The activity and enantioselectivity were not determined.

Investigation of the effect of the variation at the position T42

From the results shown in **Table 3.6** it can be concluded that neither mutants T42A nor T42A/S47A improves the activity towards tributyrin. Their enantioselectivities are a little lower than of the wild-type, $E = 205$ and 216 respectively. The corresponding enantiomeric excess of the substrate (ee_s) and of the product (ee_p) being similar with that of the wild-type came up very soon to 1 (100%) and kept constantly even after 24 h (**Figure 3.13**), i.e. the enantioselectivity like the wild-type favored the *R*-enantiomer (*R*) over the *S*-enantiomer (*S*).

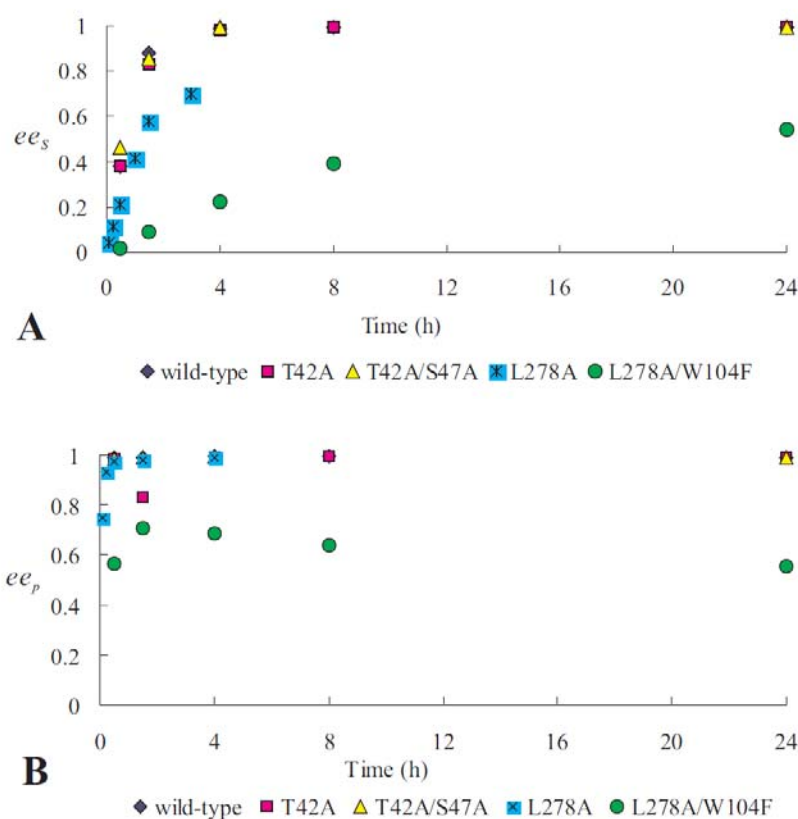


Figure 3.13: (A) The enantiomeric excess of the substrates (ee_s) and (B) of the product (ee_p). The CALB wild-type is colored blue, T42A red, T42A/S47A yellow, L278A cyan and L278A/W104F green.

Investigation of the effect of the variation at the position S47

By contrast to T42A, S47A improves somewhat activity towards tributyrin. Moreover, the effect of mutation at position 47 on the hpca and enantioselectivity was strongly dependent on the amino acids at positions 104 and 278. On the one hand, the single mutant S47A showed lower activity than the wild-type in the hpca hydrolysis and higher enantioselectivity ($E > 300$). On the other hand, the combination of S47A with L278A or the double mutant L278A/W104F led to a strong increase in hydrolysis rate towards both substrates (tributyrin and hpca), as well as decreased enantioselectivity ($E = 80$ and 5 respectively) (Table 3.6).

Investigation of the effect of variation at the position W104

The mutation W104F resulted in a lower enantioselectivity ($E = 30$) in comparison to the wild-type ($E = 300$) but lost some activity in hydrolysis of tributyrin and hpca (Table 3.6). When this mutation was combined with L278A, it showed considerably improved activity with 6-fold higher hpca hydrolysis rate than the wild-type. At the same time its enantioselectivity was further decreased from 30 to 4. From the Figure 3.13 it can be seen that L278A still prefers the *R*-enantiomer (*R*) to the *S*-enantiomer (*S*), although it strongly improved activity towards both tributyrin and hpca. However, the enantiomeric excess of the substrate (ee_s) for the double mutant L278A/W104F increased steadily to 0.5 and that of the product (ee_p) increased slightly to 0.7 in the first 2 h and then decreased slowly to 0.5, i.e. L278A/W104 has no strong bias towards the *R*-enantiomers and the stereoselectivity of CALB was then decreased. Thus, the effect of combination of mutations at position 278 (responsible for increased activity) and 104 (responsible for decreased stereoselectivity) was additive for the substrate hpca.

3.1.5 Immobilization of CALB variants

Lyophilized CALB showed no activity in the acrylation of hpc in organic solvents. Therefore, the wild-type and the mutants L278A, L278A/W104F and L278A/W104F/S47A were immobilized (2.2.4) on two hydrophobic carriers (MP1000, HP20L) to compare the activity in acrylation of hpc enantiomers.

The immobilization of CALB is shown in Table 3.7 for MP1000 and Table 3.8 for HP20L. After concentration with the Amicon concentrator, the CALB solution was diluted in buffer A containing 25% ethanol and sodium phosphate buffer at pH 6.0. This pH is in the scope of the isoelectric point (pI: pH 4 - pH 8) of CALB. The wide pI range was determined and evaluated using the Phast-system (Amersham Pharmacia Biotech) by Peter Trodler (Trodler 2008).

After addition of MP1000 or HP20L washed with 100% ethanol, immobilization was carried out for 40 h at 6°C (2.2.4). The final total protein loads of CALB wild-type as well as variants on MP1000 were between 0.4-0.7% (Table 3.7), and that on HP20L lay between 0.7-1.0% (Table 3.8).

Table 3.7: Immobilization of CALB on MP1000^a (2.2.4).

CALB	Concentrated enzyme ^b	Protein ^c		Filtrate ^d	MP1000	Protein ^e on MP1000	Total protein load ^f on MP1000	MP1000-Protein ^g (Protein)
		[ml]	[mg]					
wild-type	6.364	0.8	5.0	2.5	500	2.5	0.5	10 (50)
L278A	5.918	0.8	5.0	1.5	500	3.5	0.7	7 (50)
L278AW104F	8.054	0.6	5.0	3.0	500	2.0	0.4	13 (50)
L278AW104FS47A	2.901	1.7	5.0	2.5	500	2.5	0.5	10 (50)

^a Immobilization using 500 mg MP1000 was performed in 40 ml buffer for 40 h under stirring in cooling room (6°C). The immobilized enzyme was dried for 4 h in a fume hood.

^b Concentrated sample CALB cultivation using the Amicon concentrator.

^c The amount of protein from the concentrated sample CALB cultivation for immobilization.

^d The amount of protein from the washing solution after immobilization.

^e The amount of protein immobilized on MP1000.

^f mg protein per mg immobilizate in percent.

^g The amount of carrier with protein for the acrylation of hpc

Table 3.8: Immobilization of CALB on HP20L^a (2.2.4).

CALB	Concentrated enzyme ^b	Protein ^c		Filtrate ^d	Protein ^e on HP20L	HP20L	Total protein load ^f on HP20L	HP20L-Protein ^g (Protein)
	[mg/ml]	[ml]	[mg]	[mg]	[mg]	[mg]	[%]	[mg]([μg])
wild-type	2.226	3.19	7.1	1.5	5.6	600	0.9	6 (50)
L278A	2.331	3.17	7.4	1.6	5.8	600	1.0	5 (50)
L278AW104F	2.499	2.56	6.4	1.7	4.7	600	0.8	6 (50)
L278AW104FS47A	2.508	2.23	5.6	1.7	3.9	600	0.7	7 (50)

^a Immobilization using 600 mg carrier was performed in 40 ml buffer for 40 h under stirring in cooling room (6°C). The immobilized enzyme was dried for 4 h in a fume hood.

^b Concentrated sample CALB cultivation using the Amicon concentrator.

^c The amount of protein from the concentrated sample CALB cultivation for immobilization.

^d The amount of protein from the washing solution after immobilization.

^e The amount of protein immobilized on MP1000.

^f mg protein per mg immobilizate in percent.

^g The amount of carrier with protein for the acrylation of hpc

3.1.6 Acrylation of hpc catalyzed by CALB variants

For the activity measurement of CALB wild-type and mutants (L278A, L278A/W104F and L278A/W104F/S47A) in the acrylation of hpc with methyl acrylate (**Figure 1.11**), similar amount (about 50 μg shown in **Table 3.7** and **Table 3.8**) of CALB wild-type and variants immobilized on MP1000 and on HP20L were used in order to compare the activity of CALB variants and consider the carrier effect on activity. The time-dependent conversion to the products (hpcA) was analyzed by GC/MS measurements. It can be discerned in **Figure 3.14** that all mutants immobilized on MP1000 exhibit about 10-20% higher activity than the wild-type after three hours reaction. Mutants immobilized on HP20L exhibit 7-9% higher activity than the wild-type after one hour reaction and only 0-4% higher activity after three hours reaction. What is more interesting is the fact that using these mutants we could reach 90% conversion after 24 h (MP1000) and 29 h (HP20L), while the wild-type reached this level of conversion only after 48 h regardless of the used carrier material. This was in good agreement with the hypothesis from molecular modeling and the reliability of the two-site saturation mutagenesis library. The acrylation reaction by L278A, L278A/W104F and L278A/W104F/S47A showed a similar reaction rate. Both the double and triple mutants

contributed to full conversion by creating more space for all hpc enantiomers and decreased the enantioselectivity.

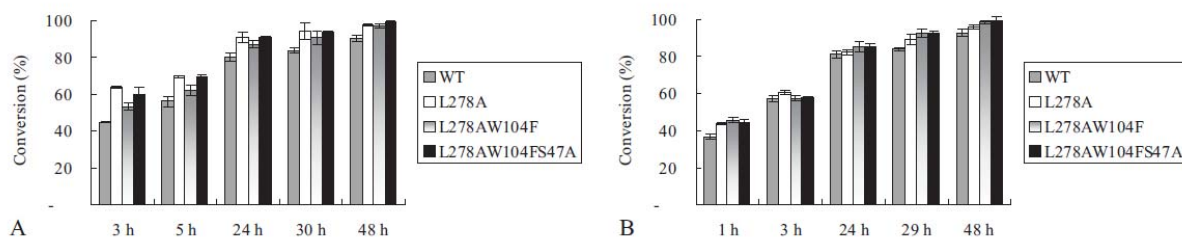


Figure 3.14: (A) Comparison of the acrylation (2.2.5.4) of hpc enantiomers of wild-type (WT) and the mutants of CALB immobilized on MP1000 and (B) on HP20L. Error bars indicate standard deviations from three independent experiments.

3.2 Cloning, expression and characterization of a cutinase from *A. brassicicola* for acrylation of 6-mercaptohexanol

A patented cutinase from *Humicola insolens* (*H. insolens*) showed high activity for the transesterification of methyl acrylate and amino- or mercaptoalcohol. For economical industrial applications, our work was to find a cutinase, which shows homology to the *H. insolens* cutinase (Hi_Cutinase) and exhibits also activity for the transesterification of methyl acrylate with amino- or mercaptoalcohol, which was 6-mercaptohexanol in our work.

3.2.1 Cloning of a cutinase from *A. brassicicola* in *P. pastoris*

3.2.1.1 Homology alignment and 3D structure of a cutinase from *A. brassicicola*

To search for a homologous protein with Hi_Cutinase, the amino acid sequence of this cutinase was used as a query for BLASTP in the NCBI BLAST databases. Eight protein candidates with high scores and low E-values were extracted from the Swiss-Prot database and aligned using Vector NTI Advance 10.3 from Invitrogen Corporation (**Figure 3.15**). It can be seen in **Figure 3.15** that the catalytic triad (Ser, His and Asp) (Ettinger et al. 1987; Martinez 1992) is conserved and that the stretch around the putative active site Ser G-G-Y-S-Q-G (Koeller and Kolattukudy 1982; Ettinger 1987) is also highly conserved in the investigated

cutinases. Moreover, four invariant cysteines (49, 129, 191 and 198) were conserved, forming two disulfide linkages in the cutinases (Ettinger 1987). According to the alignment of these cutinases, the protein sequence of a cutinase (pCUTAB1) from *A. brassicicola* (Albr) (YAO and Köller 1994) shared an identity of 61% with Hi_Cutinase. Additionally, it displayed the smallest distance in the corresponding phylogenetic tree (**Figure 3.15**).

The 3D structure of pCUTAB1 was deduced from an apo-cutinase (3DCN_A at a resolution of 1.9 Å) from *G. cingulata* (Nyon 2009), with a sequence identity of 67.7%, and visualized with PyMOL (**Figure 3.16**). In **Figure 3.16**, it can be seen that five parallel β -sheets are sandwiched by two α -helices on either side of the sheets. It shows clearly that pCUTAB1 belongs to the superfamily of α/β hydrolases, in which the catalytic triad (Ser, Asp and His) is located at one extremity of the protein ellipsoid and the nucleophilic Ser at the quite sharp turning point between β -sheet and α -helix (Longhi 1997a). It can also be noticed that the catalytic crevice of the cutinase is surrounded by two hydrophobic loops (79-86 and 179-187), in which hydrophobic amino acids (Leu, Gly, Ala Val, Pro and Ile) may compose the interfacial binding site. These amino acids are all found at homologous proteins (Martinez 1992; Jelsch et al. 1998). Despite of the possible existence of two side-chain bridges (shown in **Figure 3.16** (A)) of L80 with V183, and L181 with N83, the Ser of the catalytic triad of pCUTAB1 is not buried under the surface loops, however is accessible to solvent and substrate (**Figure 3.16**). The same features were found in other aligned cutinases too (Martinez 1992). Another interesting feature of the aligned cutinases is that the conserved S40 (pCUTAB1) (**Figure 3.15** and **Figure 3.16**), may stabilize the oxyanion hole of the cutinase (Nicolas 1996). From analysis of the alignment of cutinases and the deduced 3D conformational models, pCUTAB1 seemed to be the ideal candidate and was chosen for deeper investigation.

Results

A

		Section 1									
		1	10	20	30	40	50	55			
Huin	(1)	-----GAIENGLESGSANACPDAILL									
Fuso1	(1)	-----LPTSNPAQELEARQLGRTTRDDLINGNSASCADVIFI									
Fuso2	(1)	-----LPTSNPAQELEARQLERTTRDDLINGNSASCADVIFI									
Glc1	(1)	-----AM---AISDPQSSTRNELETGSSSACPVIYI									
Glc1i	(1)	MKFLSVLSLAITLAAAAPVEVETGV---ALETRQSSTRNELETGSSSACPVIYI									
Coca	(1)	MKFLSIIISLAVSLVAAAAPVEVGLDTGVANLEARQSSTRNELESSSSNCPKVIYI									
Magr	(1)	MQFITVALTLIALASASPIATNVEKPSPEARQLNSVRNDLISGNAAACP SVILI									
Albr	(1)	-----MMNLNLLLSKPCQASTTRNELETGSSDACPRTIFI									
Dira	(1)	---MKFFAFSMLIGEASPIVLALRRTTLEVRQLDPIIRSELEQGSSSSCPKAILI									
Consensus	(1)	TRNELE GSS ACP VI I									
† Section 2											
		(56) 56	70	80	90	100	110				
Huin	(22)	FARGSTEPGNMGITVGFALANGLESHI--RNIIWVQVGGPYDAALATNFI-ERGT									
Fuso1	(38)	YARGSTETGNLG-TLGP S IASNLES AFGKDG V W I Q V G G A Y R A T L G D N F I - E R G T									
Fuso2	(38)	FARGSTETGNLG-TLGP S IASNLES AFGKDG V W I Q V G G A Y R A T L G D N A L - E R G T									
Glc1	(30)	FARASTE PGNMGI SAGPIVADALERIYGANDVWVQVGGPYLADLASNFL-EDGT									
Glc1i	(53)	FARASTE PGNMGI SAGPIVADALERIYGANNVWVQVGGPYLADLASNFL-EDGT									
Coca	(56)	FARASTE PGNMGI SAGPIVADALESRYGASQVWVQVGGPYSDLASNFIIEGT									
Magr	(56)	FARASGEVGNMGLSAGTINVASALEREFR-NDI W V Q V G D P Y D A A L S P N F I - E A G T									
Albr	(36)	FARGSTEAGNMGALVGF TANALESAYGASNWVQVGGPYTAGLVENAL-ERGT									
Dira	(53)	FARGSTEIGNMGV SAGPAVASALEAYG-ADQI W V Q V G G P Y T A D L P S N F I - E G G T									
Consensus	(56)	FARGSTE GNMG SAGP VA ALES GA V W V Q V G G P Y A L N F L P G T									
Section 3											
		(111) 111	120	130	140	150	165				
Huin	(74)	SQANI DEGKRLFALANQKCPNTPV VAGGYSQGAALIAAAVSEL S GAVKEQVKGVA									
Fuso1	(91)	SSAAIREMLGLFQQANTKCPDATLIAGGYSQGAALAAASIEDLDSAIRDKIAGTV									
Fuso2	(91)	SSAAIREMLGLFQQANTKCPDATLIAGGYSQGAALAAASIEDLDSAIRDKIAGTV									
Glc1	(84)	SSAAINEARRLETLANTKCPNAAIVSGGYSQGTAVMAGSISGLSTTIKNQIKGVV									
Glc1i	(107)	SSAAINEARRLETLANTKCPNAAIVSGGYSQGTAVMAGSISGLSTTIKNQIKGVV									
Coca	(111)	SRVAINEAKRLFTLANTKCPNSAVVAGGYSQGTAVMASSISELSSTIQNQIKGVV									
Magr	(109)	TQGAIDEAKRMTLANTKCPNAAVVAGGYSQGTAVMFNAVSEMPAAVQDQIKGVV									
Albr	(90)	SQAAIREAQRLENLAASKCPNTPITAGGYSQGAAVMSNAIPGLSAAVQDQIKGVV									
Dira	(106)	SQSAINEAVRLENEANTKCESTPIVAGGYSQGTAVMAGAI PKLD-AVRARVVGTV									
Consensus	(111)	S AAI EA RLF LANTKCPNA VAGGYSQGTAVMA SIS LS AI QIKGVV									
† * † * †											
Section 4											
		(166) 166	180	190	200	210	220				
Huin	(129)	LFGYTKNLQNRGGIPNYPRERTKVF CNVGDVAVCTGTLIITPAHLSY TIEARGEHA									
Fuso1	(146)	LFGYTKNLQNRGRIPNYPADRTKVF CNTGDLVCTGSLIVAAPHLAYGPDARGPAP									
Fuso2	(146)	LFGYTKNLQNRGRIPNYPADRTKVF CNTGDLVCTGSLIVAAPHLAYGPDARGPAP									
Glc1	(139)	LFGYTKNLQNLGRIPNFETS KTEVYCDIADAVCYGTLFILPAHFLYQTDAAVAAP									
Glc1i	(162)	LFGYTKNLQNLGRIPNFETS KTEVYCDIADAVCYGTLFILPAHFLYQTDAAVAAP									
Coca	(166)	LSAITKNLQNLGRIPNFETS KTEVYCALADAVCYGTLFILPAHFLYQADAAATSAP									
Magr	(164)	LFGYTKNLQNRGRIPDFPTEKTEVYCNASDAVCFGTLFLLPAHFLYTTSESSAAP									
Albr	(145)	LFGYTKNLQNGRIPNFPTS KTTIYCETGDLVCGTLIITPAHL LYSDEAAVQAP									
Dira	(160)	LFGYTKNLQNNKGIKDYEQEDLQVYCEVGDVAVCTGTLIITVSHFLYLEEAAGEAP									
Consensus	(166)	LFGYTKNLQN GRIPNFPT KT VYC GDAVC GTLII PAHFLY DAA AP									
† * † * †											
Section 5											
		(221) 221	234								
Huin	(184)	RFLRDRIRA-----									
Fuso1	(201)	EFLIEKVRVVRGSA									
Fuso2	(201)	EFLIEKVRVVRGSA									
Glc1	(194)	RFLQARTIG-----									
Glc1i	(217)	RFLQARTIG-----									
Coca	(221)	RFLAARTIG-----									
Magr	(219)	NWLIRQIRA-----									
Albr	(200)	TFLRAQIDSA-----									
Dira	(215)	EFLKSKLGA-----									
Consensus	(221)	FL I A									

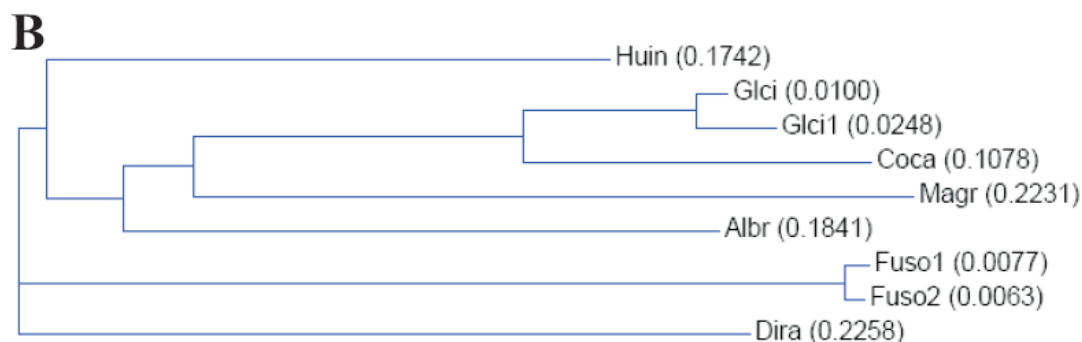


Figure 3.15: (A) Sequence alignment and (B) phylogenetic analysis of *Humicola insolens* cutinase and other fungal cutinases. It was performed using Vector NTI Advance 10.3 from Invitrogen Corporation. Cutinase sources: Huin, *Humicola insolens*, Hi_Cutinase; Fuso1, *Fusarium solani* cutinase A85F mutant, 1CUV_A; Fuso2, *Fusarium solani* cutinase T38F mutant, 1XZJ_A; Glci, *Glomerella cingulata*, Apo Cutinase Chain A, 3DCN_A; Glci1, *Glomerella cingulata*, P11373; Coca, *Colletotrichum capsic* CUTI_COLCA, P10951; Magr, *Magnaporthe grisea*, XP365241; Albr, *Alternaria brassicicola*, P41744; Dira, *Didymella rabiei*, P29292. Identical residues are highlighted in yellow and non-identical conservative in blue. The residues of the conserved catalytic triad (Ser, His and Asp) are marked with (*), while (†) indicates conserved cysteines. The conserved Ser in the oxyanion hole of the cutinases is marked with (:).

Table 3.9: Identity and distance in the phylogenetic tree to Hi_Cutinase calculated using Vector NTI Advance 10.3 from Invitrogen Corporation.

Percentage (%)	Fuso1 ^a	Fuso2 ^a	Glci ^a	Glci1 ^a	Coca ^a	Magr ^a	Albr ^a	Dira ^a
Identity	56	56	58	58	57	59	61	59
Distance	44	44	42	42	43	41	39	41

^a Cutinase sources: Fuso1, *Fusarium solani* cutinase A85F mutant, 1CUV_A; Fuso2, *Fusarium solani* cutinase T38F mutant, 1XZJ_A; Glci, *Glomerella cingulata*, Apo Cutinase Chain A, 3DCN_A; Glci1, *Glomerella cingulata*, P11373; Coca, *Colletotrichum capsic* CUTI_COLCA, P10951; Magr, *Magnaporthe grisea*, XP365241; Albr, *Alternaria brassicicola*, P41744; Dira, *Didymella rabiei*, P29292.

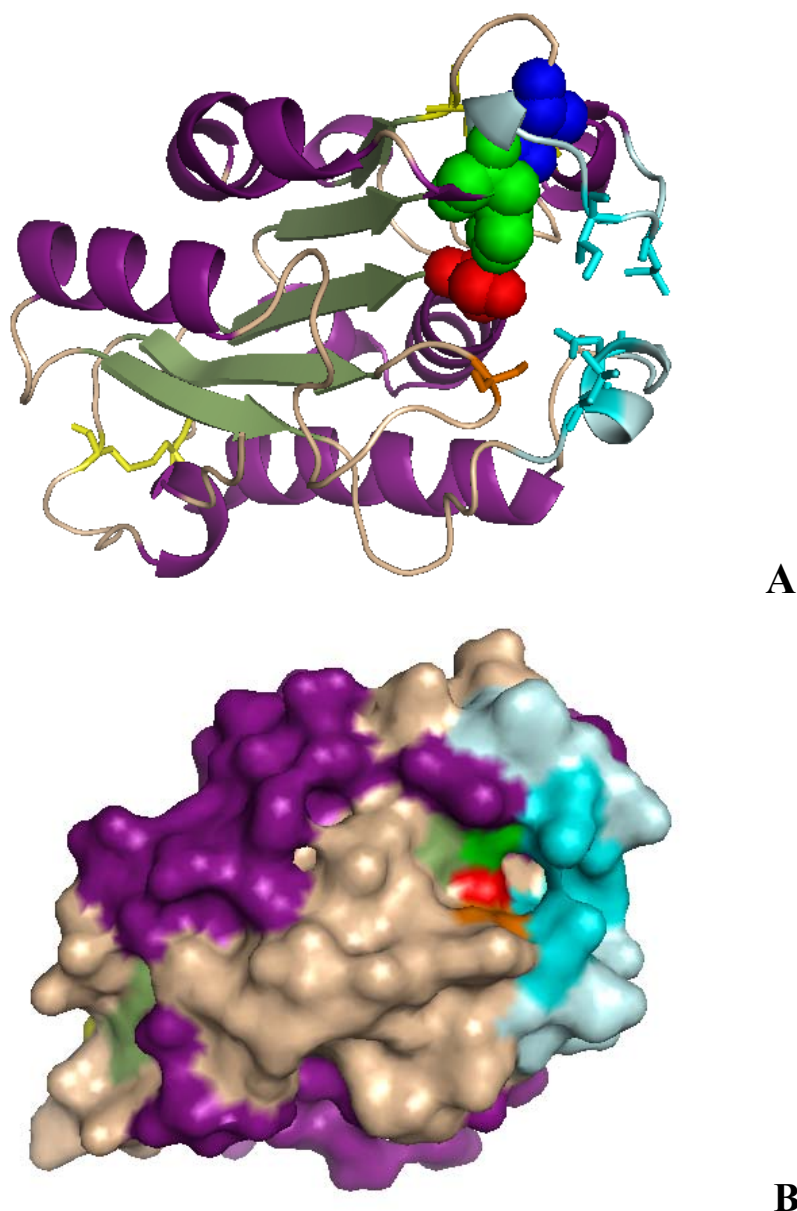


Figure 3.16: 3D structures of pCUTAB1 deduced using SWISS MODEL (Guex and Peitsch 1997; Melo and Feytmans 1998; Schwede T 2003; Arnold K. 2006) and visualized with PyMOL (DeLano 2002). The template for modelling is the apo-cutinase (3DCN_A) from *Glomerella cingulata* (Nyon 2009). The α -helices of pCUTAB1 are colored in deep purple; β -sheets in green and loops in wheat. The residues of the catalytic triad (Ser, red; His, blue green; Asp, blue) are represented in CPK. The conserved Ser in the oxyanion hole of the cutinase is represented with sticks and colored in orange. The residues in the two possible hydrophobic loops located near the active crevice are depicted in pale cyan. Two conserved side-chain bridges of L80 with V183, and L181 with N83 of pCUTAB1 are shown in sticks and marked in cyan. The cysteines are shown as yellow sticks. (A): Cartoon structure of pCUTAB1 molecule. (B): Solvent accessible surface of the deduced pCUTAB1 structure.

3.2.1.2 Cloning of *CUTAB1* in pPICZ α A

For expression of the cutinase from *A. brassicicola* in *P. pastoris*, the corresponding gene *CUTAB1* had to be cloned in the methanol-inducible expression vector pPICZ α A from Invitrogen™ (Figure 3.17). As *A. brassicicola* is a eukaryotic organism, many of its genes contain a combination of exons and introns. The intron of the cutinase from *A. brassicicola* was shown in Figure 3.18. Therefore, it is more suitable to use the mRNA as a template to synthesize cDNA using reverse transcriptase (2.2.1.5) and Oligo(dT)₁₂₋₁₈ by standard protocol (QIAGEN™), as here the introns have been excised. Total RNA was purified by the protocol of the RNasy® Plant Mini Kit (QIAGEN™) after several days of specific induction of *A. brassicicola* with cutin monomers (16-hydroxyhexadecanoic acid) (Fan and Köller 1998). After reverse transcription from mRNA to cDNA (2.2.1.5), *CUTAB1* was amplified from cDNA using primer (2.1.6: *CUTAB1_EcoRI_fw* and *CUTAB1_NotI_rev*). Figure 3.19 shows the PCR product (637 bp) of *CUTAB1* and the vector pPICZ α A_*CALB* (pPICZ α A containing the gene of the Lipase *CALB*) both digested with *EcoRI* and *NotI*. After digestion (2.2.1.8) of the PCR product (Figure 3.19) with restriction endonucleases *EcoRI* and *NotI*, *CUTAB1* was ligated (2.2.1.10) with the empty pPICZ α A vector (3543 bp) digested with the same restriction endonucleases and then pPICZ α A_*CUTAB1* was constructed after successful transformation of DH5 α and validation by sequencing. The *CUTAB1* gene contains a sequence of a potential native signal peptide of the cutinase pCUTAB1 from *A. brassicicola*. We did not know if the potential native signal peptide of pCUTAB1 shows a function in secretion of recombinant protein in *P. pastoris* or not. Therefore, for secretion of the recombinant pCUTAB1 into the medium of *P. pastoris* (2.2.2.2.3), α factor from *S. cerevisiae* was fused together with the *CUTAB1* gene under the control of 5' *AOX1* promoter, which is induced by methanol.

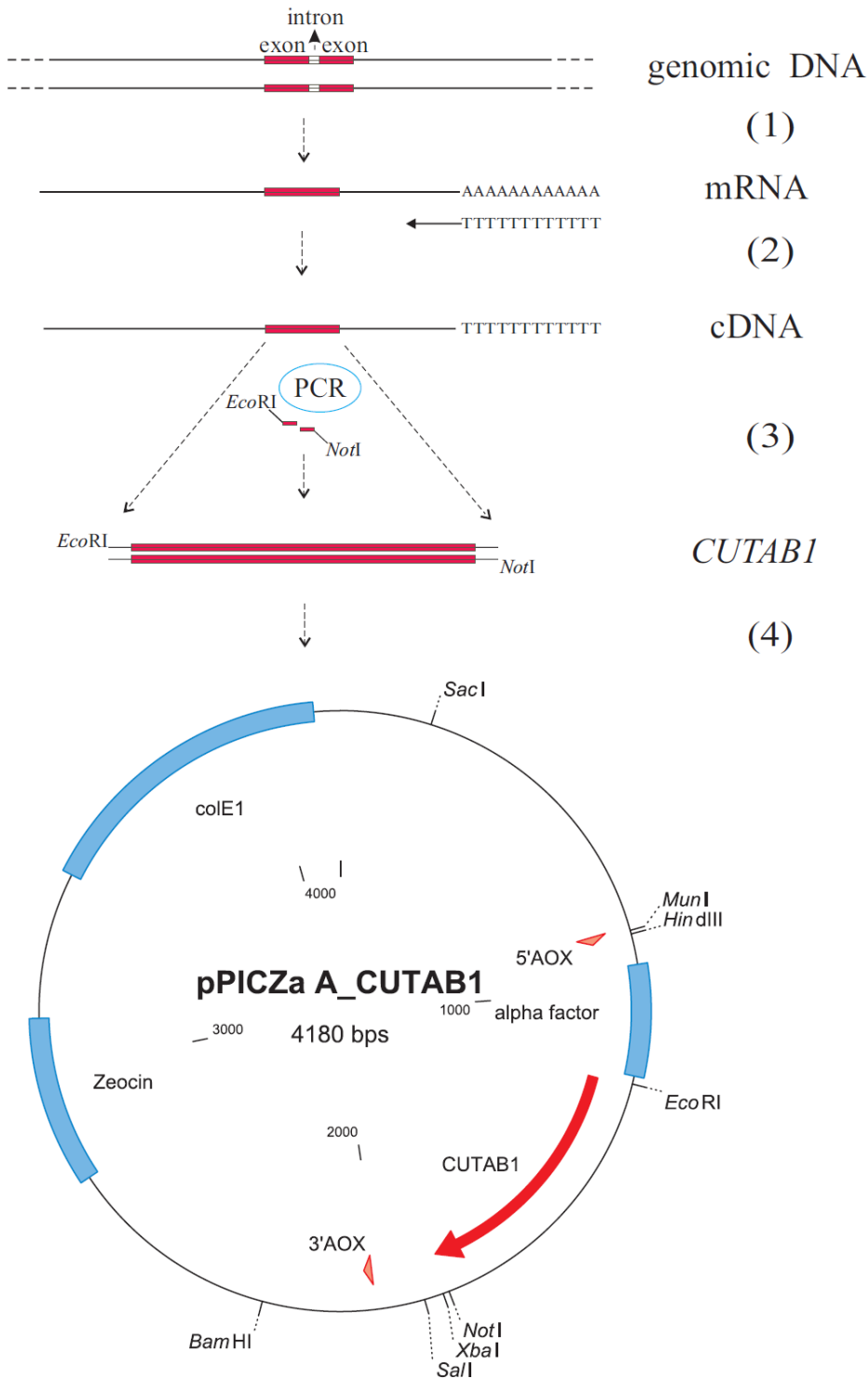


Figure 3.17: Cloning of *CUTAB1* in pPICZαA. (1) Transcription of genomic DNA of *A. brassicicola* to mRNA after induction by cutin monomers. (2) Reverse transcription from mRNA to cDNA. (3) Cutinase gene (*CUTAB1*) synthesis by PCR using two primers containing restriction sites of *EcoRI* and *NotI* respectively. (4) Construction of pPICZαA_ *CUTAB1* for expression in *P. pastoris* by insertion of *CUTAB1* in pPICZαA after digestion with restriction enzymes *EcoRI* and *NotI*.

Results

```
1  ATGATGAACC TCAACTTGTT ACTCTCGAAG CCCTGTCAGG CTAGTACTAC CAGAAACGAG
   >>.....CUTAB1.....>
   m m n l n l l l s k p c q a s t t r n e
61  CTTGAAACGG GAAGCAGCGA TGCTTGCCCA CGCACCATCT TCATCTTCGC AAGGGGAAGC
   >.....CUTAB1.....>
   l e t g s s d a c p r t i f i f a r g s
121 ACTGAAGCTG GAAACATGGT GAGTACAAGC AAATTCTCTA CAGACTCCTC CATAACAGCA
      intron
   >.....CUTAB1.....>
   t e a g n m
181 ATTAACCATC ACAGGGCGCA CTCGTCGGTC CCTTCACAGC AAACGCCCTC GAGAGCGCGT
      >>.....CUTAB1.....>
      g a l v g p f t a n a l e s a
241 ATGGGGCATC CAATGTTTGG GTCCAGGGCG TAGGTGGCCC CTATACCGCC GGTCTCGTAG
   >.....CUTAB1.....>
   y g a s n v w v q g v g g p y t a g l v
301 AGAATGCCCT TCCAGCCGGT ACTTCTCAAG CCGCCATCCG CGAAGCCCAG CGCCTCTTCA
   >.....CUTAB1.....>
   e n a l p a g t s q a a i r e a q r l f
361 ATCTCGCCGC AAGCAAATGC CCCAATACCC CCATCACTGC CGGTGGTTAC TCTCAAGGTG
   >.....CUTAB1.....>
   n l a a s k c p n t p i t a g g y s q g
421 CTGCAGTCAT GTCCAACGCG ATCCCCGGTC TCAGCGCTGC CGTACAAGAC CAAATCAAGG
   >.....CUTAB1.....>
   a a v m s n a i p g l s a a v q d q i k
481 GTGTCGTGTT GTTCGGCTAC ACTAAGAACT TGCAAATGG AGGGAGGATT CCAAACCTTC
   >.....CUTAB1.....>
   g v v l f g y t k n l q n g g r i p n f
541 CTACCAGCAA GACGACGATC TACTGTGAAA CCGGGGACTT GGTTCGCAAC GGTACACTGA
   >.....CUTAB1.....>
   p t s k t t i y c e t g d l v c n g t l
601 TCATCACGCC TGCGCATCTC CTGTACTCGG ATGAAGCTGC TGTGCAGGCA CCTACCTTCT
   >.....CUTAB1.....>
   i i t p a h l l y s d e a a v q a p t f
661 TGAGGGCTCA GATTGACTCA GCATAG
   >.....CUTAB1.....>
   l r a q i d s a -
```

Figure 3.18: Nucleotide sequence containing the intron (marked in green) and the two exons (denoted with CUTAB1) of the gene *CUTAB1* and the translated amino acid sequence.

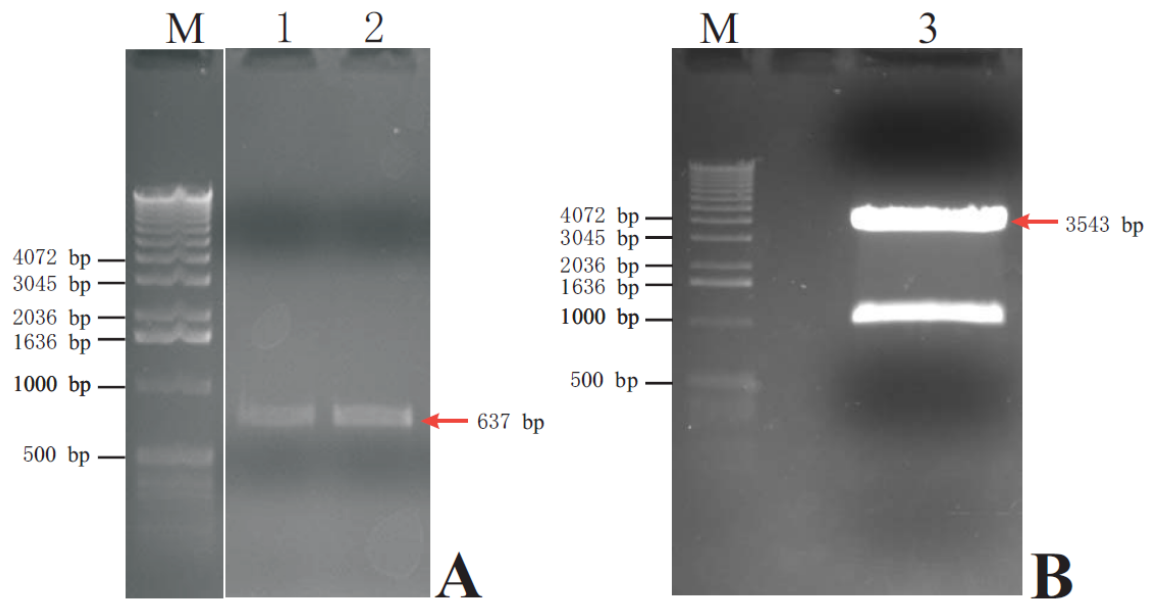


Figure 3.19: (A) PCR product (*CUTAB1*, 637 bp) and (B) Restriction of vector (pPICZαA, 3543 bp) from pPICZαA_CALB. M: 1 kb DNA marker; 1: undigested PCR product amplified from cDNA of *A. brassicicola*; 2: PCR product digested with *EcoRI* and *NotI*; 3: pPICZαA digested with *EcoRI* and *NotI*.

3.2.2 Expression of *CUTAB1* in *P. pastoris*

To overcome problems (like the inability to perform post-translational modifications) with expression of eukaryotic genes often observed in *E. coli*, *P. pastoris* X-33 was used as expression host. **Figure 3.20** shows the total experimental process from cloning of *CUTAB1* to its expression in *P. pastoris* X-33.

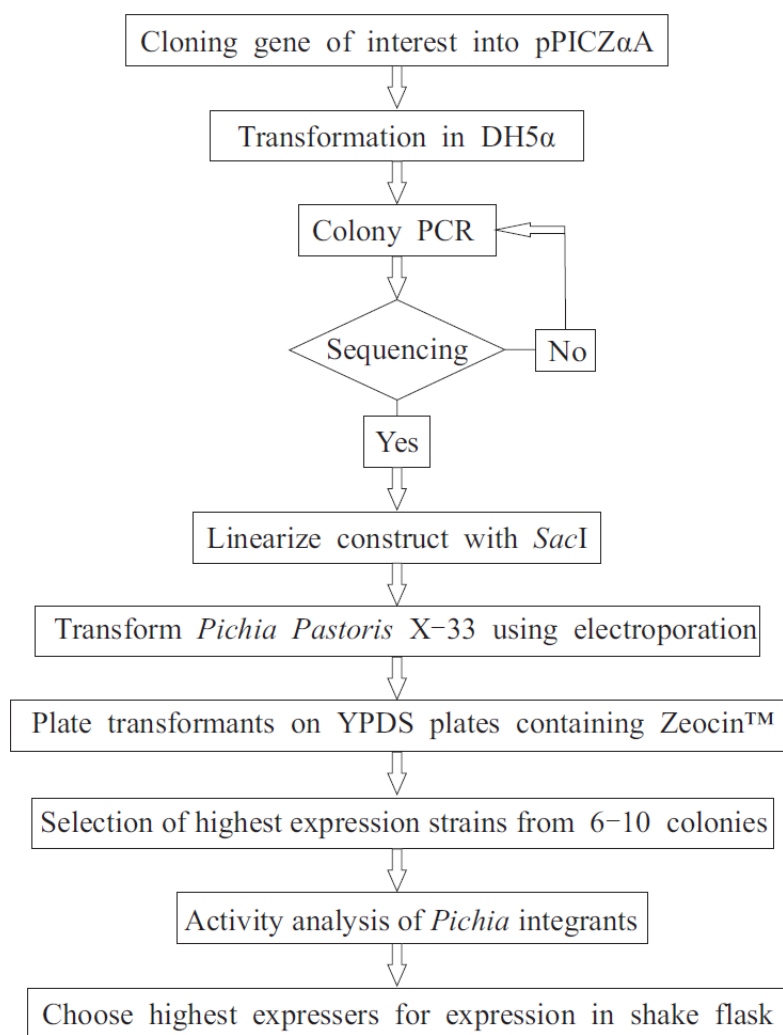


Figure 3.20: The total experimental process from cloning of *CUTAB1* to its expression in *P. pastoris* X-33.

3.2.2.1 Selection of highest expression strains for expression in small batch experimental shake flask

As shown in **Figure 3.20**, *P. pastoris* X-33 was transformed with the plasmid DNA (pPICZ α A_*CUTAB1*) linearized using the enzyme *SacI* after the successful cloning of *CUTAB1* confirmed by sequencing. Ten recombinants (colonies: A-J) from YPDS plates containing Zeocin™ were selected for small-scale expression to choose one producing cutinase. The recombinant p*CUTAB1* from colony A showed the highest volumetric activities towards both *pNPB* and *pNPP*, 396 U/ml and 2 U/ml respectively. This *P. pastoris* colony was then chosen for expression of *CUTAB1* in 2 x 200 ml shake flasks and characterized further.

3.2.2.2 Expression of *CUTAB1*

For expression (2.2.2.2.3) of *CUTAB1* in *P. pastoris*, the *P. pastoris* colony containing the gene *CUTAB1* was inoculated in 10 ml BMGY medium with Zeozin™ until culture reached an $OD_{600} = 5-15$. The cell pellet from centrifuging the culture was resuspended in 200 ml BMMY medium with 0.5% (v/v) methanol to induce expression of the gene. *P. pastoris* containing the empty vector was also cultivated as negative control. Expression during 5 days and secretion of the enzyme into the supernatant was observed by SDS-PAGE. Lane 3 and Lane 4 in **Figure 3.21** show only one thick band (≈ 24 kDa), which corresponds to the recombinant pCUTAB1. Due to the glycosylation (discussed below), the molecular mass (≈ 24 kDa) of the secreted pCUTAB1 was higher than the published mass of 21 kDa with a potential signal peptide (YAO and Köller 1994). The molecular mass of pCUTAB1 without the potential signal peptide and glycosylation should be 20 kDa. After concentration (2.2.3.1) with the Amicon concentrator™ (10 kDa membrane), smaller proteins (< 10 kDa) in the medium, e.g. peptides, were excluded and the band of pCUTAB1 from the concentrated supernatant appeared clearer (**Figure 3.21**, Lane 4). The hydrolytic activity of pCUTAB1 from crude, concentrated supernatant as well as from purified pCUTAB1 (discussed in next chapter) was measured using *p*NPP (**Table 3.10**). After concentration with exclusion of peptides from medium, the specific activities of pCUTAB1 increased 1.1-fold towards *p*NPP to 12 U/mg.

Table 3.10: Activity of pCUTAB1 produced in *P. pastoris* towards *p*NPP.

pCUTAB1	[ml] ^b	[mg/ml] ^c	[mg] ^d	<i>p</i> NPP ^a				
				Total activity [U]	Activity [U/ml]	Specific activity [U/mg]	Yield [%]	Purification factor
Crude supernatant	380	0.224	85	887	2	10	100	1
Concentrated supernatant	5	15.000	68	776	172	12	88	1.1
Purified pCUTAB1	108	0.337	36	623	6	17	70	1.6

^a Reaction mixture contained 0.65 mM *p*NPP as substrate sonically dispersed in 0.5% Triton X-100, 0.1% aqueous gum arabic, 0.1 M Tris-HCl pH 8, water, and enzyme in a total volume of 1 ml. Rate of hydrolysis was determined by spectrophotometer (2.2.3.6.2). 1 U was defined as turnover of 1 μ mol substrate per minute.

^b Volume of the protein solution [ml].

^c Concentration of protein [mg/ml].

^d Total amount of protein [mg].

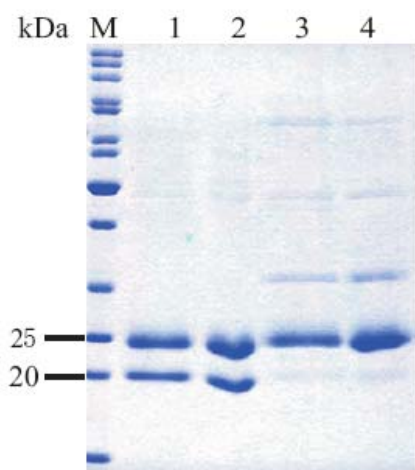


Figure 3.21: Coomassie blue stained SDS-PAGE analysis of pCUTAB1 produced in *P. pastoris* and purified. SDS-PAGE was performed on a 12% polyacrylamide gel. 2-4 μg of the total protein of the culture supernatant or purified pCUTAB1 was loaded on each lane. M indicates protein molecular weight standards (2.2.3.3: PageRuler™ Unstained Protein Ladder). Lane 1: purified pCUTAB1; Lane 2: purified pCUTAB1 processed with loading buffer without β -mercaptoethanol (explained below); Lane 3: crude supernatant from *P. pastoris* expression of CUTAB1; Lane 4: concentrated supernatant from *P. pastoris* expression of CUTAB1 using Amicon concentrator™.

3.2.2.3 Purification of recombinant pCUTAB1

In view of existence of hydrophobic patches on the surface (Figure 3.22) of pCUTAB1, hydrophobic interaction chromatography (HIC) was used to purify the protein (2.2.3.5). Recombinant pCUTAB1 was purified in a single step under native conditions using a HIC column (HiTrap™ Phenyl FF (low sub)) after expression of recombinant pCUTAB1 and concentration (2.2.3.1) of the crude culture supernatant. The purity of the purified pCUTAB1 was confirmed by SDS-PAGE (Figure 3.21). On the gel, there are two bands of purified pCUTAB1, which seemed to correspond to two forms of recombinant pCUTAB1, glycosylated and unglycosylated (discussed in next chapter). Table 3.10 shows the purification steps of recombinant pCUTAB1. The recovery of active pCUTAB1 accounted for 70% after purification, and the total active cutinase was calculated to 36 mg from 2 x 200 ml culture broth. The high protein content of recombinant pCUTAB1 in the crude culture supernatant contributed to the low purification factor. Therefore, additional purification steps were not performed.

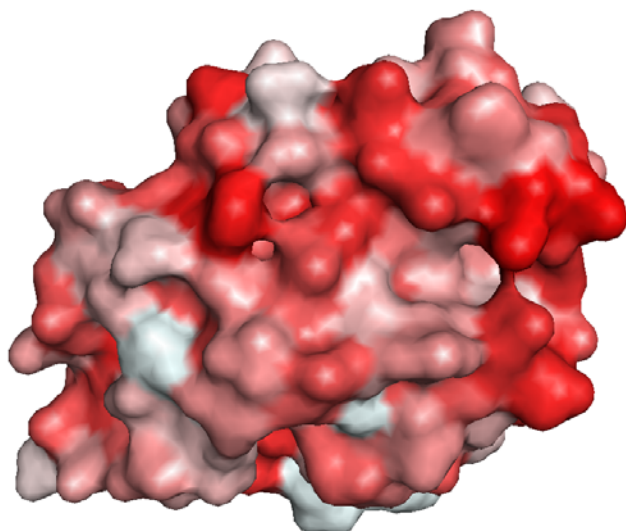


Figure 3.22: Solvent accessible surface of the deduced pCUTAB1 structure colored by hydrophobicity (hydrophobic amino acids, i.e. V, I, L, F, etc., are colored in red, hydrophilic amino acids, i.e. S, D, H, N, etc., in white).

3.2.2.4 Glycosylation of recombinant pCUTAB1

There are two bands of purified pCUTAB1 visible in lane 1 on the Coomassie blue stained SDS-PAGE (**Figure 3.21**). One band corresponds to 20 kDa, the other one to 24 kDa. The latter one was thought to be glycosylated pCUTAB1. Due to the glycosylation in *P. pastoris* (Cereghino and Cregg 2000; Daly and Hearn 2005), the molecular mass of secreted pCUTAB1 should be higher (24 kDa, **Figure 3.21** lane 1) than the published mass of 21 kDa with the potential signal peptide (YAO and Köller 1994). The molecular mass of pCUTAB1 without the potential signal peptide and glycosylation should be 20 kDa. Thus, deglycosylation was performed to check the mass of recombinant pCUTAB1. According to the manufacture's protocol, it was performed using glycosidase Endo H_f (NEB™) (Maley et al. 1989), which cleaves within the chitobiose core of high mannose and some hybrid oligosaccharides from *N*-linked glycoproteins. Only one additional band of 70 kDa corresponding to the endoglycosydase, Endo H_f, can be observed next to a distinct band of deglycosylated pCUTAB1 in lane 2 at about 20 kDa (**Figure 3.23**). The *N*-glycosylation site (178 NGTL) in pCUTAB1, predicted by NetNGlyc 1.0 of Technical University of Denmark, is shown in **Figure 3.24**.

Results

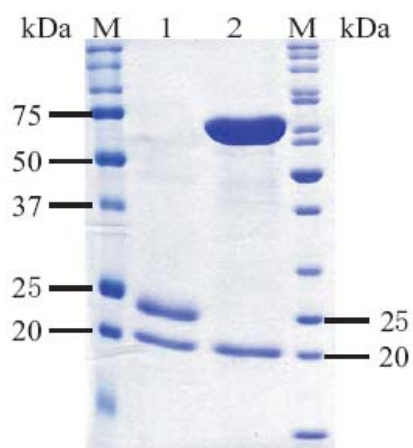


Figure 3.23: Coomassie blue stained SDS-PAGE analysis of purified and deglycosylated recombinant pCUTAB1. M indicates protein molecular weight standards (2.2.3.3: Precision Plus Protein™ all Blue Standard (left) and PageRuler™ Unstained Protein Ladder (right)). Lane 1: purified pCUTAB1; Lane 2: deglycosylated pCUTAB1 using Endo H_f (70 kDa).

```
Name: P41744 Length: 209
MMNLNLLLSKPCQASTTRNELETGSSDACPRITIFIFARGSTEAGNMGALVGPFTANALESAYGASNVVWQGVGGPYTAGL 80
VENALPAGTSQAAIREAQRLENLAASKCPNTPITAGGYSQGAAVMSNAIPGLSAAVQDQIKGVVLFGYTKNLQNGGRIPN 160
FPTSKTTIYCETGDLVCGTLIITPAHLLYSDEAAVQAPTFLRAQIDSA
..... 80
..... 160
.....N..... 240
```

(Threshold=0.5)

SeqName	Position	Potential	Jury agreement	N-Glyc result
P41744	178 NGTL	0.6303	(9/9)	++

NetNGlyc 1.0: predicted N-glycosylation sites in P41744

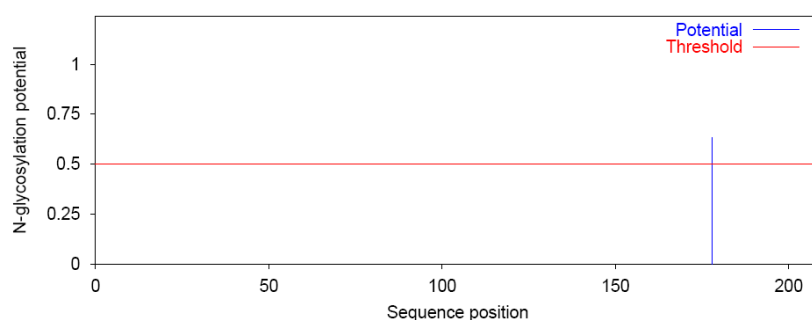


Figure 3.24: Predicted N-glycosylation sites in pCUTAB1 (P41744) of *A. brassicicola* by NetNGlyc 1.0 of the Technical University of Denmark. N-X-S/T sequons in the sequence output above are highlighted in blue. Asn predicted to be N-glycosylated is highlighted in red.

3.2.2.5 Putative signal peptide of pCUTAB1

Considering the presence of a putative signal peptide related to a high degree of hydrophobicity in the region of the protein where the signal peptide is located, the hydropathy plot of pCUTAB1 generated from the translated sequence reveals a hydrophobic segment near the amino terminus (**Figure 3.25**), which is composed of 8 amino acids; A basic amino acid Lys is close to the *N*-terminus; and an amino acid with short neutral side chain Ala is at position 14. All these characters indicated a potential signal peptide. The presumed cleavage site of pCUTAB1 was estimated between position 14 (Ala) and 15 (Ser), predicted by SignalP 3.0 Server of the Technical University of Denmark. Additionally, from the alignment of pCUTAB1 with Hi_Cutinase showing only the mature protein in **Figure 3.15**, it can be concluded that the cleavage sites of the two proteins are similar. The sequence of the mature protein of recombinant pCUTAB1 was thus estimated to contain only 195 amino acids, and its molecular weight was predicted as 20.1 kDa by Vector NTI Advance 10.3 from Invitrogen Corporation. This prediction was validated by the results from SDS-PAGE (**Figure 3.23**) after deglycosylation of recombinant pCUTAB1. The size of the deglycosylated pCUTAB1 showed about 20 kDa (lane 2 in **Figure 3.23**). Furthermore, the protein sequence deduced from the *CUTAB1* gene in the genome of *P. pastoris* contained five Cys. If the first *N*-terminal Cys (position 12) (**Figure 3.18**) would not be excised together with the putative signal peptide of pCUTAB1, the recombinant pCUTAB1 would form a dimer. In order to verify again the prediction about the cleavage of the first *N*-terminal Cys in the putative signal peptide of pCUTAB1 and exclude the existence of the dimer of recombinant pCUTAB1, purified pCUTAB1 without β -mercaptoethanol was loaded on the Coomassie blue stained SDS-PAGE in **Figure 3.21** (Lane 2). β -mercaptoethanol as a reductant is employed for scission of disulfide bonds. No dimer was observed in **Figure 3.21** (Lane 2). This result verified that the first *N*-terminal Cys was excised together with the putative signal peptide of pCUTAB1. However, exact confirmation of the signal peptide and protein size would need *N*-terminal sequencing of purified pCUTAB1, which will be performed in the future.

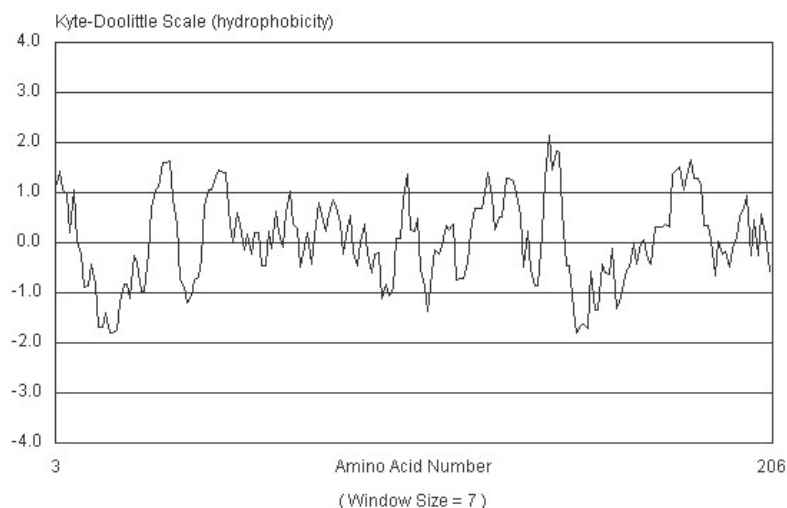


Figure 3.25: Hydropathy plot of the predicted amino acid sequence of pCUTAB1. The hydropathy plot was calculated by the method of Kyte and Doolittle (Kyte and Doolittle 1982) with a window of 7 amino acids.

3.2.3 Biochemical characterization of pCUTAB1

3.2.3.1 Kinetic constants of pCUTAB1

Kinetic constants K_m (0.55 mM) and V_{max} (31 U/mg) of the purified pCUTAB1 were determined with *p*NPP as substrate and calculated from a Lineweaver-Burk plot (**Figure 3.26**) using a least-squares best fit to the Michaelis-Menten equation.

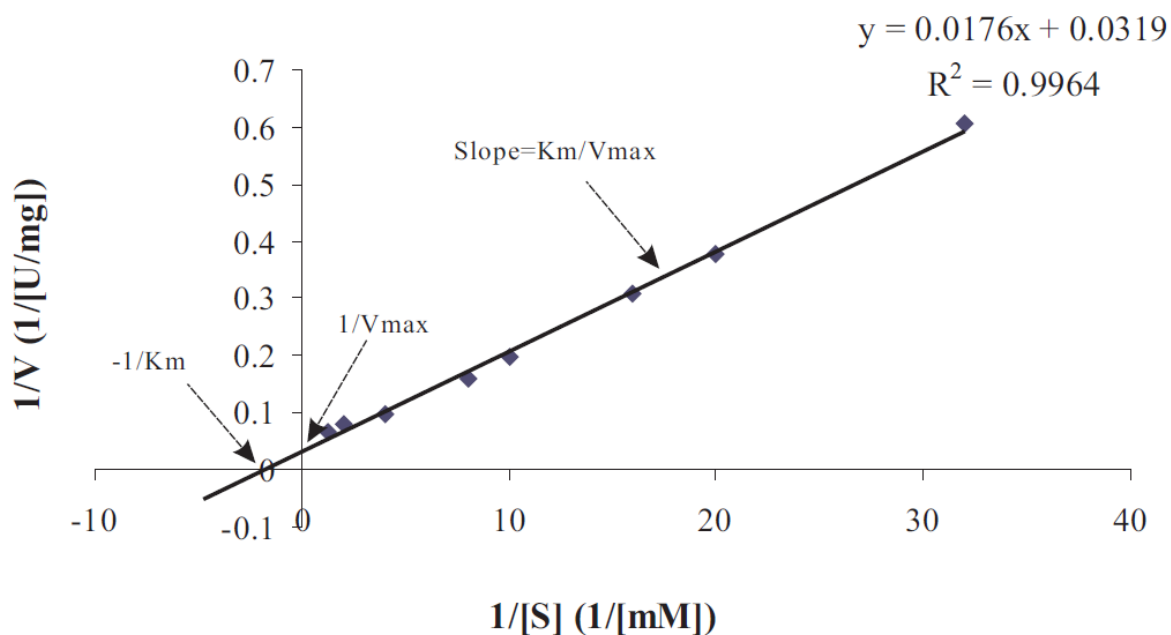


Figure 3.26: Enzyme (pCUTAB1) kinetic data on a Lineweaver-Burk plot with a Y-intercept of $1/V_{max}$, an X-intercept of $-1/K_m$ and a slope of K_m/V_{max} . Reaction mixture contained 0.03-0.8 mM pNPP sonically dispersed in 2-propanol, 900 μ l solution containing 0.5% Triton X-100, 0.1% aqueous gum arabic, 0.1 M Tris-HCl pH 8, water, and enzyme in a total volume of 1 ml. Rate of hydrolysis was determined at 410 nm by spectrophotometer. One unit [U] of hydrolase activity was defined as turnover of 1 μ mol substrate per min under assay conditions. V is the abbreviation for “velocity”. I.e. V indicates the specific activity (A [U/mg]) and [S] the concentration of the substrate pNPP.

3.2.3.2 Substrate specificity of pCUTAB1

The substrate specificity of the purified pCUTAB1 from *P. pastoris* was studied by using pNPB, pNPP, ethyl esters (butyrate and caprylate), olive oil, various glycerol esters and methyl esters of straight-chain fatty acids ranging in chain length from C₂ (acetate) to C₁₄ (myristate). The substrate specificity of the pCUTAB1 is shown in Table 3.11. It is obvious from the data that pCUTAB1 prefers relatively bulky glycerol esters to single chain aliphatic esters. The highest activity of the pCUTAB1 towards glycerol esters was observed with tributyrin (3302 U/mg) and tricaprylin (1286 U/mg). In the case of single chain aliphatic esters, pCUTAB1 showed the highest activity towards ethyl butyrate (281 U/mg) and methyl butyrate (257 U/mg) as substrates. The activity of pCUTAB1 with pNP esters was measured towards pNPB (2868 U/mg) and pNPP (17 U/mg). Along with the increased acyl chain length, the activity of pCUTAB1 decreased.

Table 3.11: Substrate spectrum of pCUTAB1.

Substrate (ab.)	Specific activity ^b (U/mg)
Methyl acetate (M-C ₂) ^a	41 ± 1
Methyl propionate (M-C ₃) ^a	157 ± 4
Methyl butyrate (M-C ₄) ^a	257 ± 10
Ethyl butyrate (E-C ₄) ^a	281 ± 13
Methyl caproate (M-C ₆) ^a	125 ± 1
Methyl caprylin (M-C ₈) ^a	129 ± 3
Ethyl caprylin (E-C ₈) ^a	125 ± 2
Methyl decanoate (M-C ₁₀) ^a	161 ± 3
Methyl laurate (M-C ₁₂) ^a	197 ± 6
Methyl myristate (M-C ₁₄) ^a	145 ± 2
Tributylin (Tri-C ₄) ^a	3302 ± 160
Tricaprylin (Tri-C ₈) ^a	1286 ± 55
Tripalmitin (Tri-C ₁₆) ^{a,c}	637 ± 13
Triolein (Tri-C ₁₈) ^{a,c}	62 ± 2
Tristearin (Tri-C _{18:1}) ^a	436 ± 21
olive oil ^a	391 ± 16
<i>p</i> -nitrophenyl butyrate (<i>p</i> NPB) ^d	2868 ± 135
<i>p</i> -nitrophenyl palmitate (<i>p</i> NPP) ^d	17 ± 1

^a Reaction mixture contained 5% (v/v) soluble substrates and 1% (w/v) solid substrates emulsified in 2% aqueous gum arabic, water, and enzyme in a total volume of 20 ml. Rate of hydrolysis was determined at pH 8 and at 40°C by continuous titration of the liberated acids with the pH-stat.

^b Expressed as units per milligram. One unit of hydrolase activity was defined as 1 µmol of acids released by enzyme per min under assay conditions.

^c Solid substrates were emulsified in water and the solubility was low.

^d Reaction mixture contained 100 µl 6.5 mM *p*NP ester sonically dispersed in 2-propanol and 900 µl solution containing 0.5% Triton X-100, 0.1% aqueous gum arabic, 0.1 M Tris-HCl pH 8, water, and enzyme in a total volume of 1 ml. Rate of hydrolysis was determined at 410 nm by spectrophotometer.

3.2.3.3 Temperature optimum of pCUTAB1

The temperature profile of pCUTAB1 is shown in **Figure 3.27**. All measurements were carried out at pH 8 with *p*NPP as substrate. The highest activity was observed at 40°C. Further increasing of the temperature (more than 50°C) resulted in an inactivation of the enzyme (data not shown).

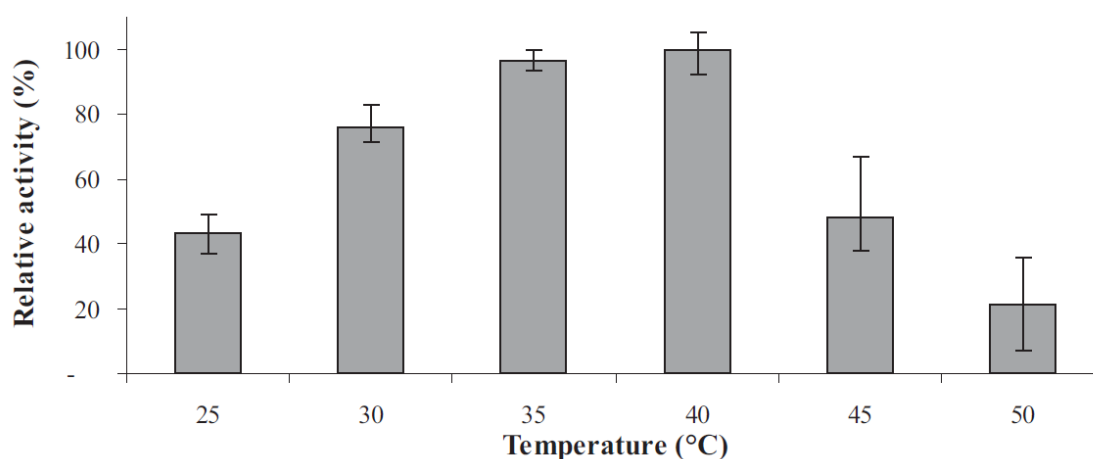


Figure 3.27: Relative activity of pCUTAB1 at different temperatures. The activity of pCUTAB1 towards *p*NPP at 40°C is designated as 100%. The measurement was carried out at pH 8 using *p*NPP as substrate by spectrophotometer and the reaction mixture was as described in legend of Table 3.11. The determination of the activity of pCUTAB1 was performed three times and the error bars indicate the deviations.

3.2.3.4 pH optimum of pCUTAB1

As the optimal temperature of pCUTAB1 was determined to be 40°C, identification of the pH optimum was measured at room temperature (22°C) and 40°C. pCUTAB1 showed higher activity at more alkaline conditions ranging from pH 7 to pH 10 at both room temperature and 40°C (**Figure 3.28**).

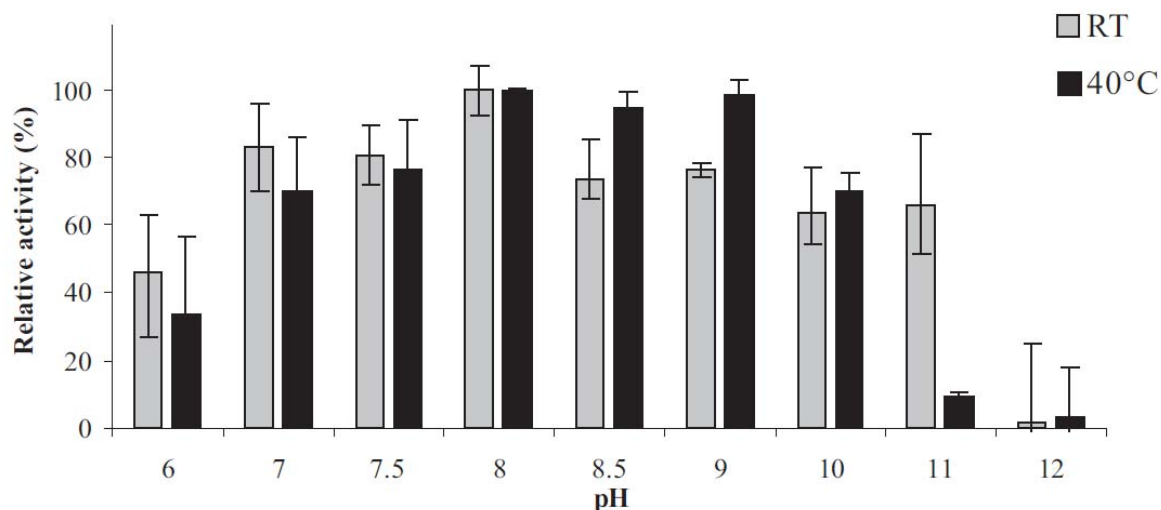


Figure 3.28: Relative activity of pCUTAB1 at different pH values. The activity of pCUTAB1 towards *p*NPP at pH 8 is designated as 100%. The measurement was carried out at room temperature (RT) and 40°C using *p*NPP as substrate and the reaction mixture was as described in legend of Table 3.11. The determination of the activity of pCUTAB1 was performed three times and the error bars indicate the deviations.

3.2.3.5 Temperature and pH stability of pCUTAB1

In order to determine the temperature stability of pCUTAB1, enzyme was incubated in buffer containing 0.5% Triton X-100, 0.1% aqueous gum arabic, 0.1 M Tris-HCl pH 8 and water at optimum temperature (40°C) for 24 h. The samples were measured every half an hour in the first 2 h and then every hour until 4 h. Only in the first half an hour, the activity decreased to 84% and was then almost unchanged until 24 h (**Figure 3.29**). That indicates high stability of the enzyme at 40°C.

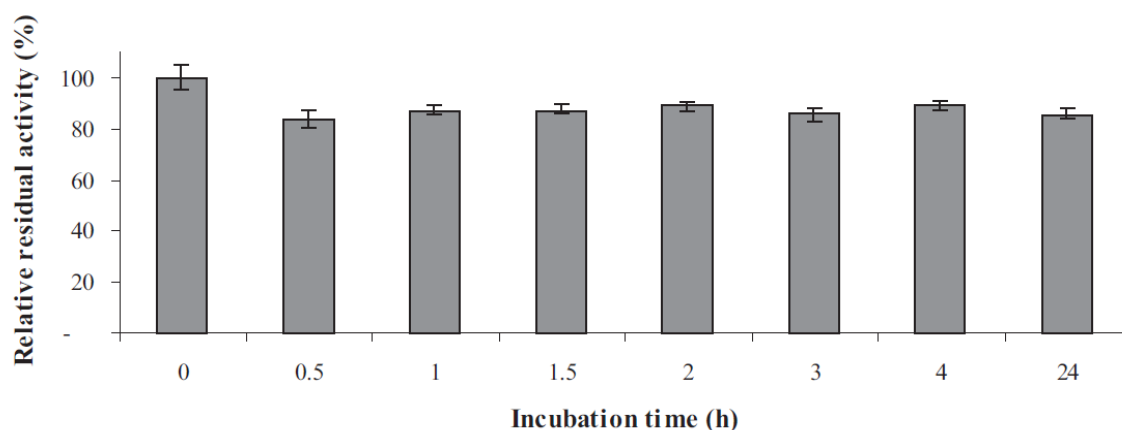


Figure 3.29: Relative residual activity of pCUTAB1 after long time incubation at 40°C. The initial activity of pCUTAB1 was designated as 100%. The measurement was carried out at pH 8 using *p*NPP as substrate and the reaction mixture was as described in legend of Table 3.11. The determination of the activity of pCUTAB1 was performed three times and the error bars indicate the deviations.

For pH stability determination of pCUTAB1, the activity was measured at pH 8. After incubation at pH 8, more than 80% of initial activity of pCUTAB1 remained after 24 h (Figure 3.30).

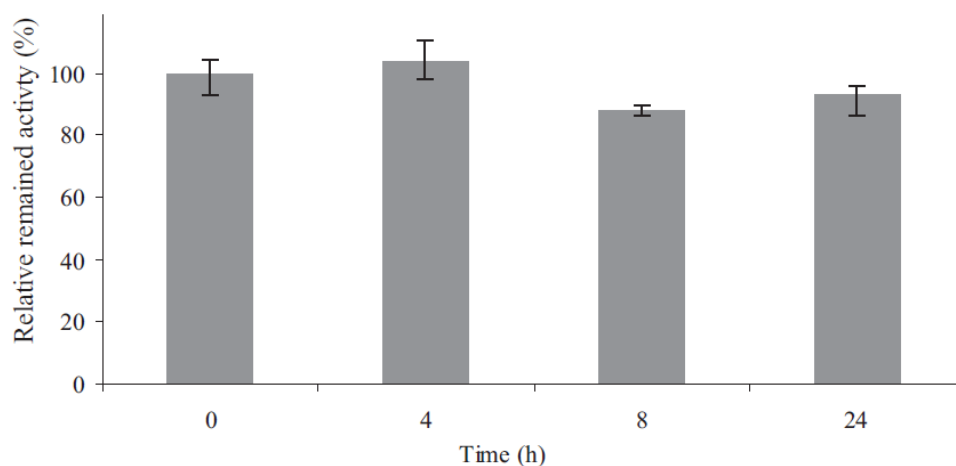


Figure 3.30: Relative residual activity of pCUTAB1 after incubation at pH 8 and room temperature. The initial activity of pCUTAB1 at pH 8 was designated as 100%. The measurement using *p*NPP as substrate was performed at 410 nm spectrophotometrically. The reaction mixture was as described in legend of Table 3.11. The determination of the activity of pCUTAB1 was performed three times and the error bars indicate the deviations.

3.2.4 Immobilization of pCUTAB1 on MP1000

In order to perform transesterification in organic solvents in which lyophilized enzyme showed only very low activity (data not shown), enzymes were immobilized (2.2.4) by adsorption onto the hydrophobic carrier, the macroporous polypropylene support MP1000. Since the culture supernatant contained a high amount of pCUTAB1, additional purification steps were not performed before immobilization. The immobilization of pCUTAB1 is shown in **Table 3.12**. After concentration with an Amicon concentrator (2.2.3.1), the cutinase solution (15 mg/ml) was diluted in 39.7 ml buffer A containing 25% (v/v) ethanol and sodium phosphate buffer at pH 5.5. This pH 5.5 is in the vicinity of the isoelectric point (pI: pH 5.2 - pH 7.0) of pCUTAB1 (**Figure 3.31**). The pI was determined and evaluated using the Phast-system (Amersham Pharmacia Biotech) by Peter Trodler. After addition of degreased MP1000, immobilization was carried out for 40 h at 6°C.

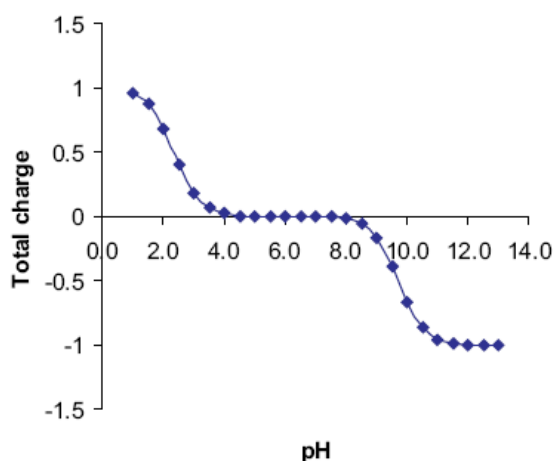


Figure 3.31: Titration curve of pCUTAB1. pI was between pH 5.2 - pH 7.0.

Table 3.12: Immobilization of pCUTAB1 on MP1000^a.

Concentrated enzyme ^b	Protein ^c		Filtrate ^d	MP1000	Protein ^e on MP1000	Total protein load ^f on MP1000	MP1000-Protein ^g (Protein)
[mg/ml]	[ml]	[mg]	[mg]	[mg]	[mg]	[%]	[mg]([μg])
15	0.3	4.5	1.6	500	2.9	0.6	9 (50)

^a Immobilization using 500 mg MP1000 was performed in 40 ml buffer for 40 h under stirring in cooling room (6°C). The immobilized enzyme was dried for 4 h in a fume hood.

^b Concentrated sample pCUTAB1 cultivation using the Amicon concentrator.

^c The amount of protein from the concentrated sample pCUTAB1 cultivation for immobilization.

^d The amount of protein from the washing solution after immobilization.

^e The amount of protein immobilized on MP1000.

^f mg protein per mg immobilizate in percent.

^g The amount of carrier with protein for the acrylation of 6-mercaptohexanol

3.2.5 Acrylation of 6-mercaptohexanol catalyzed by lipase and cutinase

In order to test the transesterification activity of cutinase pCUTAB, lipase CALB and its mutants, similar amount (about 50 μg) of cutinase and lipase immobilized on MP1000 was used for the acrylation. Although the optimal temperatures of cutinase pCUTAB1 and lipase CALB were around 40°C, the acrylation of 6-mercaptohexanol (**Figure 1.12**) was performed at room temperature (22°C) in our work, due to formation of side products, such as michael addition products (**Figure 3.33**) at higher temperature (data not shown). The control test was performed without enzyme and showed no formation of acrylated mercaptohexanol. In the transesterification, methyl acrylate was used as both substrate and solvent. Samples were withdrawn per hour or per two hours for analysis with GC/MS. The activities were calculated from the peak area ratios from remaining 6-mercaptohexanol and products (**Figure 3.32**). From the Figure, it can be seen that pCUTAB1 exhibits about 10% higher activity than the CALB wild-type within five hours of reaction. The CALB mutants L278AW104F and L278AW104FS47A show lower activity than the CALB wild-type, L278A and the cutinase pCUTAB1, as the two mutants modified for the improvement of the acrylation of hpc (3.1) may not be optimal catalyst for the acrylation of 6-mercaptohexanol. Moreover, 90% conversion after 3 h was reached using the cutinase pCUTAB1, while the lipase wild-type CALB, mutants L278A and L278AW104F reached this level of conversion only after 7 h.

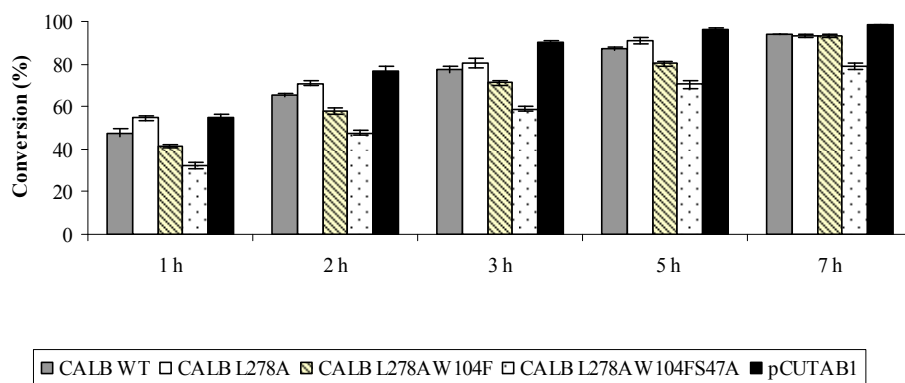


Figure 3.32: Conversion of the acrylation of 6-mercaptohexanol by cutinase pCUTAB1, lipase CALB wild-type (WT) and mutants (L278A, L278AW104F, L278AW104FS47A) immobilized on MP1000. Error bars indicate standard deviations from three independent experiments.

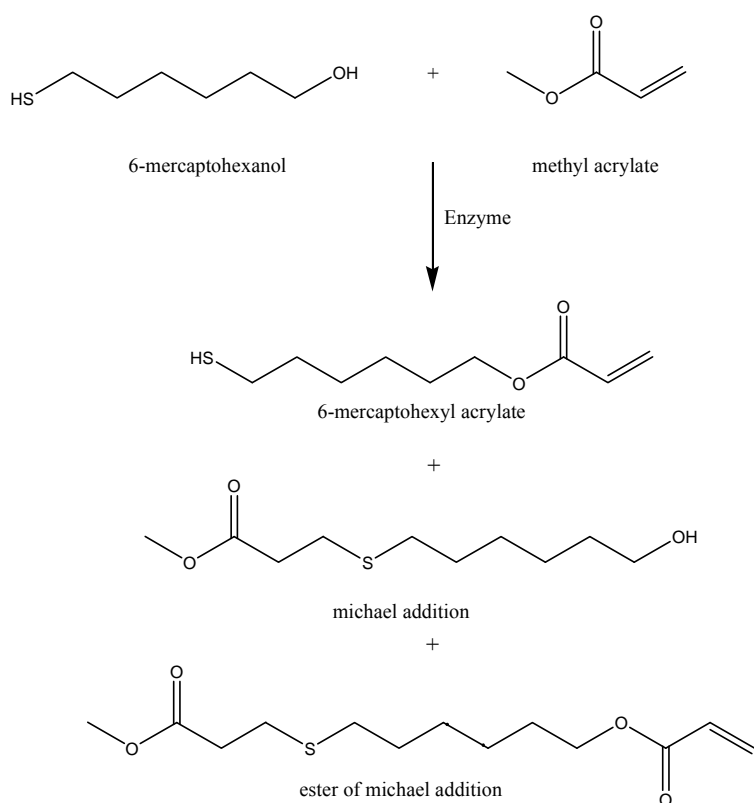


Figure 3.33: Enzyme catalyzed acrylation of 6-mercaptohexanol at 40°C or using molecular sieve at room temperature. Molecular weights: Mr. 134 (6-mercaptohexanol), Mr. 86 (methyl acrylate), Mr. 174 (6-mercaptohexyl acrylate), Mr. 206 (Michael addition product), Mr. 258 (ester of Michael addition product).

4 Discussion

4.1 Improved acrylation of hydroxypropylcarbamate by rational protein design of *C. antarctica* lipase B

4.1.1 Library creation for CALB using the *E. coli* expression system

The *CALB* gene (Appendix) was amplified by Monika Rusnak (Rusnak 2004) from genomic DNA of *C. antarctica*, revealing two discrepancies from the published CALB sequence (CAA83122) on the amino acid level (T57A, A89T). The two deviations appeared in two independent amplifications, where the gene was amplified from two different extracts of genomic DNA. Therefore, they are most likely natural variations of the lipase gene occurring in *C. antarctica* as a consequence of evolution and not of errors produced during the PCR amplification. The lipase encoded by amplified *CALB* displayed comparable activity to the published values of the wild-type CALB when expressed in *P. pastoris*, thus, we continued the work with the amplified gene (Rotticci-Mulder 2001; Rusnak 2004). Nevertheless, an influence of the deviations on lipase activity is still not clarified.

E. coli expression system allows screening for hydrolytic activity toward hydrophobic substrates. In our study, Origami[®] B cells expressing CALB wild-type showed clear halo formation on agar plates supplemented with tributyrin. A preselection of active clones prior to the complex screening assays using specific substrates is possible. Therefore, this system was used in this study for library creation and screening for CALB variants.

For a suitable library, the mutagenesis efficiency is also important. A low percentage of mutants in a library will increase the colony number and a consumption of labor, time and materials, while the low number of active variants will lead to missing a best variant due to a too high percentage of mutants resulted from our epPCR. In saturation mutagenesis, one amino acid is substituted by other 19 amino acids. Therefore, the higher the ratio of substitution is, the less is the requirement of the necessary number of colonies to be screened. The reason of low percentage of mutants by the sequential introduction of mutations method including two-steps PCR might be the high number of mismatches in degenerate primers and the wild-type like sequences bound tightly to the template, and then the new synthesized wild-type sequence in PCR increased the amount of the wild-type DNA in second round of PCR.

However, the novel technology of the QuikChange[®] Multi system had optimized the mutagenesis at multiple sites in a single round (Hogrefe et al. 2002; Stratagene 2003).

A high-throughput assay for the library screening is indispensable. Apart from the popular tributyrin assay (2.2.5.1), a new developed hpca assay (2.2.5.2) successfully satisfied this requirement. Colonies containing the pColdIII construct of CALB variants with clear halos on tributyrin plates were further functionally expressed in a 96-well microtiter plate scale in comparable amounts and checked by the hpca assay, as shown in **Figure 3.5** and **Figure 3.8**. This high-throughput activity assay was functionally verified by negative and positive control. Control cells lacking the lipase gene did not show observable reduction of absorption values at 581 nm (**Figure 3.8**), which is a prerequisite for a reliable assay system for the identification of active clones. As positive control, the wild-type CALB and mutant L278A exhibited significant decreasing of absorption at 581 nm (**Figure 3.8**). Moreover, a good correlation between the slopes and the concentrations with a double increasing series of CALB wild-type (**Figure 3.5**) shows that not only qualitative but also quantitative determination of hydrolysis of hpca by this method was possible in microtiter plate. Therefore the hpca assay was validated to be a suitable screening method for the two-site saturation mutagenesis library.

4.1.2 Modification of enzyme properties

CALB is an enzyme that has been proved to be a highly useful and versatile biocatalyst for many applications. CALB being a robust and stable enzyme has shown very enantio- and regioselectivity and high activity in organic solvents (Anderson 1998). CALB can catalyze the transesterification of hpc with methyl acrylate (**Figure 1.11**). However, wild-type CALB can not reach full conversion in an acceptable time scale for a commercial application. For increasing the activity of an enzyme towards a specific substrate, besides a classic method such as improving reaction conditions in view of experiment, specific characters can be altered by methods of directed evolution and rational protein design.

Directed evolution as a powerful tool has been used in industrial processes not only for improving the utility of enzymes, but also for generating variants that illuminate the relationship between enzyme sequences, structure and function. The most widely used method for generating of variants with random mutations is epPCR, which is designed to alter and enhance the natural error rate of the polymerase (Leung 1989; Cadwell and Joyce 1992). *Taq* polymerase (Saiki et al. 1988; Huang et al. 1992) is commonly used because of its naturally high error rate. The choice of model and parameters can affect the estimate of

mutation rate per cycle by sampling sequences from an *in vitro* PCR experiment (Pritchard et al. 2005). In our study, the mutation rate might have been too high to create enough active lipases in the library constructed through epPCR. Therefore it could be improved by changing parameters and conditions in PCR to get sufficient quantity of active variants for screening. However, finding optimal conditions not only for epPCR but also for a specific reaction still requires a great deal of experimental screening.

Rational design of enzymes would relieve the need for screening large numbers of biocatalysts to suit a target reaction and allow the introduction of new or improved enzymatic activities. For rational design, bioinformatical tools are required to investigate the relationship between the substrate and the enzyme. In the CALB-catalyzed acrylation of hpc, the reason for no full conversion catalyzed by the wild-type in short time scale can be understood by the model of (Orrenius 1998) (**Figure 4.1**). In this model, the fast-reacting enantiomer (e.g. the *R*-enantiomer of the secondary alcohols) orients its medium-sized substituent into the stereospecificity pocket constituted by the side chains of T42, S47 and W104, and its large substituent points towards the active-site entrance. Thus, the hydrogen bonds (e.g. ($H_{NE2} - O_{alc}$)) between the hydrogen atom of the catalytic His and the oxygen of the alcohol moiety essential for catalysis are formed. However, the *S*-enantiomer has to orient large substituents in the stereospecificity pocket to allow the formation of the catalytically essential hydrogen bonds, although it is sterically hindered. This model illustrates the preference of the *R*-enantiomer for the wild-type CALB and a much lower reaction rate resulted from the *S*-enantiomer of the secondary alcohol in the acrylation, which was verified by the molecular modeling with a larger distance of $H_{NE2} - O_{alc}$ (**Table 3.2**). This finding was in agreement with the usual stereochemical outcome of reactions catalyzed by lipases CALB (Kazlauskas 1991). Moreover, this model shows how CALB discriminates between the enantiomers of secondary alcohols and this involves the binding of the two enantiomers in two different models (**Figure 4.1**) in transition state to allow catalysis, yielding the possibility to kinetically resolve the two enantiomers. However, our aim was not to increase the enantioselectivity, but to decrease the enantioselectivity and increase the total activity towards the substrate hpc. The activity was strongly increased by the mutant L278A resulting from both the investigation of molecular modeling and the saturation mutagenesis library at positions 277, 278 and 281. On one hand, the substitution of L278 for Ala shortens the distance between the hydrogen atom of the catalytic His and the oxygen of the alcohol moiety, thus facilitated formation of the corresponding hydrogen bond between them. On the other hand, this mutation provides more space for the entrance of the substrates. However, in preparative hydrolysis, the reaction rate

of L278A still declined over time. As the enzymatic activity was stable (proven by reuse of the lipase), the slightly time-dependent decline in rate might be the result of the consumption of the favorable substrate of the primary alcohol and the *R*-enantiomer of the secondary alcohols and somewhat lower activity towards the *S*-enantiomer 2hpc compared to the *R*-enantiomer of the secondary alcohols due to the steric hindrance caused by the large-sized substituent of the secondary alcohols in the medium-sized stereospecificity pocket. This finding diverted our interest to target positions T42, S47 and W104 (**Figure 3.6** and **Figure 3.7**), known to have high impact on the stereospecificity of CALB (Uppenberg 1995; Patkar 1998; Rotticci et al. 2001; Magnusson 2005a). In the modeling studies by Magnusson (Magnusson 2005b), the *R*-enantiomer had similar orientation in both CALB wild-type and the mutant W104A. The redesigned stereospecificity pocket of the W104A mutant comfortably accommodates the much larger groups of the *S*-enantiomer than that of the wild-type lipase. This change transformed the strongly *R*-selective wild-type CALB into an *S*-selective mutant. The *S* selectivity increased with temperature and it was dominated by entropy. Therefore, in our study the position 104 was targeted to set up a two-site saturation mutagenesis library (L278X/W104X). Mutant L278A/W104F from the library screening showed higher activity than the wild-type and a decreased stereoselectivity verified by determination of enantioselectivity (**Table 3.6**). These findings were in agreement with the results from molecular modeling and correlated with the position L278 responsible for the activity and W104 responsible for the stereoselectivity. Furthermore, S47 in CALB is positioned behind the aromatic ring of W104 in the so called stereoselectivity pocket (**Figure 3.6**). Effects of a combination of mutant S47A with the two best mutants, L278A and L278A/W104F on hpc were investigated as well. Due to very low expression of the active CALB variants in *E. coli*, functional expression of recombinant protein by *P. pastoris* was necessary. In this expression system the high concentration and purity of the lipase were obtained by secretion of CALB to the media. This allowed more accurate characterization of the mutants and the final transesterification of hpc with methyl acrylate by immobilized CALB variants.

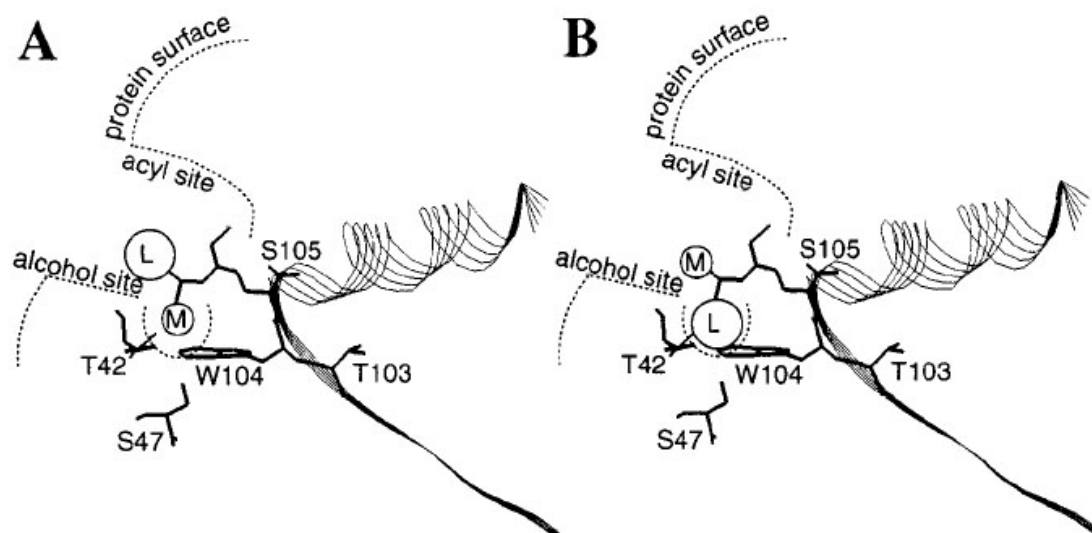


Figure 4.1: Two productive binding modes in the developed model by (Orrenius 1998) that rationalizes the enantioselectivity of CALB. (A) Fast-reacting enantiomer. (B) Slow-reacting enantiomer. (M) medium-sized substituent; (L) large substituent. (modified from (Ottosson et al. 2001)).

4.1.3 Expression of CALB variants in *P. pastoris* and characterization

Yeast expression vector (pPICZ α A) containing the genes for CALB wild-type and mutants were constructed and introduced into *P. pastoris*. Supernatants from the culture of those CALB variants were analyzed by SDS-PAGE (Figure 3.12), which displayed a major band of 36 kDa. The calculated molecular weight of CALB is 33 kDa, and the higher molecular weight obtained was attributed to the glycosylation (Rotticci-Mulder 2001). One *N*-glycosylation site is present in CALB (Uppenberg 1994) which was found to be *N*-glycosylated when produced in *A. oryzae* and in the native host (Hoegh et al. 1995). Therefore, the activity of the secreted CALB should not be disturbed by glycosylation. For deglycosylation, endoglycosidase F (Hoegh 1995) and endoglycosidase H were used (Rotticci-Mulder 2001), giving the same decrease in molecular weight and confirming the *N*-glycosylation on the lipase region. It was thus assumed that the lipases produced in the different hosts received similar extent of glycosylation (Rotticci-Mulder 2001).

Characterization of CALB wild-type and variants was performed using a standard tributyrin assay, the newly developed hpca assay and comparison of the enantioselectivity. L278A showed the highest activity towards tributyrin and the double fold higher activity towards hpca than the wild-type (Table 3.6), resulting from the more rapid hydrolysis of the ester due

to the enlarged substrate entrance site. In comparison of the enantioselectivity (**Table 3.6**) using 1-phenylethylpropionate as substrate, the obviously lowered enantioselectivity ($E = 95$) of L278A than that of the wild-type could be resulted from the shortened distance and subsequent formation of the indispensable hydrogen bond between $H_{NE2} - O_{alc}$ in the transition state for the *S*-enantiomer (**Table 3.2**), although this mutant still has a bias of the *R*-enantiomer (*R*) over the *S*-enantiomer (*S*) like the wild-type CALB (shown in **Figure 3.13**). The *R*-selectivity of L278A could be attributed to the steric hindrance in the stereospecificity pocket, which was enlarged by the mutation W104F. This helped us to understand the further lowered enantioselectivity ($E = 4$) of the double mutant L278A/W104F by comparison with L278A and the wild-type and meanwhile the higher activities towards both tributyrin and hpca than the wild-type (**Table 3.6**). Moreover, it could be observed that L278A/W104F had almost no bias towards the *R*- and *S*-enantiomers, resulting from the enantiomeric excess of the product (ee_p) which value remained 50% even after 24 h reaction (**Figure 3.13**). Therefore, it could be concluded that the effect of combination of mutations at position 278 (responsible for increased activity) and 104 (responsible for decreased stereoselectivity) was additive for the substrate hpca, although the activity of the double mutant was a little lower than that of L278A (**Table 3.6**). Furthermore, since the positions S47 and T42 behind the W104 (**Figure 1.3**) are also in the stereoselectivity pocket, the effects of mutants (S47A and T42A) were also investigated. The mutant S47A exhibited a small combination effect on the enantioselectivity when combined with L278A and L278A/W104F due to the little enlarged stereospecificity pocket (**Table 3.6**). No improvement of activity or enantioselectivity by T42A was observed (**Table 3.6** and **Figure 3.13**), although T42A provides also slightly larger stereospecificity pocket. The loss of the hydroxyl group of T42 due to the substitution for Ala and thus the missing of the corresponding hydrogen bond might destabilize the substrate.

4.1.4 Acrylation of hpc with methyl acrylate by CALB variants

For better commercial applications, CALB variants were successfully created by rational protein design and by the thereby constructed two-site saturation mutagenesis library. The reaction time of the acrylation of hpc was strongly reduced by the CALB variants (L278A, L278A/W104F and L278A/W104F/S47A) immobilized on MP1000 and HP20L. Although the effect of two carriers on the activity showed no big difference, the higher activity of the mutants than the wild-type was achieved by immobilization on the carrier MP1000 (polypropylene). The carrier HP20L may not be a suitable carrier for immobilization of the

mutants due to the carrier material (polystyrol). The conformation of the immobilized enzyme might change, resulting in a lower stability and/or activity of the enzyme immobilized on HP20L compared to the enzyme immobilized on MP1000. L278A immobilized on MP1000 exhibited the fastest reaction velocity, but even so the mutants L278A/W104F and L278A/W104F/S47A showed faster conversions than the wild-type, resulting from the release of the steric hindrance caused by the *S*-enantiomer of the secondary alcohols in the medium-sized stereospecificity pocket. The reason of the relatively lower reaction rate of L278A/W104F and L278A/W104F/S47A when compared to L278A might be that too much introduced mutations may destabilize the protein or cause structure changes affecting the enzyme's activity. Moreover, immobilization using unpurified concentrated enzyme may also contribute to the deviations. More accurate comparison can be performed in the future using the immobilized enzymes after purification and using the same active site concentration, which can be more exactly determined by a active site titration method of lipase (Rotticci et al. 2000).

These results indicated again that those regions which are important for enzyme substrate selectivity can be investigated by molecular modeling and rational designed for different purpose and that will satisfy the need of industrial use with regard to reduction of time and energy consume, eventually, improving of product quality and purity as well. On the other hand, the enzyme engineering can reduce the amount of colonies to be screened. The constantly increasing knowledge about enzyme catalysis allows the improvement of the enzyme performance using the approach of rational redesign. When a suitable catalyst does not exist for a desired application, the best candidate(s) of the favorite enzymes could be redesigned according expectations.

4.2 Cloning, expression and characterization of a cutinase from *A. brassicicola* for acrylation of 6-mercaptohexanol

4.2.1 Homology alignment and cloning of *CUTAB1* in *P. pastoris*

In order to find a homologous protein to the cutinase (Hi_Cutinase) from *H. insolens* for the transesterification of methyl acrylate with mercaptohexanol or aminohexanol, a search with BLASTP in NCBI BLAST (Basic Local Alignment Search Tool) databases was performed

using the sequence of Hi_Cutinase as a query. BLASTP searching is based on the relatedness of any favorite query sequence to other known proteins. Higher scores and lower E values indicate homology and more similarity, although one can not conclude that two sequences having lower scores and higher E values are 100% non-homologous.

The aligned sequences (**Figure 3.15 A**) around the catalytic residues like stretch G-G-Y-S-Q-G are highly conserved among the known fungal cutinases (Ettinger 1987). In respect to the conserved four Cys residues, disulfide bonds near the active residues (**Figure 4.2**) might stabilize the preformed active center within the framework of the α/β fold (Martinez 1992; Ollis 1992). Besides the conserved catalytic triad (Ser, His and Asp) and a Ser in oxyanion hole (Nicolas 1996), pCUTAB1 shared the highest percentage of the sequence identity and the shortest distance in phylogenetic analysis (**Table 3.9**) with Hi_Cutinase. Moreover, their deduced 3D structures showed high similarity (3.2.1.1) in secondary structure folds (**Figure 4.2**), although there were definite deviations of the actual crystal structures.

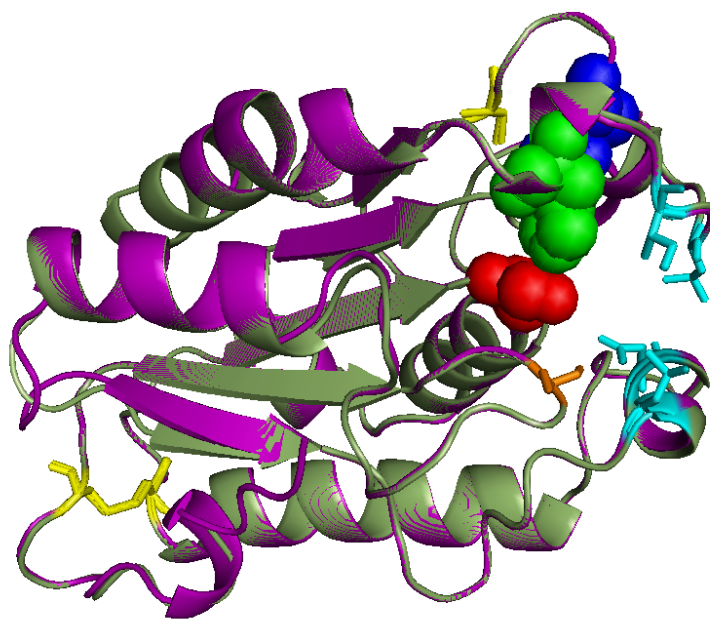


Figure 4.2: 3D structures alignment of pCUTAB1 and Hi_Cutinase deduced using SWISS MODEL (Guex and Peitsch 1997; Melo and Feytmans 1998; Schwede T 2003; Arnold K. 2006) and visualized with PyMOL (DeLano 2002). The template for modeling is the apo-cutinase (3DCN_A) from *Glomerella Cingulata* (Nyon 2009). The sequence of pCUTAB1 is coloured in deep purple; that of Hi_Cutinase in green. The residues of the catalytic triad (Ser, red; His, blue green; Asp, blue) are represented in CPK. The conserved Ser in the oxyanion hole of the cutinase is represented with sticks and coloured in orange. Two conserved side-chain bridges of L80 with V183, and L181 with N83 of pCUTAB1 and those of Hi_cutinase in the two possible hydrophobic loops are shown in sticks and marked in cyan. The cysteines are shown as yellow sticks.

For cloning of *CUTAB1* into pPICZ α A, cDNA was synthesized from mRNA, which was strongly induced *in vitro* by cutin monomers (16-hydroxyhexadecanoic acid) and repressed by glucose (Fan and Köller 1998; Rubio et al. 2008). This induction indicated its nature as cutinase, as reported for other fungal cutinases (Abu Bakar et al. 2005). The location of the intron (nucleotide positions 139-194 in **Figure 3.18**) was identical with the intron site found in all other cutinases (Ettinger 1987; Sweigard et al. 1992). After successful cloning including restriction digestion, ligation and transformation, *CUTAB1* was expressed in *P. pastoris*.

4.2.2 Expression of *CUTAB1* in *P. pastoris*

Heterologous expression is an important step on the way to gene products with high enzymatic activities. Codon usage preference of different expression systems should be considered. Gene expression is regulated by the complex interplay of transcriptional activity, tRNA availability and mRNA stability. Konu et al. (Konu and Li 2002) found that mRNA expression levels correlated with the presence of G or C at the third nucleotide position of mice and rat codons. *CUTAB1* encoding 209 amino acids and consists of 627 base pairs of nucleotides. Therein, 87 triple codes ends in C and 47, 41 and 34 triple codes end in T, G and A, respectively. This preference of ending with C is similar to other filamentous fungi (Ballance 1991). In view of successful expression of *CALB* from *C. antarctica* with a high percent of 3rd GC (72.3%) in *P. pastoris* (3rd GC: 42.15%), expression of a native cutinase from *A. brassicicola* with a similar percent of 3rd GC (64.13%) in *P. pastoris* should be unproblematic.

The site of recombination can affect expression in *P. pastoris* and an occurrence of multiple copies integrated at the *AOX1* locus can happen (Invitrogen). Therefore, six to ten recombinants should be examined, since it is unpredictable which construct or isolate will express the target protein better. In our previous work about expression of *CALB* in *P. pastoris*, a strongly decreased activity of a variant with a C-terminal His-tag was observed (Rusnak 2004). As far as we know, it was the first time that pCUTAB1 from filamentous fungi was produced as a native cutinase at high levels in *P. pastoris*, although a cutinase with a His-tag produced in *P. pastoris* has already been reported (Wang et al. 2002). The possibility to achieve a high level expression of the cutinase gene in *P. pastoris* renders this enzyme therefore very attractive for application in industry.

As is often the case in other eukaryotic systems, the glycosylation recognition sequon in *P. pastoris* is N-X-S/T (Yan et al. 1999). The glycosylation is more readily achieved if the

sequon is N-X-T rather than N-X-A (Bause and Legler 1981). The chain length of the oligosaccharides can depend on surrounding residues where hydrophilic residues may result in the sequon having longer oligosaccharides (Lis and Sharon 1993). For example, if residue surrounding the glycosylation recognition sequon (N-X-S/T) is a hydrophobic residue, such as Trp (Yan 1999) or Phe (Shakin-Eshleman et al. 1996), the initial step of addition of Glc3Man9GlcNAc2 is inhibited. Negatively-charged amino acids such as Glu and Asp also partially inhibit occupancy, whereas positively charged amino acids such as Lys, His and Arg promote core glycosylation and increase the occupancy levels (Yan 1999). The X-residue of pCUTAB1 (178 NGTL sequence) is Gly, which is a hydrophobic amino acid. Therefore, the level of the corresponding core glycosylation and occupancy on recombinant pCUTAB1 may not be very high. Additionally, the glycosylated sites of pCUTAB1 lay near the end of the C-terminus, the glycosylation of the protein may be processed incompletely as a result of strong methanol induction and therefore rapid formation of recombinant protein in *P. pastoris* (Daly and Hearn 2005). SDS-PAGE analysis of purified pCUTAB1 (**Figure 3.21**) agreed with this prediction. Although the bands of unglycosylated pCUTAB1 (≈ 20 kDa) in the supernatant samples (**Figure 3.21**, lane 3 and 4) were not very distinct, the partial glycosylation of pCUTAB1 was confirmed by deglycosylation (**Figure 3.23**) after purification of the protein. Most exported eukaryotic proteins contain typical elements in their signal peptides (Ettinger 1987; Sweigard 1992): a central hydrophobic core, a basic amino acid like Arg or Lys close to the N-terminus, a more polar C-terminus and amino acids with short neutral side chains at 1- and 3-position of the native N-terminus as recognition sites for signal peptidase (Müller 1992). The most pronounced difference between the cutinase from *A. brassicicola* and all other cutinases is the sequence at N-terminus (YAO and Köller 1994). The Arg at position 38 as the first highly conserved amino acid in most cutinases (**Figure 3.15**) stands close to or at the signal cleavage site. In contrast, a basic amino acid Lys locates close to the N-terminus of pCUTAB1. Although the conserved sequence (-L-E-A/T-R-Q-L/S-) does not exist in the *A. brassicicola* signal peptide, the N-terminus of pCUTAB1 contains a short hydrophobic core, followed by more polar residues and several neutral amino acids (-A-S-T-T-) as putative signal cleavage sites of pCUTAB1. Furthermore, the signal peptide of the pCUTAB1 is shorter than those of other cutinases. As indicated by the export of yeast invertase with randomly replaced signal sequences, the signal recognition for export is not highly specific (Kaiser et al. 1987). However, other parameters such as recognition by signal peptidases and gene expression might be influenced by signal peptide (Kaiser 1987). More interestingly, an extra Cys in addition to four conserved Cys residues (**Figure 3.15**) was observed at the N-

terminal region of pCUTAB1. It had been reported that introduction of an extra single Cys by mutagenesis led to huge structural changes by forming an intramolecular disulfide bridge (Brissos et al. 2008). Therefore, in view of the result about no existence of a dimer or oligomers (**Figure 3.21**), the extra Cys in pCUTAB1 was estimated to be present in the putative signal peptide, thus cleaved.

4.2.3 Biochemical characterization of pCUTAB1

Cutinase pCUTAB1 displayed hydrolytic activity towards a broad variety of esters, from soluble synthetic esters (e.g. *p*NP esters) to insoluble long-chain glycerol esters. The preference of cutinase pCUTAB1 to glycerol ester tributyrin resulting from comparison of various substrates was the same as that of the lipase CALB (Rusnak 2004) and that of the Hi_Cutinase (Sandal et al. 1998) (**Table 4.1**). This could be attributed to the similar catalytic mechanism and stretch around the active site Ser, -G-G-Y-S-Q-G- (Koeller and Kolattukudy 1982; Ettinger 1987) for cutinase and -G-Y/H-S-X-G- for lipase respectively. The optimum pH of pCUTAB1 was around 8, which is also similar to other cutinases (Carvalho 1998), besides the cutinase from *H. insolens* (Sandal 1998) (**Table 4.1**). The temperature optimum of pCUTAB1 was 40°C and the activity at 45°C retained about 50% indicating its potential thermophilic property in aqueous solution. In the stability storage tests of pCUTAB1 for temperature and pH (**Figure 3.29** and **Figure 3.30**), it showed that pCUTAB1 was stable at 40°C and pH 8 in the solution containing Triton X-100, which have been reported to recover the activity of pCUTAB1 (Trail and Koeller 1993) and a cutinase from *F. solani* (Kolattukudy et al. 1981; Koeller and Kolattukudy 1982).

In a word, the cutinase pCUTAB1 from *A. brassicicola* showed many similar characters including the molecular weight, the isoelectric point of the protein, and the optimum pH as well as substrate, when compared with the Hi_Cutinase from *H. insolens*, although the expression systems were different, *P. pastoris* and *S. cerevisiae* respectively. The comparison of the two cutinases was summarised in **Table 4.1**. It could be concluded that the cutinase pCUTAB1 from *A. brassicicola* was the best candidate for our study of the acrylation of 6-mercaptohexanol.

Table 4.1: Comparison of the characters of the cutinases from *H. insolens* (Sandal et al. 1998) and *A. brassicicola*

Origin of the cutinase	<i>H. insolens</i>	<i>A. brassicicola</i>
Expression system	<i>S. cerevisiae</i>	<i>P. pastoris</i>
Molecular weight	20-21 kD	20-21 kD
Isoelectric point of the protein	pH 3.5-9.5	pH 5.2-7.2
Optimum pH	pH 8	pH 8
Substrate specificity	Tributylin (pH 9): 1500 U/mg	Tributylin (pH 8): 3302 U/mg
	Olive oil (pH 9): 500 U/mg	Olive oil (pH 8): 391 U/mg
Sequence identity	61%	

4.2.4 Acrylation of 6-mercaptohexanol

Cutinase is able to catalyze transesterification (alcoholysis) reaction of butyl acetate with hexanol in organic media (isooctane) (Cunnah et al. 1996; Lamare 1997; Serralha 1998). However, the discovery of the acrylation of 6-mercaptohexanol with methyl acrylate catalyzed by cutinase was a breakthrough in this area. Comparison of transesterification effect of 6-mercaptohexanol with methyl acrylate catalyzed by lipase CALB and cutinase pCUTAB1 showed that the cutinase had a higher activity (**Figure 3.32**). This could be attributed to the more opened activity crevice of the cutinase in comparison to the relatively deeper activity hole of CALB (**Figure 4.3**), although the substrate entrance site of CALB had been enlarged by mutation L278A. The lower activity of the mutants L278AW104F and L278AW104FS47A indicated that an enzyme modified for one substrate may not be suitable for another substrate. If we want to improve the acrylation of 6-mercaptohexanol with methyl acrylate, mutagenesis of the cutinase pCUTAB1 can be performed using the rational protein design, which method had been successfully applied to improve acrylation of hpc with methyl acrylate by modified CALB mutants (3.1). Besides the cutinase (pCUTAB1) from *A. brassicicola*, the cutinase from *H. insolens* can also be cloned and expressed in *P. pastoris* for better comparison with pCUTAB1. Furthermore, the acrylation of polyacrylate with mercaptohexanol can be studied in the future using the cutinase pCUTAB1 or pCUTAB1 mutants.

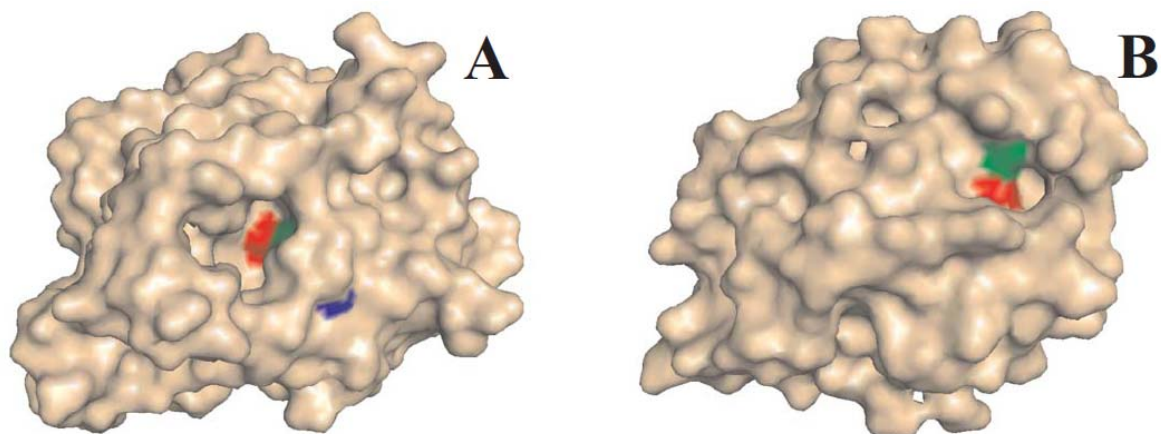


Figure 4.3: (A) Solvent accessible surface of CALB wild-type and (B) the deduced pCUTAB1 structure using SWISS MODEL (Guex and Peitsch 1997; Melo and Feytmans 1998; Schwede T 2003; Arnold K. 2006) and visualized with PyMOL (DeLano 2002). The template for modeling of pCUTAB1 is the apo-cutinase (3DCN_A) from *Glomerella Cingulata* (Nyon 2009). The residues of the catalytic triad are coloured: Ser in red; His in green and Asp in Blue.

References

- Abu Bakar, F. D., A. M. Abdul Murab, et al. (2005). "Induction and expression of cutinase activity during saprophytic growth of the fungal plant pathogen, *Glomerella cingulata*." Asia Pac J Mol Biol Biotechnol **13**: 63-69
- Anderson, E. M., K. M. Larsson, et al. (1998). "One Biocatalyst–Many Applications: The Use of *Candida antarctica* B-Lipase in Organic Synthesis." Biocatal. Biotransformation **16**(3): 181-204.
- Arnold K., B. L., Kopp J., and Schwede T. (2006). "The SWISS-MODEL Workspace: A web-based environment for protein structure homology modelling." Bioinformatics **22**: 195-201.
- Arroyo, M. and J. V. Sinisterra (1994). "High enantioselective esterification of 2-arylpropionic acids catalyzed by immobilized lipase from *Candida antarctica*: a mechanistic approach." J. Org. Chem **59**(16): 4410-4417.
- Balcaño, V. M., A. L. Paiva, et al. (1996). "Bioreactors with immobilized lipases: state of the art." Enzyme and microbial technology **18**(6): 392-416.
- Ballance, D. J. (1991). "Transformation systems for filamentous fungi and an overview of fungal gene structure." Molecular Industrial Mycology: systems and applications for filamentous fungi: 1-29.
- Ballou, C. (1976). "Structure and biosynthesis of the mannan component of the yeast cell envelope." Adv Microb Physiol **14**(11): 93-158.
- Bardwell, J. C. A. (1994). "Building bridges: disulphide bond formation in the cell." Molecular Microbiology **14**(2): 199-205.
- Bause, E. and G. Legler (1981). "The role of the hydroxy amino acid in the triplet sequence Asn-Xaa-Thr (Ser) for the N-glycosylation step during glycoprotein biosynthesis." Biochem. J **195**: 639-644.
- Beisson, F., A. Tiss, et al. (2000). "Methods for lipase detection and assay: a critical review." European Journal of Lipid Science and Technology **102**(2): 133-153.
- Berman, H. M., T. Battistuz, et al. (2002). "The protein data bank."

- Binns, F., P. Harffey, et al. (1998). "Studies of lipase-catalyzed polyesterification of an unactivated diacid/diol system." Journal of Polymer Science Part A Polymer Chemistry **36**(12): 2069-2080.
- Bornscheuer, U. T., J. Altenbuchner, et al. (1999). "Directed evolution of an esterase: screening of enzyme libraries based on pH-indicators and a growth assay." Bioorganic & medicinal chemistry **7**(10): 2169-2173.
- Bornscheuer, U. T., C. Bessler, et al. (2002). "Optimizing lipases and related enzymes for efficient application." Trends in Biotechnology **20**(10): 433-437.
- Bornscheuer, U. T. and R. J. Kazlauskas (2006). Hydrolases in organic synthesis: regio- and stereoselective biotransformations, Wiley-VCH.
- Bornscheuer, U. T. and M. Pohl (2001). "Improved biocatalysts by directed evolution and rational protein design." Current Opinion in Chemical Biology **5**(2): 137-143.
- Bosley, J. A. and A. D. Peilow (1997). "Immobilization of lipases on porous polypropylene: reduction in esterification efficiency at low loading." Journal of the American Oil Chemists' Society **74**(2): 107-111.
- Brakmann, S. and A. Schwienhorst (2004). Evolutionary methods in biotechnology: clever tricks for directed evolution, Wiley-VCH.
- Brissos, V., E. P. Melo, et al. (2008). "Biochemical and structural characterisation of cutinase mutants in the presence of the anionic surfactant AOT." BBA-Proteins and Proteomics **1784**(9): 1326-1334.
- Brzozowski, A. M., U. Derewenda, et al. (1991). "A model for interfacial activation in lipases from the structure of a fungal lipase-inhibitor complex." Nature **351**(6326): 491-494.
- Cadwell, R. C. and G. F. Joyce (1992). "Randomization of genes by PCR mutagenesis." Genome Research **2**(1): 28-33.
- Carlqvist, P., M. Svedendahl, et al. (2005). "Exploring the active-site of a rationally redesigned lipase for catalysis of Michael-type additions." ChemBioChem **6**(2): 331-336.
- Carter, P. and J. A. Wells (1988). "Dissecting the catalytic triad of a serine protease." Nature **332**(6164): 564-568.
- Carvalho, C. M. L., M. R. Aires-Barros, et al. (1998). "Cutinase structure, function and biocatalytic applications." Electronic Journal of Biotechnology **1**: 28-29.
- Cereghino, J. L. and J. M. Cregg (2000). "Heterologous protein expression in the methylotrophic yeast *Pichia pastoris*." FEMS Microbiol. Rev. **24**(1): 45-66.

- Chen, C. S., Y. Fujimoto, et al. (1982). "Quantitative analyses of biochemical kinetic resolutions of enantiomers." J. Am. Chem. Soc **104**(25): 7294-7299.
- Chen, C. S., S. H. Wu, et al. (1987). "Quantitative analyses of biochemical kinetic resolution of enantiomers. 2. Enzyme-catalyzed esterifications in water-organic solvent biphasic systems." J. Am. Chem. Soc **109**(9): 2812-2817.
- Cherepanov, A. V. and S. de Vries (2001). "Binding of Nucleotides by T4 DNA Ligase and T4 RNA Ligase: Optical Absorbance and Fluorescence Studies." Biophysical Journal **81**(6): 3545-3559.
- Cherry, J. R., M. H. Lamsa, et al. (1999). "Directed evolution of a fungal peroxidase." Nature biotechnology **17**(4): 379-384.
- Cole, P. A. (1996). "Chaperone-assisted protein expression." Structure **4**(3): 239-242.
- Cregg, J. M., T. S. Vedvick, et al. (1993). "Recent advances in the expression of foreign genes in *Pichia pastoris*." Bio/technology **11**(8): 905-910.
- Cunnah, P. J., M. R. Aires-Barros, et al. (1996). "Esterification and transesterification catalysed by cutinase in reverse micelles of CTAB for the synthesis of short chain esters." Biocatalysis and biotransformation(Print) **14**(2): 125-146.
- Daly, R. and M. T. W. Hearn (2005). "Expression of heterologous proteins in *Pichia pastoris*: a useful experimental tool in protein engineering and production." Journal of Molecular Recognition **18**(2): 119-138.
- DeLano, W. L. (2002). "The PyMOL Molecular Graphics System." from <http://www.pymol.org>.
- DeSantis, G., K. Wong, et al. (2003). "Creation of a productive, highly enantioselective nitrilase through gene site saturation mutagenesis (GSSM)." J. Am. Chem. Soc **125**(38): 11476-11477.
- Dower, W. J., J. F. Miller, et al. (1988). "High efficiency transformation of *E. coli* by high voltage electroporation." Nucleic Acids Research **16**(13): 6127-6146.
- Egmond, M. R. and C. J. Van Bommel (1997). "Impact of structural information on understanding lipolytic function." Methods in enzymology **284**: 119-129.
- Eigen, M. and W. Gardiner (1984). "Evolutionary molecular engineering based on RNA replication." Pure Appl. Chem **56**: 967-978.
- Ellis, S. B., P. F. Brust, et al. (1985). "Isolation of alcohol oxidase and two other methanol regulatable genes from the yeast *Pichia pastoris*." Molecular and Cellular Biology **5**(5): 1111-1121.

- Ettinger, W. F., S. K. Thukral, et al. (1987). "Structure of cutinase gene, cDNA, and the derived amino acid sequence from phytopathogenic fungi." Biochemistry **26**(24): 7883-7892.
- Faber, K. (2000). Biotransformations. Heidelberg, Springer.
- Faber, K. and S. Riva (1992). "Enzyme-catalyzed irreversible acyl transfer." Synthesis(Stuttgart)(10): 895-910.
- Fan, C. Y. and W. Köller (1998). "Diversity of cutinases from plant pathogenic fungi: differential and sequential expression of cutinolytic esterases by *Alternaria brassicicola*." FEMS Microbiology Letters **158**(1): 33-38.
- Fersht, A. (1984). Enzyme structure and mechanism. New York.
- Fontes, N., M. C. Almeida, et al. (1998). "Cutinase activity and enantioselectivity in supercritical fluids." Ind. Eng. Chem. Res **37**(8): 3189-3194.
- Genencor (1988). Increasing pharmacological effect of agricultural chemicals. United States Patent **88-08945**.
- Goldstein, J., N. S. Pollitt, et al. (1990). "Major Cold Shock Protein of *Escherichia coli*." Proceedings of the National Academy of Sciences **87**(1): 283-287.
- Goncalves, A. M., E. Schacht, et al. (1999). "Stability studies of a recombinant cutinase immobilized to dextran and derivatized silica supports." Enzyme and Microbial Technology **24**(1-2): 60-66.
- Goncalves, A. P. V., J. M. S. Cabral, et al. (1996). "Immobilization of a recombinant cutinase by entrapment and by covalent binding." Applied biochemistry and biotechnology **60**(3): 217-228.
- Goncalves, A. P. V., J. M. Lopes, et al. (1996a). "Zeolites as supports for enzymatic hydrolysis reactions. Comparative study of several zeolites." Journal of Molecular Catalysis. B, Enzymatic **1**(2): 53-60.
- Grinna, L. S. and J. F. Tschopp (1989). "Size distribution and general structural features of N-linked oligosaccharides from the methylotrophic yeast, *Pichia pastoris*." Yeast **5**(2): 107-115.
- Grochulski, P., Y. Li, et al. (1994). "Two conformational states of *Candida rugosa* lipase." Protein Science **3**(1): 82-91.
- Guex, N. and M. C. Peitsch (1997). "SWISS-MODEL and the Swiss-PdbViewer: An environment for comparative protein modelling." Electrophoresis **18**: 2714-2723.
- Haeffner, F., T. Norin, et al. (1998). "Molecular Modeling of the Enantioselectivity in Lipase-Catalyzed Transesterification Reactions." Biophys. J. **74**(3): 1251-1262.

- Hajjar, A. B., P. F. Nicks, et al. (1990). "Preparation of monomeric acrylic ester intermediates using lipase catalysed transesterifications in organic solvents." Biotechnol. Lett. **12**: 825-830.
- Hauer, B., D. Haering, et al. (2003). Enzymatic synthesis of polyol acrylatesenzymatic synthesis of polyol acrylates. European Patent. **EP1448785**.
- Hayette, M. P., G. Strecker, et al. (1992). "Presence of human antibodies reacting with *Candida albicans* O-linked oligomannosides revealed by using an enzyme-linked immunosorbent assay and neoglycolipids." Journal of Clinical Microbiology **30**(2): 411-417.
- Hill, A. C. (1898). "Reversible zymohydrolysis." J. Chem. Soc **73**: 634-658.
- Hoegh, I., S. Patkar, et al. (1995). "Two lipases from *Candida antarctica*: cloning and expression in *Aspergillus oryzae*." Revue canadienne de botanique **73**: 869-875.
- Hogrefe, H. H., J. Cline, et al. (2002). "Creating randomized amino acid libraries with the QuikChange? Multi Site-Directed Mutagenesis Kit: Drug discovery and genomic technologies." Biotechniques **33**(5): 1158-1165.
- Houde, A., A. Kademi, et al. (2004). "Lipases and their industrial applications." Applied Biochemistry and Biotechnology **118**(1): 155-170.
- Huang, M. M., N. Arnheim, et al. (1992). "Extension of base mispairs by Taq DNA polymerase: implications for single nucleotide discrimination in PCR." Nucleic Acids Research **20**(17): 4567-4573.
- Invitrogen "A Manual of Methods for Expression of Recombinant Proteins Using pPICZ and pPICZ α in *Pichia pastoris*, Catalog no. K1740-01".
- Itakura, K., T. Hirose, et al. (1977). "Expression in *Escherichia coli* of a chemically synthesized gene for the hormone somatostatin." Science **198**(4321): 1056-1063.
- Ivanov, A. E. and M. P. Schneider (1997). "Methods for the immobilization of lipases and their use for ester synthesis." Journal of Molecular Catalysis. B, Enzymatic **3**(6): 303-309.
- Jaeger, K. E., B. W. Dijkstra, et al. (1999). "BACTERIAL BIOCATALYSTS: Molecular Biology, Three-Dimensional Structures, and Biotechnological Applications of Lipases." Annual Reviews in Microbiology **53**(1): 315-351.
- Jaeger, K. E. and M. T. Reetz (1998). "Microbial lipases form versatile tools for biotechnology." Trends in Biotechnology **16**(9): 396-403.
- Jelsch, C., S. Longhi, et al. (1998). "Packing forces in nine crystal forms of cutinase." Proteins: Structure, Function, and Genetics **31**: 320-333.

- Jelsch, C., S. Longhi, et al. (1998). "Packing forces in nine crystal forms of cutinase." Proteins: Structure, Function, and Genetics **31**: 320-333.
- Johnston, M. (1987). "A model fungal gene regulatory mechanism: the GAL genes of *Saccharomyces cerevisiae*." Microbiology and Molecular Biology Reviews **51**(4): 458-476.
- Kaiser, C. A., D. Preuss, et al. (1987). "Many random sequences functionally replace the secretion signal sequence of yeast invertase." Science **235**(4786): 312-317.
- Kastle, J. H. and A. S. Loevenhart (1900). "Concerning lipase, the fat-splitting enzyme, and the reversibility of its action." Am. Chem. J **24**: 491-525.
- Kazlauskas, R. J. (2000). "Molecular modeling and biocatalysis: explanations, predictions, limitations, and opportunities." Current Opinion in Chemical Biology **4**(1): 81-88.
- Kazlauskas, R. J. and U. T. Bornscheuer (1998). "Biotransformations with lipases." Biotechnology **8**: 37-191.
- Kazlauskas, R. J., A. N. E. Weissfloch, et al. (1991). "A Rule to Predict Which Enantiomer of a Secondary Alcohol Reacts Faster in Reactions Catalyzed by Cholesterol Esterase, Lipase from *Pseudomonas cepacia*, and Lipase from *Candida rugosa*." J. Org. Chem. **56**: 2656-2665.
- Kirk, O. and M. W. Christensen (2002). "Lipases from *Candida antarctica*: Unique Biocatalysts from a Unique Origin." Org Process Res Dev **6**(4): 446-451.
- Klibanov, A. M. (1986). "Enzymes that work in organic solvents." Chemtech **16**(6): 354-359.
- Klibanov, A. M. (2001). "Improving enzymes by using them in organic solvents." Nature a-z index **409**(6817): 241-246.
- Koeller, K. M. and C. H. Wong (2001). "Enzymes for chemical synthesis." Nature a-z index **409**(6817): 232-240.
- Koeller, W. and P. E. Kolattukudy (1982). "Mechanism of action of cutinase: chemical modification of the catalytic triad characteristic for serine hydrolases." Biochemistry **21**(13): 3083-3090.
- Kolattukudy, P. E. (1981). "Structure, biosynthesis, and biodegradation of cutin and suberin." Annual Review of Plant Physiology **32**(1): 539-567.
- Kolattukudy, P. E., R. E. Purdy, et al. (1981). "Cutinases from fungi and pollen." Methods in enzymology **71**: 652-664.
- Konu and M. D. Li (2002). "Correlations Between mRNA Expression Levels and GC Contents of Coding and Untranslated Regions of Genes in Rodents." Journal of Molecular Evolution **54**(1): 35-41.

- Koutz, P., G. R. Davis, et al. (1989). "Structural comparison of the *Pichia pastoris* alcohol oxidase genes." Yeast **5**(3): 167-177.
- Krishnakant, S. and D. Madamwar (2001). "Ester synthesis by lipase immobilized on silica and microemulsion based organogels (MBGs)." Process Biochem **36**: 607-611.
- Kyte, J. and R. F. Doolittle (1982). "A simple method for displaying the hydropathic character of a protein." Journal of Molecular Biology **157**(1): 105-132.
- Laemmli, U. K. (1970). "Cleavage of structural proteins during the assembly of the head of bacteriophage T4." Nature **227**(5259): 680-685.
- Lamare, S. and M. D. Legoy (1995). "Working at controlled water activity in a continuous process: the gas/solid system as a solution." Biotechnology and Bioengineering **45**(5): 387-397.
- Lamare, S., R. Lortie, et al. (1997). "Kinetic studies of *Fusarium solani* pisi cutinase used in a gas/solid system: transesterification and hydrolysis reactions." Biotechnology and Bioengineering **56**(1): 1-8.
- Lauwereys, M., P. De Geus, et al. (1991). Cloning, expression and characterization of cutinase, a fungal lipolytic enzyme. Lipases-structure, Function and Genetic Engineering. L. Alberghina, R. D. Schmid and R. Verger. Weinheim, Germany, VCH Weinheim: 243–251.
- Leung, D. W., E. Chen, et al. (1989). "A method for random mutagenesis of a defined DNA segment using a modified polymerase chain reaction." Technique **1**(1): 11-15.
- Liebeton, K., A. Zonta, et al. (2000). "Directed evolution of an enantioselective lipase." Chemistry & Biology **7**(9): 709-718.
- Lis, H. and N. Sharon (1993). "Structural and functional aspects." European Journal of Biochemistry **218**(1): 1-27.
- Liu, D., R. D. Schmid, et al. (2006). "Functional expression of *Candida antarctica* lipase B in the *Escherichia coli* cytoplasm--a screening system for a frequently used biocatalyst." Appl. Microbiol. Biotechnol. **72**(5): 1024-1032.
- Liu, D., R. D. Schmid, et al. (2006). "Functional expression of *Candida antarctica* lipase B in the *Escherichia coli* cytoplasm—a screening system for a frequently used biocatalyst." Appl. Microbiol. Biotechnol. **72**(5): 1024-1032.
- Longhi, S., M. Mannesse, et al. (1997a). "Crystal structure of cutinase covalently inhibited by a triglyceride analogue." Protein Sci. **6**(2): 275-286.
- Lueking, A., C. Holz, et al. (2000). "A system for dual protein expression in *Pichia pastoris* and *Escherichia coli*." Protein Expression and Purification **20**(3): 372-378.

- Magnusson, A. (2005). Rational redesign of *Candida antarctica* lipase B. Department of Biochemistry. Stockholm, Royal Institute of Technology, School of Biotechnology.
- Magnusson, A. O., J. C. Rotticci-Mulder, et al. (2005a). "Creating space for large secondary alcohols by rational redesign of *Candida antarctica* lipase B." Chembiochem **6**(6): 1051-1056.
- Magnusson, A. O., M. Takwa, et al. (2005b). "An S-selective lipase was created by rational redesign and the enantioselectivity increased with temperature." Angewandte Chemie (International ed. in English) **44**(29): 4582-4585.
- Maley, F., R. B. Trimble, et al. (1989). "Characterization of glycoproteins and their associated oligosaccharides through the use of endoglycosidases." Analytical Biochemistry **180**(2): 195-204.
- Mandel, M. and A. Higa (1970). "Calcium-dependent bacteriophage DNA infection." J Mol Biol **53**(1): 159-162.
- Mannesse, M. L. M., R. C. Cox, et al. (1995). "Cutinase from *Fusarium solani* pisi Hydrolyzing Triglyceride Analogs. Effect of Acyl Chain Length and Position in the Substrate Molecule on Activity and Enantioselectivity." Biochemistry **34**(19): 6400-6407.
- Martinelle, M., M. Holmquist, et al. (1995). "On the interfacial activation of *Candida antarctica* lipase A and B as compared with *Humicola lanuginosa* lipase." Biochim. Biophys. Acta **1258**(3): 272-276.
- Martinez, C., P. de Geus, et al. (1993). "Engineering cysteine mutants to obtain crystallographic phases with a cutinase from *Fusarium solani* pisi." Protein Engineering Design and Selection **6**(2): 157-165.
- Martinez, C., P. Geus, et al. (1992). "Fusarium solani cutinase is a lipolytic enzyme with a catalytic serine accessible to solvent." Nature **356**: 615-618.
- Mei, Y., L. Miller, et al. (2003). "Imaging the distribution and secondary structure of immobilized enzymes using infrared microspectroscopy." Biomacromolecules **4**(1): 70-74.
- Melo, F. and E. Feytmans (1998). "Assessing Protein Structures with a Non-local Atomic Interaction Energy." Journal of Molecular Biology **277**: 1141-1152.
- Miyazaki, K. and F. H. Arnold (1999). "Exploring nonnatural evolutionary pathways by saturation mutagenesis: rapid improvement of protein function." Journal of molecular evolution **49**(6): 716-720.

- Mouratou, B., P. Kasper, et al. (1999). "Conversion of tyrosine phenol-lyase to dicarboxylic amino acid β -lyase, an enzyme not found in nature." Journal of Biological Chemistry **274**(3): 1320-1325.
- Müller, M. (1992). "Proteolysis in protein import and export: Signal peptide processing in eu- and prokaryotes." Cellular and Molecular Life Sciences (CMLS) **48**(2): 118-129.
- Mullis, K., F. Faloona, et al. (1986). Specific enzymatic amplification of DNA in vitro: the polymerase chain reaction, Cold Spring Harbor Symposia on Quantitative Biology. **51**: 263-273.
- Murphy, C. A., J. A. Cameron, et al. (1996). "Fusarium polycaprolactone depolymerase is cutinase." Applied and Environmental Microbiology **62**(2): 456-460.
- Neumann, E., M. Schaefer-Ridder, et al. (1982). "Gene transfer into mouse lyoma cells by electroporation in high electric fields." The EMBO Journal **1**(7): 841-845.
- Nicolas, A., M. Egmond, et al. (1996). "Contribution of cutinase serine 42 side chain to the stabilization of the oxyanion transition state." Biochemistry **35**: 398-410.
- Noble, M. E. M., A. Cleasby, et al. (1994). "Analysis of the structure of *Pseudomonas glumae* lipase." Protein Engineering Design and Selection **7**(4): 559-562.
- Nyon, M. P., D. W. Rice, et al. (2009). "Catalysis by *Glomerella cingulata* cutinase requires conformational cycling between the active and inactive states of its catalytic triad." J Mol Biol. **385**(1): 226-235.
- Ohtani, T., H. Nakatsukasa, et al. (1998). "Enantioselectivity of *Candida antarctica* lipase for some synthetic substrates including aliphatic secondary alcohols." Journal of Molecular Catalysis. B, Enzymatic **4**(1-2): 53-60.
- Okkels, J. S., A. Svendsen, et al. (1997). New lipolytic enzyme with high capacity to remove lard in one wash cycle. United States Patent. **97-05735**.
- Ollis, D. L., E. Cheah, et al. (1992). "The Alpha/Beta-Hydrolase Fold." Protein Eng. **5**(3): 197-211.
- Orrenius, C., F. Haeffner, et al. (1998). "Chiral recognition of alcohol enantiomers in acyl transfer reactions catalysed by *Candida antarctica* lipase B." Biocatalysis and biotransformation(Print) **16**(1): 1-15.
- Ottosson, J., J. C. Rotticci-Mulder, et al. (2001). "Rational design of enantioselective enzymes requires considerations of entropy." Protein Science **10**(9): 1769-1774.
- Park, D. W., S. Haam, et al. (2004). "Enzymatic esterification of β -methylglucoside with acrylic/methacrylic acid in organic solvents." J. Biotechnol. **107**(2): 151-160.

- Park, S., K. L. Morley, et al. (2005). "Focusing mutations into the *P. fluorescens* esterase binding site increases enantioselectivity more effectively than distant mutations." Chemistry & Biology **12**(1): 45-54.
- Parvaresh, F., H. Robert, et al. (1992). "Gas phase transesterification reactions catalyzed by lipolytic enzymes." Biotechnology and Bioengineering **39**(4): 467-473.
- Pasteur, L. (1906). Researches on the molecular asymmetry of natural organic products, Edinburgh : Alembic Club ; Chicago : University of Chicago Press.
- Patkar, S., J. Vind, et al. (1998). "Effect of mutations in *Candida antarctica* B lipase." Chem. Phys. Lipids **93**: 95-101.
- Pritchard, L., D. Corne, et al. (2005). "A general model of error-prone PCR." Journal of theoretical biology **234**(4): 497-509.
- Purdy, R. E. and P. E. Kolattukudy (1975). "Hydrolysis of plant cuticle by plant pathogens. Purification, amino acid composition, and molecular weight of two isoenzymes of cutinase and a nonspecific esterase from *Fusarium solani* f. *psii*." Biochemistry **14**(13): 2824-2831.
- Rakels, J. L. L., A. J. J. Straathof, et al. (1993). "A simple method to determine the enantiomeric ratio in enantioselective biocatalysis." Enzyme and microbial technology **15**(12): 1051-1056.
- Reetz, M. T., M. Bocola, et al. (2005). "Expanding the range of substrate acceptance of enzymes: combinatorial active-site saturation test." Angewandte Chemie (International ed. in English) **44**(27): 4192-4196.
- Reetz, M. T. and K. E. Jaeger (1999). "Superior biocatalysts by directed evolution." Topics in current chemistry **200**(3): 1-57.
- Reslow, M., P. Adlercreutz, et al. (1987). "Organic solvents for bioorganic synthesis." Applied Microbiology and Biotechnology **26**(1): 1-8.
- Rizzi, M., P. Stylos, et al. (1992). "A kinetic study of immobilized lipase catalyzing the synthesis of isoamyl acetate by transesterification in n-hexane." Enzyme Microb Technol **14**: 709-713.
- Rossi, R., A. Montecucco, et al. (1997). "Functional characterization of the T4 DNA ligase: a new insight into the mechanism of action." Nucleic Acids Research **25**(11): 2106-2113.
- Rotticci-Mulder, J. C., M. Gustavsson, et al. (2001). "Expression in *Pichia pastoris* of *Candida antarctica* Lipase B and Lipase B Fused to a Cellulose-Binding Domain." Protein Expression and Purification **21**(3): 386-392.

- Rotticci, D. (2000). Understanding and Engineering the Enantioselectivity of *Candida antarctica* Lipase B towards sec-Alcohols, Royal Institute of Technology, Sweden.
- Rotticci, D., F. Hecfner, et al. (1998). "Molecular recognition of sec-alcohol enantiomers by *Candida antarctica* lipase B." J. Mol. Catal., B Enzym. **5**(1-4): 267-272.
- Rotticci, D., T. Norin, et al. (2000). "An active-site titration method for lipases." BBA-Molecular and Cell Biology of Lipids **1483**(1): 132-140.
- Rotticci, D., J. Ottosson, et al. (2001). "*Candida antarctica* lipase B: a tool for the preparation of optically active alcohols." Methods in Biotechnology **15**: 261-276.
- Rotticci, D., J. C. Rotticci-Mulder, et al. (2001). "Improved Enantioselectivity of a Lipase by Rational Protein Engineering." Chembiochem **2**(10): 766-770.
- Rubio, M. B., R. E. Cardoza, et al. (2008). "Cloning and characterization of the Thcut1 gene encoding a cutinase of *Trichoderma harzianum* T34." Current genetics **54**(6): 301-312.
- Rusnak, M. (2004). Untersuchungen zur enzymatischen Enantiomerentrennung von Glykolethern und Etablierung neuer Methoden des synthetischen Shufflings. Institute of Technical Biochemistry. Stuttgart, Stuttgart University: 1–183.
- Saiki, R. K., D. H. Gelfand, et al. (1988). "Primer-directed enzymatic amplification of DNA with a thermostable DNA polymerase." Science **239**(4839): 487-491.
- Sambrook, J., D. W. Russell, et al. (2001). Molecular Cloning: A Laboratory Manual (3-Volume Set), Cold Spring Harbor Laboratory Press.
- Sandal, T., S. kauppinen, et al. (1998). Enzyme with lipolytic activity. United States Patent. **5827719**.
- Schmid, A., J. S. Dordick, et al. (2001). "Industrial biocatalysis today and tomorrow." Nature **409**(6817): 258-268.
- Schmid, R. D. and R. Verger (1998). "Lipases: interfacial enzymes with attractive applications." Angew. Chem. Int. Ed. Engl. **37**(12): 1608-1633.
- Schoemaker, H. E., D. Mink, et al. (2003). Dispelling the myths-biocatalysis in industrial synthesis. **299**: 1694-1697.
- Schrag, J. D. and M. Cygler (1997). "Lipases and alpha/beta hydrolase fold." Methods in enzymology **284**: 85-107.
- Schwede T, K. J., Guex N, and Peitsch MC (2003). "SWISS-MODEL: an automated protein homology-modeling server. Research." Nucleic Acids **31**: 3381-3385.
- Scorer, C. A., R. G. Buckholz, et al. (1993). "The intracellular production and secretion of HIV-1 envelope protein in the methylotrophic yeast *Pichia pastoris*." Gene(Amsterdam) **136**(1-2): 111-119.

- Sereti, V., H. Stamatis, et al. (1997). "Improved stability and reactivity of *Fusarium solani* cutinase in supercritical CO₂." Biotechnology Techniques **11**: 661-665.
- Serralha, F. N., J. M. Lopes, et al. (1998). "Zeolites as supports for an enzymatic alcoholysis reaction." Journal of Molecular Catalysis. B, Enzymatic **4**(5-6): 303-311.
- Shakin-Eshleman, S. H., S. L. Spitalnik, et al. (1996). "The Amino Acid at the X Position of an Asn-X-Ser Sequon Is an Important Determinant of N-Linked Core-glycosylation Efficiency." Journal of Biological Chemistry **271**(11): 6363-6366.
- Shapiro, A. L., E. Vinuela, et al. (1967). "Molecular weight estimation of polypeptide chains by electrophoresis in SDS-polyacrylamide gels." Biochem Biophys Res Commun **28**(5): 815-820.
- Sharma, R., Y. Chisti, et al. (2001). "Production, purification, characterization, and applications of lipases." Biotechnology Advances **19**(8): 627-662.
- Shaw, J. F., R. C. Chang, et al. (1990). "Lipolytic activities of a lipase immobilized on six selected supporting materials." Biotechnology and Bioengineering **35**(2): 132-137.
- Sjursnes, B., C. Valente, et al. (1998). "Interactions between water and medium effects on enzymes in organic media: kinetics of cutinase catalysed esterification with mutual solvation of reactants." Biotechnology and Bioengineering **1**(3).
- Soares, C. M., V. H. Teixeira, et al. (2003). "Protein structure and dynamics in nonaqueous solvents: insights from molecular dynamics simulation studies." Biophysical journal **84**(3): 1628-1641.
- Soliday, C. L. and P. E. Kolattukudy (1983). "Primary structure of the active site region of fungal cutinase, an enzyme involved in phytopathogenesis." Biochemical and biophysical research communications **114**(3): 1017-1022.
- Spee, J. H., W. M. de Vos, et al. (1993). "Efficient random mutagenesis method with adjustable mutation frequency by use of PCR and dITP." Nucleic Acids Research **21**(3): 777-778.
- Spiegelman, S., I. Haruna, et al. (1965). "The synthesis of a self-propagating and infectious nucleic acid with a purified enzyme." Proceedings of the National Academy of Sciences **54**(3): 919-927.
- Stark, M. B. and K. Holmberg (1989). "Covalent immobilization of lipase in organic solvents." Biotechnology and Bioengineering **34**(7): 942-950.
- Stemmer, W. P. C. (1994a). "DNA shuffling by random fragmentation and reassembly: in vitro recombination for molecular evolution." Proceedings of the National Academy of Sciences **91**(22): 10747-10751.

- Stemmer, W. P. C. (1994b). "Rapid evolution of a protein in vitro by DNA shuffling." Nature **370**(6488): 389-391.
- Straathof, A. J. J. and J. A. Jongejan (1997). "The enantiomeric ratio: origin, determination and prediction." Enzyme and Microbial Technology **21**(8): 559-571.
- Stratagene (2003). "kits feature X110-Gold, X. L. QuikChange® II XL Site-Directed Mutagenesis Kit."
- Suen, W. C., N. Zhang, et al. (2004). "Improved activity and thermostability of *Candida antarctica* lipase B by DNA family shuffling." Protein Engineering Design and Selection **17**(2): 133-140.
- Svendsen, A. (2004). Enzyme functionality: design, engineering, and screening, CRC Press.
- Sweigard, J. A., F. G. Chumley, et al. (1992). "Cloning and analysis of CUT1, a cutinase gene from *Magnaporthe grisea*." Molecular Genetics and Genomics **232**(2): 174-182.
- Telefoncu, A., E. Dlnckaya, et al. (1990). "Preparation and characterization of pancreatic lipase immobilized in Eudragit-matrix." Applied biochemistry and biotechnology **26**(3): 311-317.
- Tetsuya Ohru, N., S. Yasuhito Sakakibara, et al. (1975). Process for continuously synthesizing acrylic acid esters. United States Patent. **3875212**.
- Trail, F. and W. Koeller (1993). "Diversity of cutinases from plant pathogenic fungi: Purification and characterization of two cutinases from *Alternaria brassicicola*." Physiological and Molecular Plant Pathology **42**: 205-220.
- Trodler, P. (2008). Untersuchung von Lipasen - Elektrostatik, Selektivität und Einfluss von Lösungsmitteln auf Struktur und Dynamik. Institute of Technical Biochemistry. Stuttgart, Stuttgart University.
- Trodler, P., J. Pleiss, et al. (2008). "Modeling structure and flexibility of *Candida antarctica* lipase B in organic solvents." BMC Structural Biology **8**(1): 9.
- Tschopp, J. F., G. Sverlow, et al. (1987). "High-level secretion of glycosylated invertase in the methylotrophic yeast, *Pichia pastoris*." Bio/technology **5**(12): 1305-1308.
- Uppenberg, J., M. T. Hansen, et al. (1994). "The sequence, crystal structure determination and refinement of two crystal forms of lipase B from *Candida antarctica*." Structure **2**(4): 293-308.
- Uppenberg, J., N. Ohrner, et al. (1995). "Crystallographic and molecular-modeling studies of lipase B from *Candida antarctica* reveal a stereospecificity pocket for secondary alcohols." Biochemistry **34**(51): 16838-16851.

- Uyama, H., S. Suda, et al. (1997). "Extremely efficient catalysis of immobilized lipase in ring-opening polymerization of lactones." Chemistry Letters **26**(11): 1109-1110.
- Van den Burg, B., G. Vriend, et al. (1998). Engineering an enzyme to resist boiling, National Acad Sciences. **95**: 2056-2060.
- Van der Hijden, H. T., J. D. Marugg, et al. (1994). Enzyme containing surfactants compositions. United States Patent. **94-04771**.
- Van Tol, J. B. A., J. A. Jongejan, et al. (1991). "Enantioselective enzymatic catalysis. 2. Applicability of methods for enantiomeric ratio determinations." Recl. Trav. Chim. Pays-Bas **110**: 255-262.
- Verger, R. (1997). "'Interfacial activation' of lipases: facts and artifacts." Trends in Biotechnology **15**(1): 32-38.
- Villeneuve, P., J. M. Muderhwa, et al. (2000). "Customizing lipases for biocatalysis: a survey of chemical, physical and molecular biological approaches." Journal of Molecular Catalysis. B, Enzymatic **9**(4-6): 113-148.
- Walbot, V. (2000). "Saturation mutagenesis using maize transposons." Current opinion in plant biology **3**(2): 103-107.
- Wang, G. Y., T. J. Michailides, et al. (2002). "Molecular cloning, characterization, and expression of a redox-responsive cutinase from *Monilinia fructicola* (Wint.) Honey." Fungal Genetics and Biology **35**(3): 261-276.
- Warwel, S., G. Steinke, et al. (1996). "An efficient method for lipase-catalyzed preparation of acrylic and methacrylic acid esters." Biotechnol. Tech. **10**: 283-286.
- Weber, K. and M. Osborn (1969). "The Reliability of Molecular Weight Determinations by Dodecyl Sulfate-Polyacrylamide Gel Electrophoresis." Journal of Biological Chemistry **244**(16): 4406-4412.
- White, C. E., N. M. Kempf, et al. (1994). "Expression of highly disulfide-bonded proteins in *Pichia pastoris*." Structure **2**(11): 1003-1005.
- Wisdom, R. A., P. Dunnill, et al. (1984). "Enzyme esterification of fats: factors influencing the choice of support for immobilized lipase." Enzyme Microb Technol **6**: 443-446.
- Yan, B., W. Zhang, et al. (1999). "Sequence Pattern for the Occurrence of N-Glycosylation in Proteins." Journal of Protein Chemistry **18**(5): 511-521.
- Yang, D. S. C. and C. L. Hew (2001). "Low-temperature increases the yield of biologically active herring antifreeze protein in *Pichia pastoris*." Protein Expression and Purification **21**: 438-445.

- Yang, J., Y. Koga, et al. (2002). Modifying the chain-length selectivity of the lipase from *Burkholderia cepacia* KWI-56 through in vitro combinatorial mutagenesis in the substrate-binding site, Oxford Univ Press. **15**: 147-152.
- YAO, C. and W. Köller (1994). "Diversity of cutinases from plant pathogenic fungi: cloning and characterization of a cutinase gene from *Alternaria brassicicola*." Physiological and Molecular Plant Pathology **44**: 81-92.
- Zhang, N., W. C. Suen, et al. (2003). "Improving tolerance of *Candida antarctica* lipase B towards irreversible thermal inactivation through directed evolution." Protein Engineering Design and Selection **16**(8): 599-605.
- Zheng, L., U. Baumann, et al. (2004). "An efficient one-step site-directed and site-saturation mutagenesis protocol." Nucleic acids research **32**(14): e115.

Appendix

Sequence of *Candida antarctica* lipase B (CALB)

calb_ncbi	CTACCTTCGGTTTCGGACCCCTGCCTTTTCGCAGCCCCAAGTCGGTGCTCGATGCGGGTCTG	60
calb_iso	CTACCTTCGGTTTCGGACCCCTGCCTTTTCGCAGCCCCAAGTCGGTGCTCGATGCGGGTCTG	20
calb_ncbi	ACCTGCCAGGGTGCTTCGCCATCCTCGGTCTCCAAACCCATCCTTCTCGTCCCCGGAACC	120
calb_iso	ACCTGCCAGGGTGCTTCGCCATCCTCGGTCTCCAAACCCATCCTTCTCGTCCCCGGAACC	40
calb_ncbi	GGCACCACAGGTCCACAGTCGGTTCGACTCGAACTGGATCCCCCTCTCAAGCAGTTGGGT	180
calb_iso	GGCACCACAGGTCCACAGTCGGTTCGACTCGAACTGGATCCCCCTCTCAAGCAGTTGGGT	60
calb_ncbi	TACACACCCTGCTGGATCTCACCCCGCCGTTTCATGCTCAACGACACCCAGGTCAACACG	240
calb_iso	TACACACCCTGCTGGATCTCACCCCGCCGTTTCATGCTCAACGACACCCAGGTCAACACG	80
calb_ncbi	GAGTACATGGTCAACGCCATCACCTCTCTACGCTGGTTCGGGCAACAACAAGCTTCCC	300
calb_iso	GAGTACATGGTCAACGCCATCACCTCTCTACGCTGGTTCGGGCAACAACAAGCTTCCC	100
calb_ncbi	GTGCTTACCTGGTCCCAGGGTGGTCTGGTTGCACAGTGGGGTCTGACCTTCTTCCCAGT	360
calb_iso	GTGCTTACCTGGTCCCAGGGTGGTCTGGTTGCACAGTGGGGTCTGACCTTCTTCCCAGT	120
calb_ncbi	ATCAGGTCCAAGTTCGATCGACTTATGGCCTTTGCGCCCGACTACAAGGGCACCCGTCCTC	420
calb_iso	ATCAGGTCCAAGTTCGATCGACTTATGGCCTTTGCGCCCGACTACAAGGGCACCCGTCCTC	140
calb_ncbi	GCCGGCCCTCTCGATGCACTCGCGGTTAGTGCACCCCTCCGTATGGCAGCAAACCACCGGT	480
calb_iso	GCCGGCCCTCTCGATGCACTCGCGGTTAGTGCACCCCTCCGTATGGCAGCAAACCACCGGT	160
calb_ncbi	TCGGCACTCACACCCGCACTCCGAAACGCAGGTGGTCTGACCCAGATCGTGCCACACC	540
calb_iso	TCGGCACTCACACCCGCACTCCGAAACGCAGGTGGTCTGACCCAGATCGTGCCACACC	180
calb_ncbi	AACCTCTACTCGCGACCGGACGAGATCGTTTCAGCCTCAGGTGTCCAACCTGCCACTCGAC	600
calb_iso	AACCTCTACTCGCGACCGGACGAGATCGTTTCAGCCTCAGGTGTCCAACCTGCCACTCGAC	200
calb_ncbi	TCATCTACCTCTTCAACGGAAAGAACGTCCAGGCACAGGCCTGTGTGGGCCGCTGTTC	660
calb_iso	TCATCTACCTCTTCAACGGAAAGAACGTCCAGGCACAGGCCTGTGTGTGGGCCGCTGTTC	220
calb_ncbi	GTCATCGACCATGCAGGCTCGCTCACCTCGCAGTTCTCCTACGTCGTCGGTTCGATCCGCC	720
calb_iso	GTCATCGACCATGCAGGCTCGCTCACCTCGCAGTTCTCCTACGTCGTCGGTTCGATCCGCC	240
calb_ncbi	CTGGCTCCACCACGGGCCAGGCTCGTAGTGCAGACTATGGCATTACGGACTGCAACCCCT	780
calb_iso	CTGGCTCCACCACGGGCCAGGCTCGTAGTGCAGACTATGGCATTACGGACTGCAACCCCT	260
calb_ncbi	CTTCCCGCCAATGATCTGACTCCCGAGCAAAGGTGCGCGGCTGCGCTCCTGGCGCCG	840
calb_iso	CTTCCCGCCAATGATCTGACTCCCGAGCAAAGGTGCGCGGCTGCGCTCCTGGCGCCG	280
calb_ncbi	GCAAGCTGCAGCCATCGTGGCGGGTCCAAAGCAGAAGTGCAGGCCGACCTCATGCCCTAC	900
calb_iso	GCAAGCTGCAGCCATCGTGGCGGGTCCAAAGCAGAAGTGCAGGCCGACCTCATGCCCTAC	300
calb_ncbi	GCCCGCCCTTTGCACTAGGCAAAGGACCTGCTCCGGCATCGTCAACCCCTGA	954
calb_iso	GCCCGCCCTTTGCACTAGGCAAAGGACCTGCTCCGGCATCGTCAACCCCTGA	317

Sequence alignment of the published *CALB* sequence (calb_ncbi: CAA83122) and the recombinant *CALB* gene used in our work (calb_iso). Silent mutations are marked in yellow. The positions of mutations (T57A, A89T) are indicated with red. The protein sequence of the recombinant *CALB* is represented in blue.

Curriculum vitae

Personal Information

Name: Danni Liu

Nationality: Chinese (P. R. China)

Tel: +49 711 4103140

Mobil: +49 176 48756666

Email: danni.liu@gmx.de

Education

- 11/2005 - present **PhD-thesis work at the Institute for Technical Biochemistry, University of Stuttgart, Germany**
Title: Enzymes for Industrial Acrylation: Redesign of *Candida antarctica* Lipase B and Characterization of a New Cutinase from *Alternaria brassicicola*
- 03/2005-10/2005 **Diploma thesis at the Institute for Technical Biochemistry, University of Stuttgart, Germany**
Title: Improvement of Functional Expression of *Candida antarctica* Lipase B in *Escherichia coli*
- 10/2001-02/2005 **Study of technical Biology at the University of Stuttgart, Germany**
Degree: Diplom-Biologin (technisch orientiert)
- 02/2004-08/2004 **Research assistant at Fraunhofer Institute IGB, molecular Biotechnology**
- 09/1992-07/1997 **Study of Medicine at the Xi'an Jiao Tong University, China**
Degree: Bachelor of Medicine

Publications

Liu D, Schmid R. D. and Rusnak M. “Functional expression of *Candida antarctica* lipase B in the *Escherichia coli* cytoplasm--a screening system for a frequently used biocatalyst”. Appl. Microbiol. Biotechnol. 2006. **72**(5): p. 1024-1032.

Liu D., Trodler P., Eiben S., Müller M., Pleiss J., Maurer C. S., Branney C., Schmid R. D. and Hauer B. “Improved Acrylation of hydroxypropylcarbamates by rational design of *Candida antarctica* lipase B”. Chembiochem, Submitted.

Liu D., Schmid R. D., Hauer B., “Functional expression and characterization of a new cutinase from *Alternaria brassicicola* in *Pichia pastoris* for industrial acrylation”. Appl. Microbiol. Biotechnol., Submitted.

Patent

Liu D., Schmid R. D., Rusnak M., Branney C., Haering D., Hauer B.. “Functional expression of triacylglycerol lipases”, DE 102006016023.1, BASF AG, Germany, 2006.

Liu D., Trodler P., Eiben S., Müller M., Pleiss J., Maurer C. S., Branney C., Schmid R. D., Hauer B., “Improved Acrylation of hydroxypropylcarbamates by rational design of *Candida Antarctica* lipase B”, AE 20070139, BASF AG, Germany, 2007.